WVT-TR-75058

AD A018 727

APPLICATION OF FILAMENT WINDING TO CANNON AND CANNON COMPONENTS. PART II: RESIDUAL STRESS ANALYSIS

October 1975

BENET WEAPONS LABORATORY
WATERVLIET ARSENAL
WATERVLIET, N.Y. 12189

TECHNICAL REPORT

AMCMS No. 3297.06.6681

Pron No. M1-3-23032

DISCLAIMER

The findings in this report are not to be construed as an official Department of the Army position unless so designated by other authorized documents.

The use of trade name(s) and/or manufacturer(s) in this report does not constitute an official indorsement or approval.

DISPOSITION

Destroy this report when it is no longer needed. Do not return it to the originator.

UNCLASSIFIED

SECURITY CLASSIFICATION OF THIS PAGE *(When Data Entered)*

REPORT DOCUMENTATION PAGE

READ INSTRUCTIONS BEFORE COMPLETING FORM

1. REPORT NUMBER: WVT-TR-75058	2. GOVT ACCESSION NO.
3. RECIPIENT'S CATALOG NUMBER	
4. TITLE *(and Subtitle)*: Application of Filament Winding to Cannon and Cannon Components. Part II: Residual Stress Analysis	5. TYPE OF REPORT & PERIOD COVERED
	6. PERFORMING ORG. REPORT NUMBER
7. AUTHOR(s): Giuliano D'Andrea, Robert Cullinan, Royce W. Soanes	8. CONTRACT OR GRANT NUMBER(s)
9. PERFORMING ORGANIZATION NAME AND ADDRESS: Benet Weapons Laboratory, Watervliet Arsenal, Watervliet, N.Y. 12189, SARWV-RT	10. PROGRAM ELEMENT, PROJECT, TASK AREA & WORK UNIT NUMBERS: AMCMS No. 3297.06.6681, Pron No. M1-3-23032
11. CONTROLLING OFFICE NAME AND ADDRESS: U.S. Army Armament Command, Rock Island, Illinois 61201	12. REPORT DATE: October 1975
	13. NUMBER OF PAGES: 103
14. MONITORING AGENCY NAME & ADDRESS *(if different from Controlling Office)*	15. SECURITY CLASS. *(of this report)*: UNCLASSIFIED
	15a. DECLASSIFICATION/DOWNGRADING SCHEDULE

16. DISTRIBUTION STATEMENT *(of this Report)*

Approved for public release; distribution unlimited

17. DISTRIBUTION STATEMENT *(of the abstract entered in Block 20, if different from Report)*

18. SUPPLEMENTARY NOTES

19. KEY WORDS *(Continue on reverse side if necessary and identify by block number)*

Composite Materials
Gun Barrels
Guns
Recoilless Guns
Rifles
Residual Stress
Filaments
Winding

20. ABSTRACT *(Continue on reverse side if necessary and identify by block number)*

The feasibility of utilizing high strength steel wire filaments for lightweight composite gun tubes has been demonstrated in Watervliet Arsenal Technical Report WVT-7205. This study investigates the variation in gun tube strength due to the residual stresses introduced during the filament winding operation. Four composite test specimens of 106mm caliber have been designed, fabricated, and tested for residual stress studies. Graphical outputs are included to show correlation between theory and experiments.

DD FORM 1 JAN 73 1473 EDITION OF 1 NOV 65 IS OBSOLETE

UNCLASSIFIED

SECURITY CLASSIFICATION OF THIS PAGE *(When Data Entered)*

WVT-TR-75058

AD

APPLICATION OF FILAMENT WINDING TO CANNON AND CANNON COMPONENTS. PART II: RESIDUAL STRESS ANALYSIS

Guiliano D'Andrea

Robert Cullinan

Royce W. Soanes

October 1975

BENET WEAPONS LABORATORY
WATERVLIET ARSENAL
WATERVLIET, N.Y. 12189

TECHNICAL REPORT

AMCMS No. 3297.06.6681

Pron No. M1-3-23032

TABLE OF CONTENTS

ILLUSTRATIONS

TABLES

FOREWORD

1. The authors wish to thank the following individuals for their excellent assistance, cooperation and contributions:

Dr. J. Zweig, Lt Arnold M. Manaker, Paul J. Croteau, Philip J. Giordano, Ralph E. Peterson, and Harold S. Scheck.

2. Special thanks to Mrs. Patricia Clinton for the preparation of the manuscript.

OBJECTIVE

The objective of this program is to develop within the Army Armament Command the fabrication technology and design concepts necessary for the application of filament wound fiber reinforced composites to cannon and cannon components.

Particular emphasis of this phase of the study is being placed on the development of a theoretical technique which would predict the residual stresses introduced during the filament winding operation. Results from this analysis are to be used in the development of lightweight, high strength, reusable composite systems such as recoilless rifles.

BACKGROUND

As mentioned in ref 1, there are two main approaches for eliminating the problem of strain incompatibility which arises when a low modulus (fiberglass) jacket is coupled with a high modulus liner (steel). The first approach is to bring the modulus of the jacket more in line with, or greater than, that of the liner (ref 1 deals with this aspect).

The second approach is to make sure that the compressive stresses, introduced during the filament winding operation, are only favorable in reducing system weight, and do not contribute unnecessary or adverse stresses to the supporting liner.

---

[1]Cullinan, R., et al, "Application of Filament Winding to Cannon and Cannon Components. Part I: Steel Filament Composites," April 1972, Watervliet Arsenal Technical Report WVT-7205.

This report concerns itself primarily with the second approach; it links the variation in the composite vessel's strength to the residual stresses introduced during the filament winding operation. A number of reports have been documented in the study of residual stresses.[2,3] This work will (a) provide the residual stress (induced during fabrication) as a function of the design and fabrication procedures, and (b) will correlate theoretical and experimental results obtained in the development of the lightweight 106mm recoilless rifle consisting of a steel liner and a composite jacket made of continuous steel filaments embedded in an epoxy matrix or binder.

APPROACH TO THE PROBLEM

The approach will consist of an experimental program complimented by a theoretical study to establish (a) the magnitude of the displacement field during the winding of pressure vessels and (b) to provide the engineer, in charge of the overall design, with graphical or

---

[2]Stone, F. E., "Study of Residual Stresses in Thick Glass-Filament-Reinforced Laminates," October 1965, AD623051.

[3]Stone, F. E. and Greszczuk, L. B., "Study of Residual Stresses in Thick Glass-Filament-Reinforced Laminates," October 1965, AD623051.

numerical data which could be readily used in making manufacturing changes "on the spot" to obtain the desired performance of the weapon.

There are two phases which will be considered: the uncured state, and the cured state.

Before elaborating on the two phases, a description of the fabrication process is next described to facilitate understanding of the theory.

FABRICATION AND TESTING

A. EQUIPMENT

Filament Winder

The winding machine utilized throughout this study is a commercial-type winder shown in Figure 1. This simple horizontal type winder has a chain driven carriage and is capable of winding both helical (15° to 85°) and circumferential modes. A detailed description of the winder, its setup and operation can be found in reference 1.

B. MATERIALS

Steel Filaments

The filament utilized throughout this study was 0.006" stainless steel wire (National-Standard Corp. NS-355) whose physical and mechanical properties are shown in Tables 1 and 2. This wire was supplied in five pound spools.

The most important justification for using steel wire in composites, besides the obvious advantages of high strength and modulus, is

---

[1] Cullinan, R., et al, "Application of Filament Winding to Cannon and Cannon Components. Part I: Steel Filament Composites," April 1972, Watervliet Arsenal Technical Report WVT-7205.

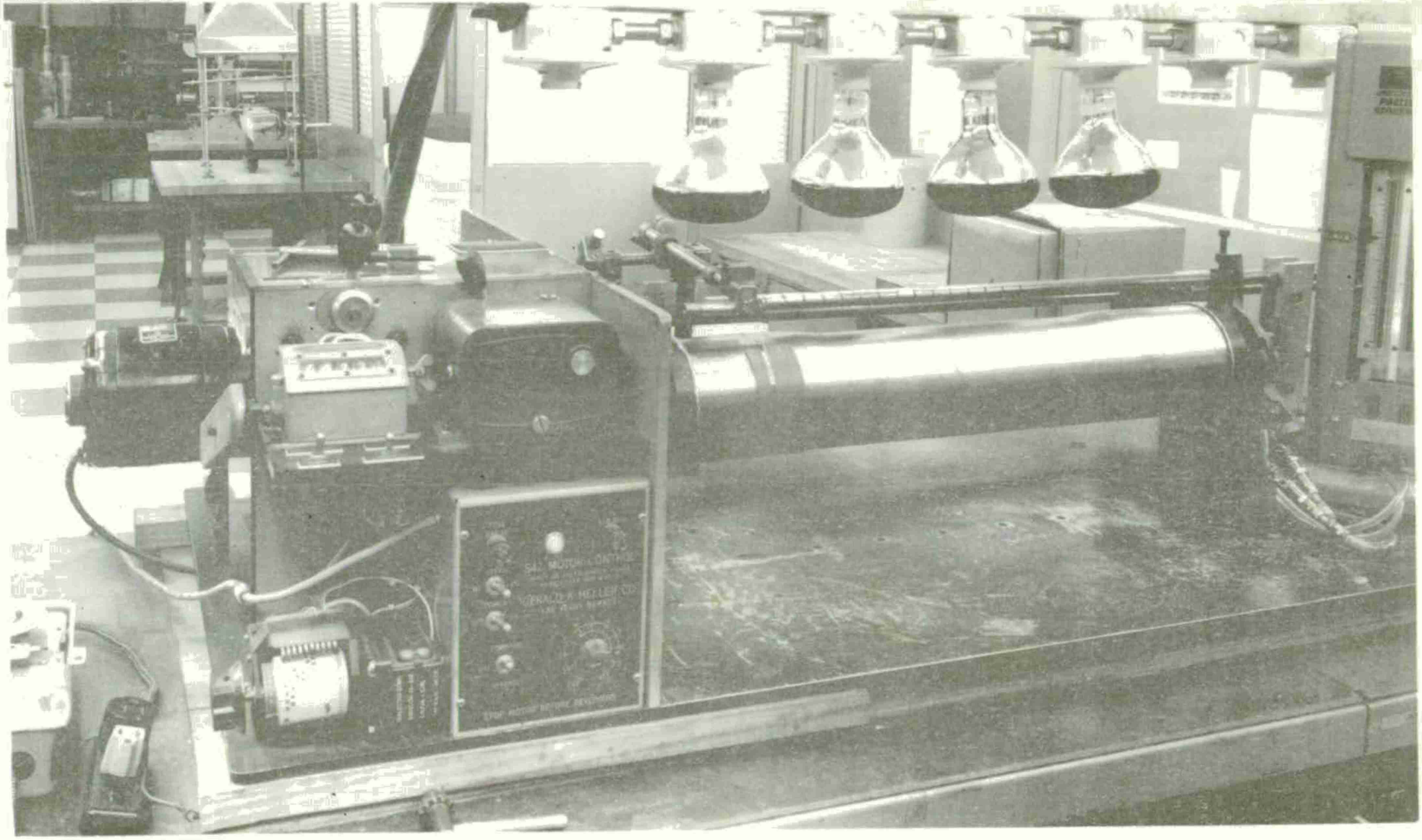

Figure 1. Overall View of the Filament Winder Showing Mounted Test Cylinder, Air Gage Assembly and I-R Lamps Used to Gel Resin.

its extremely high composite efficiency. Composite efficiency is the ratio of the composites' test strength to theoretical composite strength. For steel wire this ratio is $\geq$ 90% whereas for glass it can be as low as 60%[4].

A high composite efficiency indicates that most of the filament's strength goes into the composite's strength because there is no loss of filament strength as a result of mechanical damage from the winding operation, and there is a good bond between the filament and the matrix. As will be shown later, this high composite efficiency enables one to more effectively design a composite structure from the mechanical properties of the raw material.

Resin

In all cases, the epoxy matrix used in the fabrication was an epoxy-anhydride-amine system of the following formulation:

100 parts EPON 828 (Shell Corp)

80 parts CIBA 906 (CIBA Co)

2 parts BDMA (benzyldimethylamine)

Liners

A finish machined 106mm M40A1 gun tube was procured and modified for use as a rifled steel liner. These tubes are made of "gun steel"(modified 4130 steel) with the properties shown in Table 3. The conventional tube (Fig 2) is approximately nine foot long and starting from the muzzle end, four 25" sections were cut off. These four cylinders (OCL-4, 6, 7, 10) were further machined to the dimensions shown in Fig 3.

---

[4]Rosato, D. V. and Grove, C. S., "Filament Winding", John Wiley & Son, New York, N. Y. 1964, p 180

TABLE 1. PHYSICAL AND CHEMICAL PROPERTIES OF NS-355 WIRE*

CHEMICAL			PHYSICAL	
C	0.10	- .18	Density (lb/in^3)	.282
Ni	4.0	- 5.0	Thermal Expansion Coefficient (in/in/°F)	6.4×10^{-6}
Mo	2.0	- 3.0		
Cr	14.4	- 16.0		

CORROSION RESISTANT

TABLE 2. MINIMUM TENSILE STRENGTHS (KSI) VS WIRE DIAMETER*

Wire Diameter (in)	Standard Music Wire	NS-355 Rocket Wire
0.004	439	475
0.005	426	460
0.006	415	450
0.007	407	440
0.008	399	430
0.009	393	430
0.010	387	430
0.012	377	420
0.015	365	420
0.020	350	400
0.030	330	393
Elastic Modulus ($x10^6$ psi)	30	29.3

* SOURCE: NATIONAL STANDARD CO. (1971)

C. FABRICATION

Winding

The fabrication of the test cylinders utilized the solvent-wipe technique shown in Fig 4 and is explained in detail in reference 1.

C.T.C.* Constant tensioning devices, of the type shown in Fig 5, were used to pre-set the load on the wire spools. Fig 6 shows the stand with four such tensioning devices. This was the setup used throughout this phase of the study.

The C.T.C. device would apply a pre-determined load on the individual spools; however, the overall tension of the wires as they reached the mandrel was higher. This increase in tension was a result of the frictional drag on the wires as they traveled through the solvent-wipe process. Actual load on the wires was determined, at the delivery eye before and after winding, with a "fish scale" type scale. Overall tension was monitored during the winding operation with a hand held tensiometer.

Deflection Monitoring

In order to measure the internal dimensions of the cylinders, before and after winding, and to monitor deflection during winding, a modified air gage was used. A conventional 106mm air gage routinely used at Watervliet Arsenal for the dimensional inspection of the land and

---

[1] Cullinan, R., et al, "Application of Filament Winding to Cannon and Cannon Components. Part I: Steel Filament Composites," April 1972, Watervliet Arsenal Technical Report WVT-7205.

* Compensating Tension Controls, Inc., Orange, N. J.

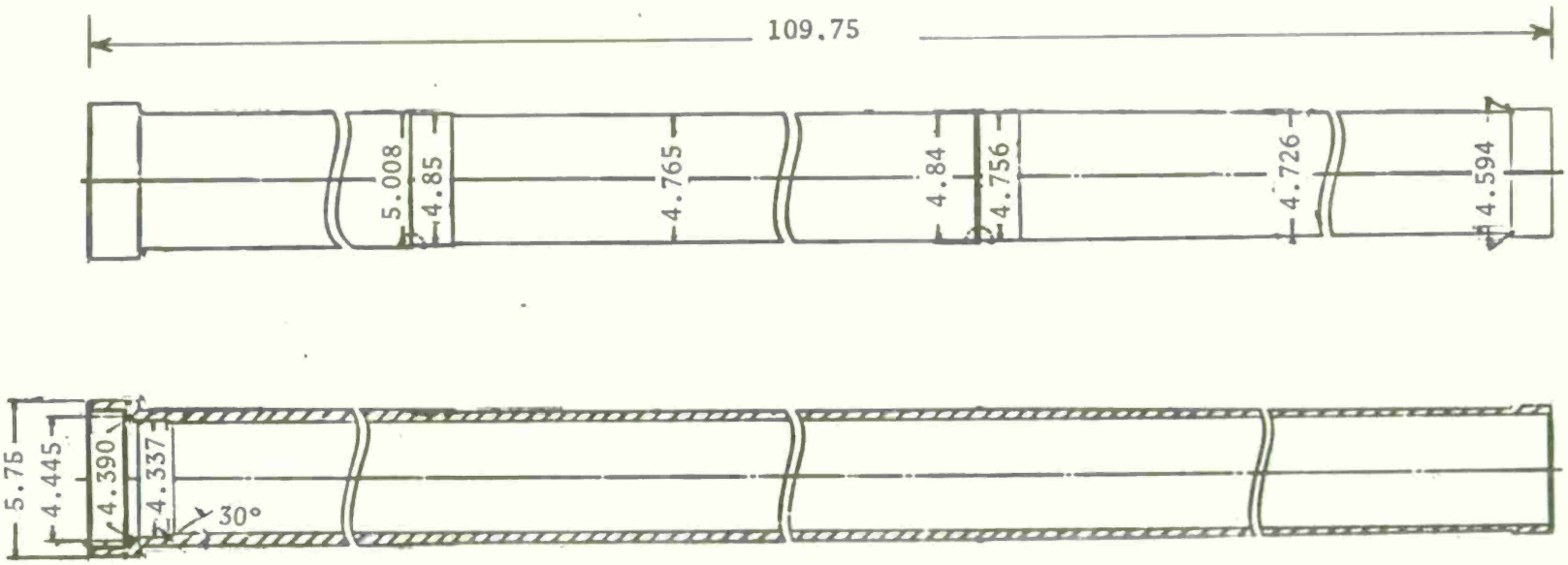

Figure 2. Drawing of Conventional 106mm M40A1 Gun Tube.

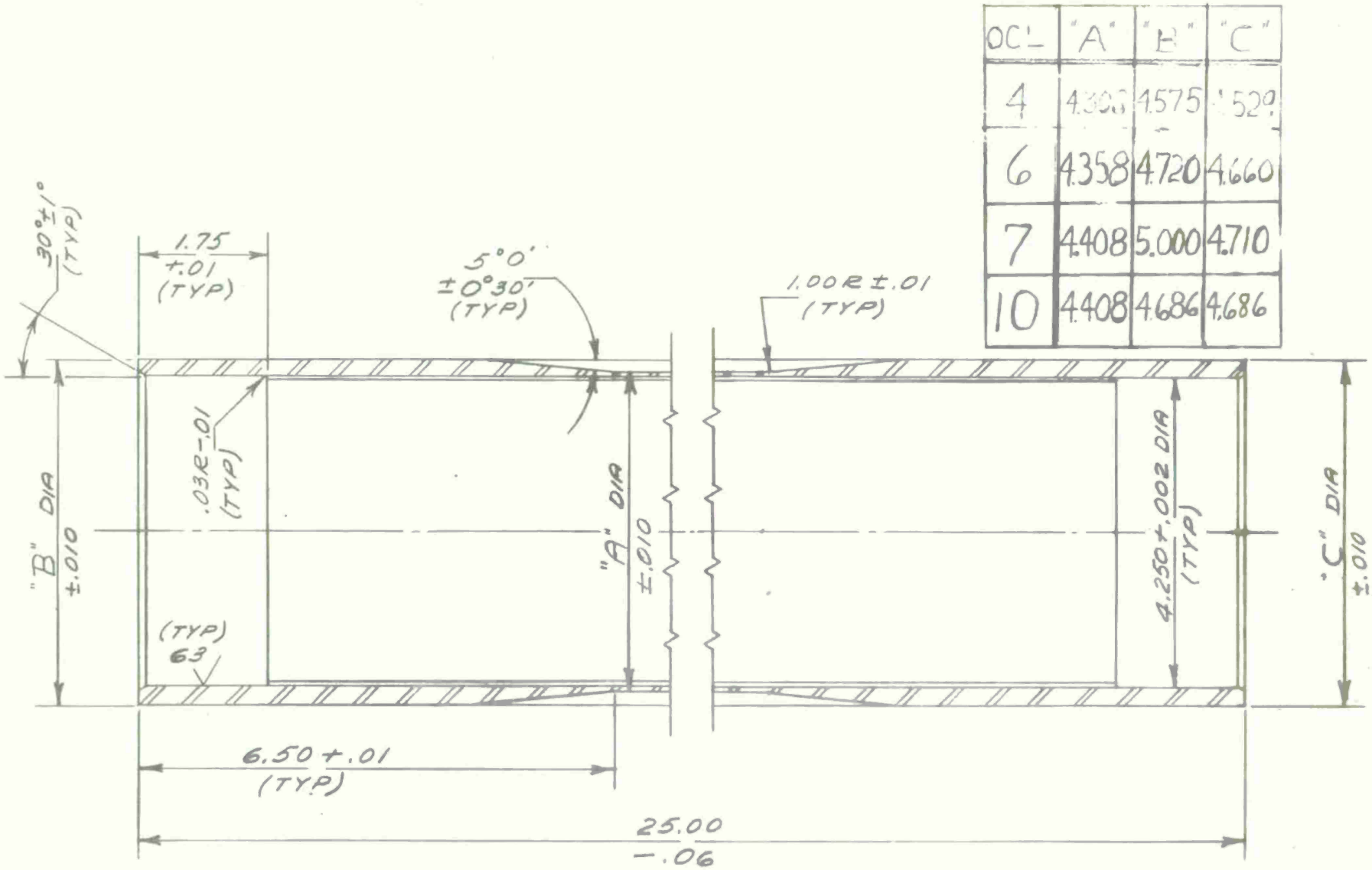

OCL	"A"	"B"	"C"
4	4.300	4.575	4.520
6	4.358	4.720	4.660
7	4.408	5.000	4.710
10	4.408	4.686	4.686

Figure 3. Dimensional Drawing of Steel Liner Test Cylinders.

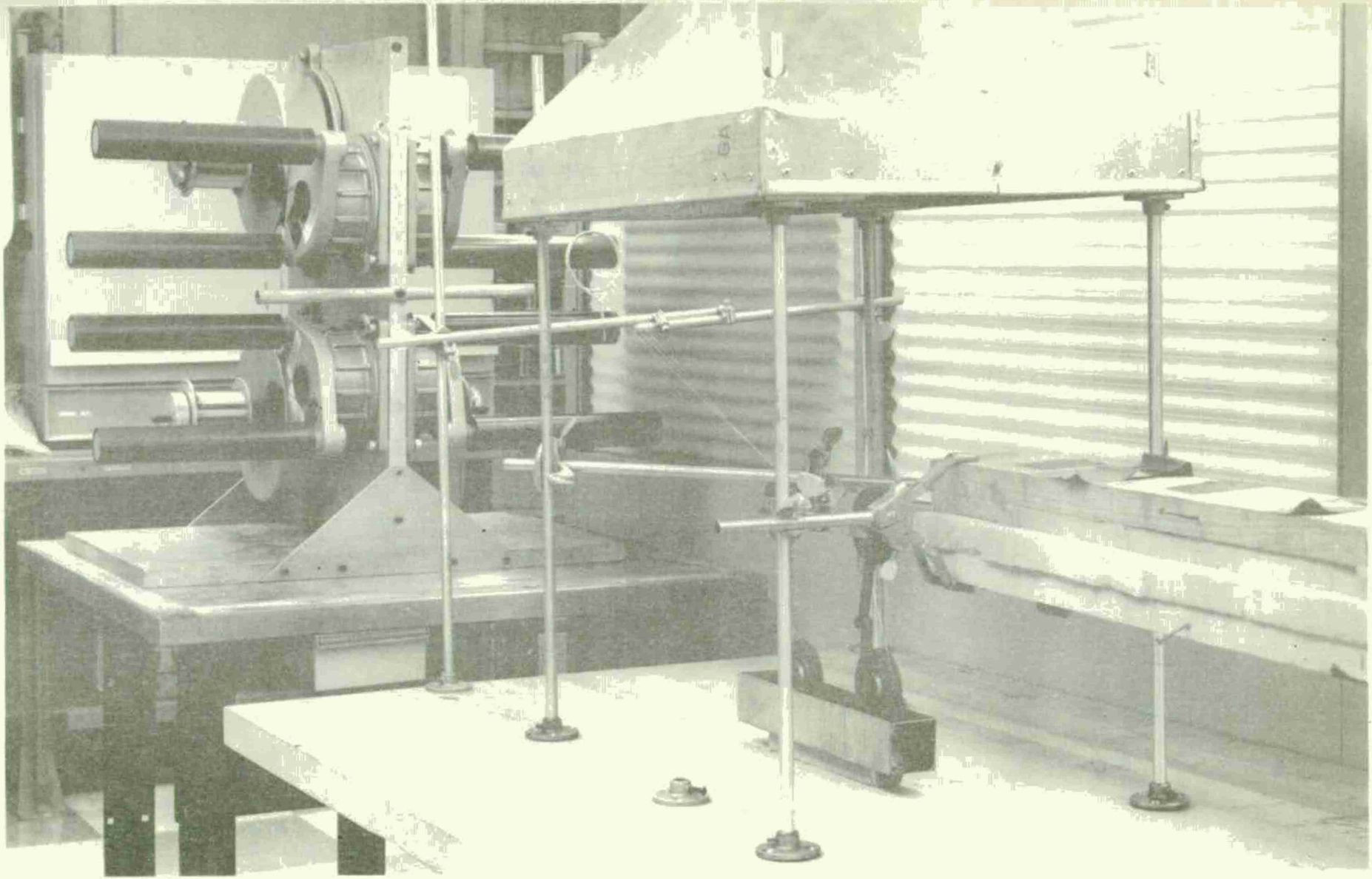

Figure 4. View of Solvent-Wipe Cleaning Process. Wires are Run Through Solvent Bath and Wiped on Foam Pads on Their Way to the Winder. An Exhaust Hood is Shown Mounted Over the Bath.

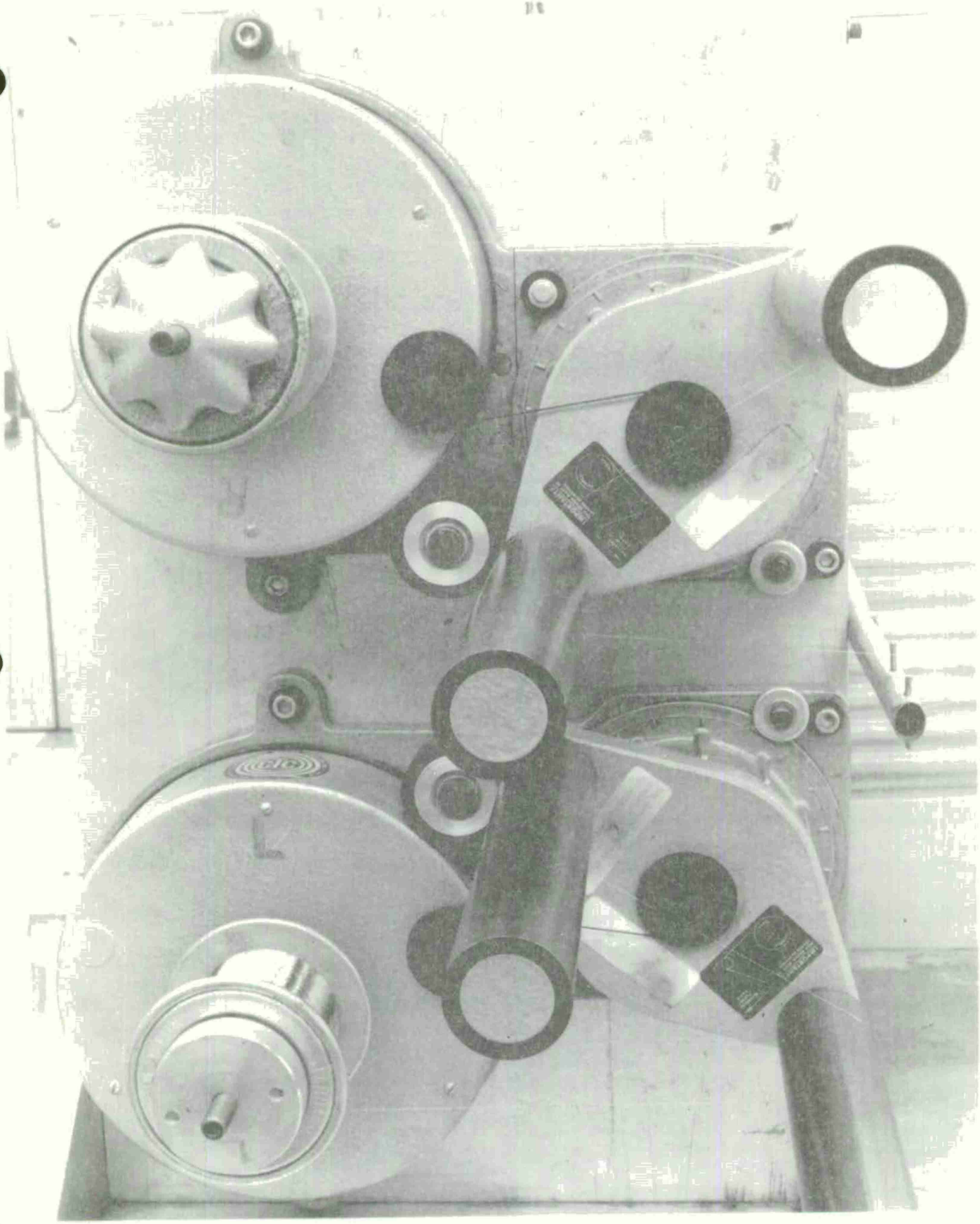

Figure 5. Close-Up of the Tensioning Devices Used to Set a Pre-Load on Individual Spools. The Compensating Rollers Take up any Slack and Maintain the Desired Load.

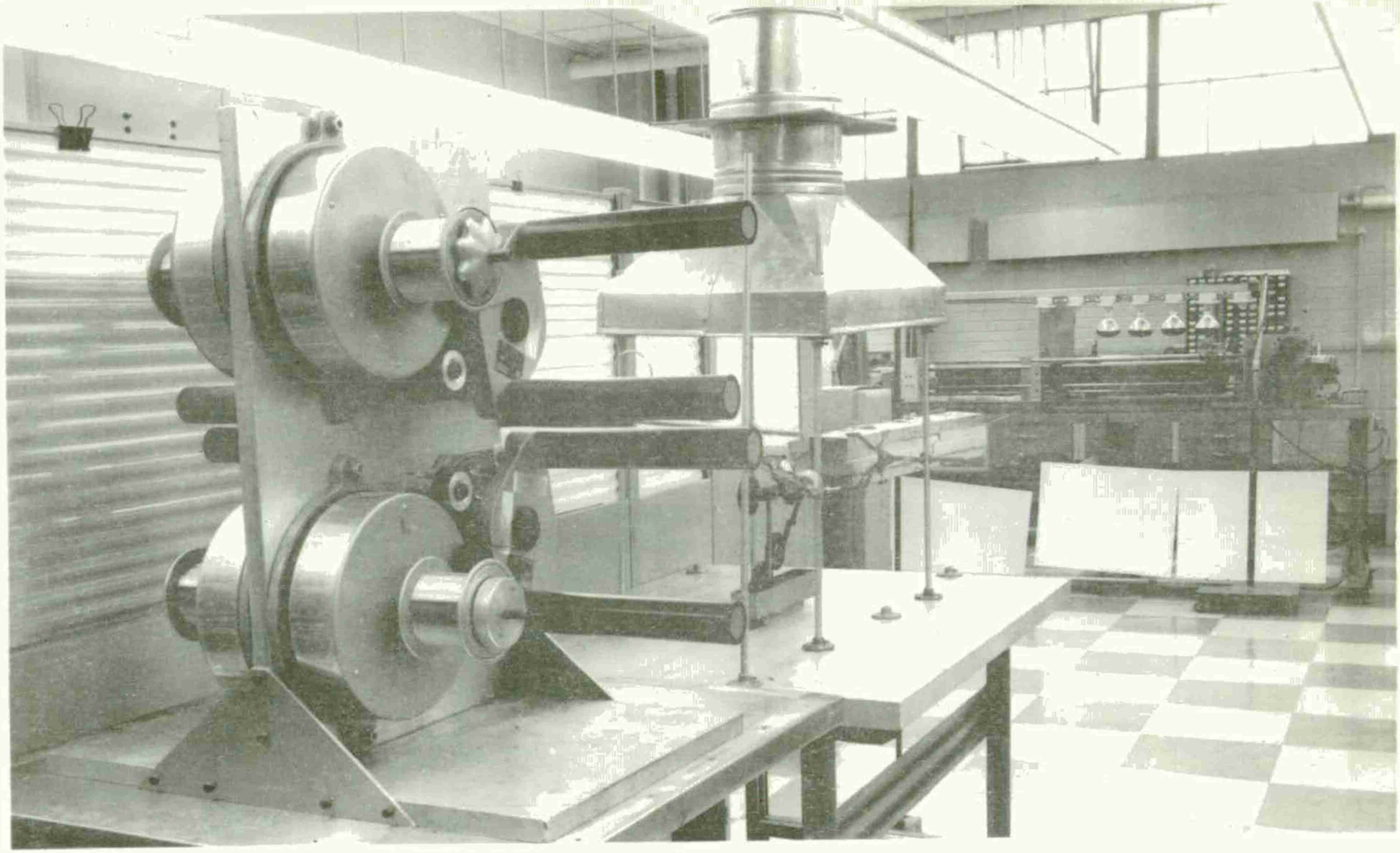

Figure 6. View of Stand with Four Tension Devices Mounted. Distance from Wipes to Winder was 16 feet to Facilitate Drying of Wire.

groove (top and bottom of rifling) diameters was modified for this work (Fig 7).

The gage head consists of two separate air actuated probes (90° apart) as shown in Fig 8. These probes for the rifling and bore are calibrated with the master, and this standard is noted on the air column. The gage is then inserted into the cylinders and readings are recorded at various locations throughout the bore. These readings are taken from the calibrated air columns and are recorded as ± thousandths of inch deviation from the standard.

Utilizing the air gage, a technique was developed to monitor the deflection (at one specific location in the tube) throughout the winding operation. One of the aluminum end caps used to support and drive the cylinders during winding was modified to allow the air gage to be mounted and held rigidly in the tube. The other end cap was bored out in the center to allow for the exit of the gage's air lines. "Quick disconnect" connectors allowed for the easy connection of these air lines to those that ran to the air column. After every layer was wound, the increased deflection of the liner, at a point 12.5" (mid-point) down the tube was measured. A view of this air gage assembly is shown in Fig 9 while Fig 10 is a view of the assembled cylinder with the air gage apparatus.

Composite Cylinders

The actual winding and recorded deflection data for each of the four cylinders are shown in Appendix A. The filament volume ratio of the four cylinders was calculated to be 75%.

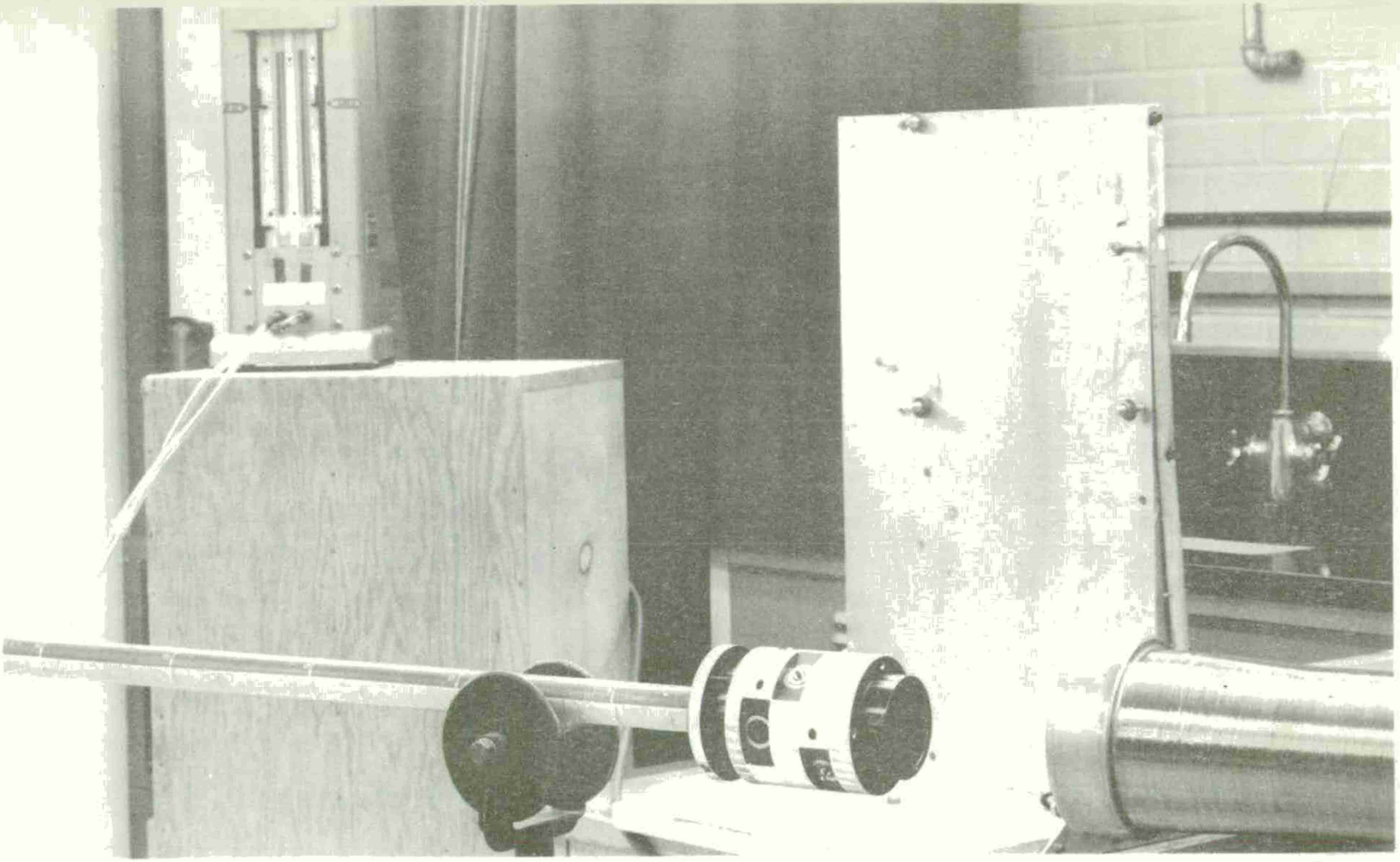

Figure 7. Air Gage with Recording Air Column that was Used for I.D. Inspection of Cylinders Before and After Winding.

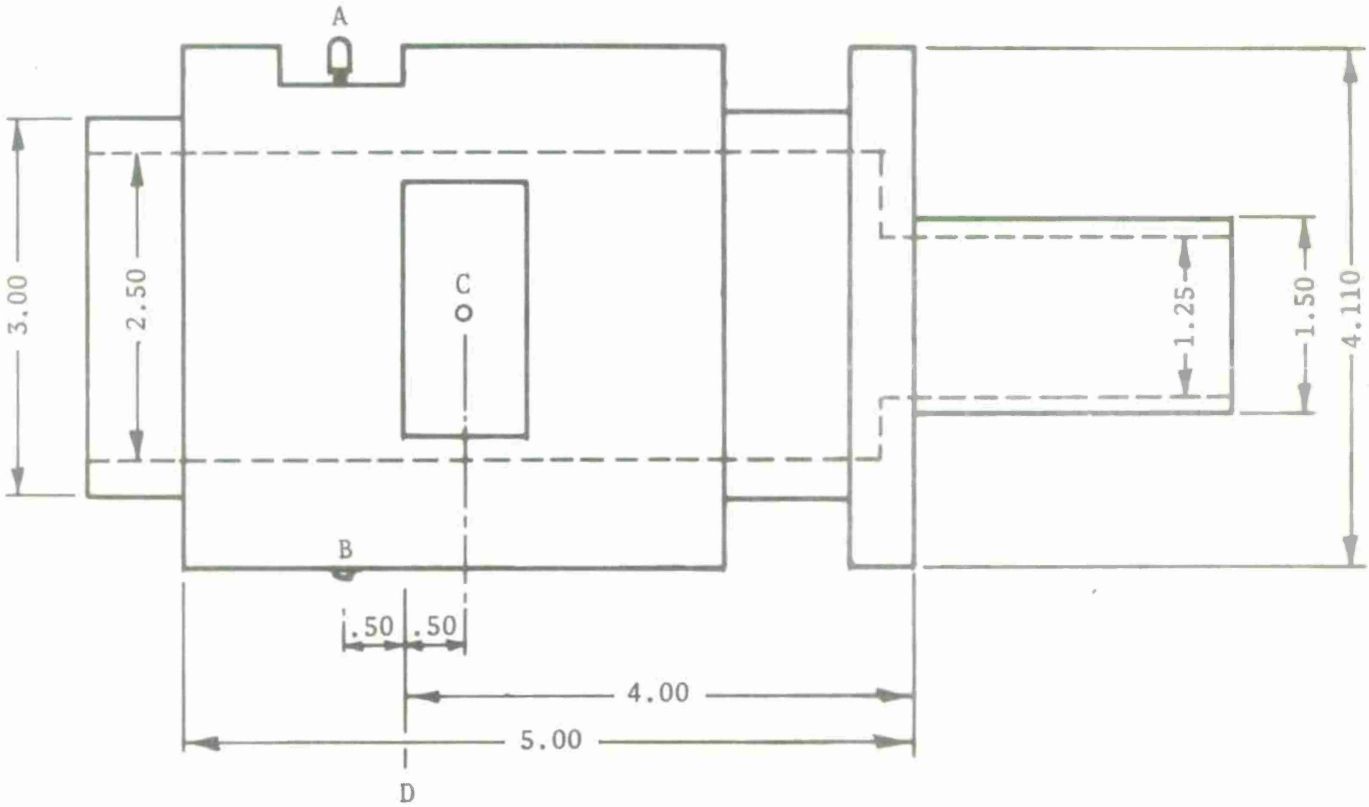

A = Rifling Probe
B = Rifling Button
} Leading Probe Which Measures The Diameter Of The Groove (Bottom) Of The Rifling

C = Bore Probe (Button Not Shown) — This Probe Measures The Land (Top) Of The Rifling

NOTE: The Bore Probe Is Measuring A Diameter Which Is 90° From The Diameter Being Measured By The Rifling Probe

D = Mid-Point — (The Point From Where The Travel Distances Are Measured.) This Puts The True Location Of The Rifling Probe + .50" Further And The Bore Probe -.50" Behind.

FIGURE 8. Sketch Of Air Gage Head

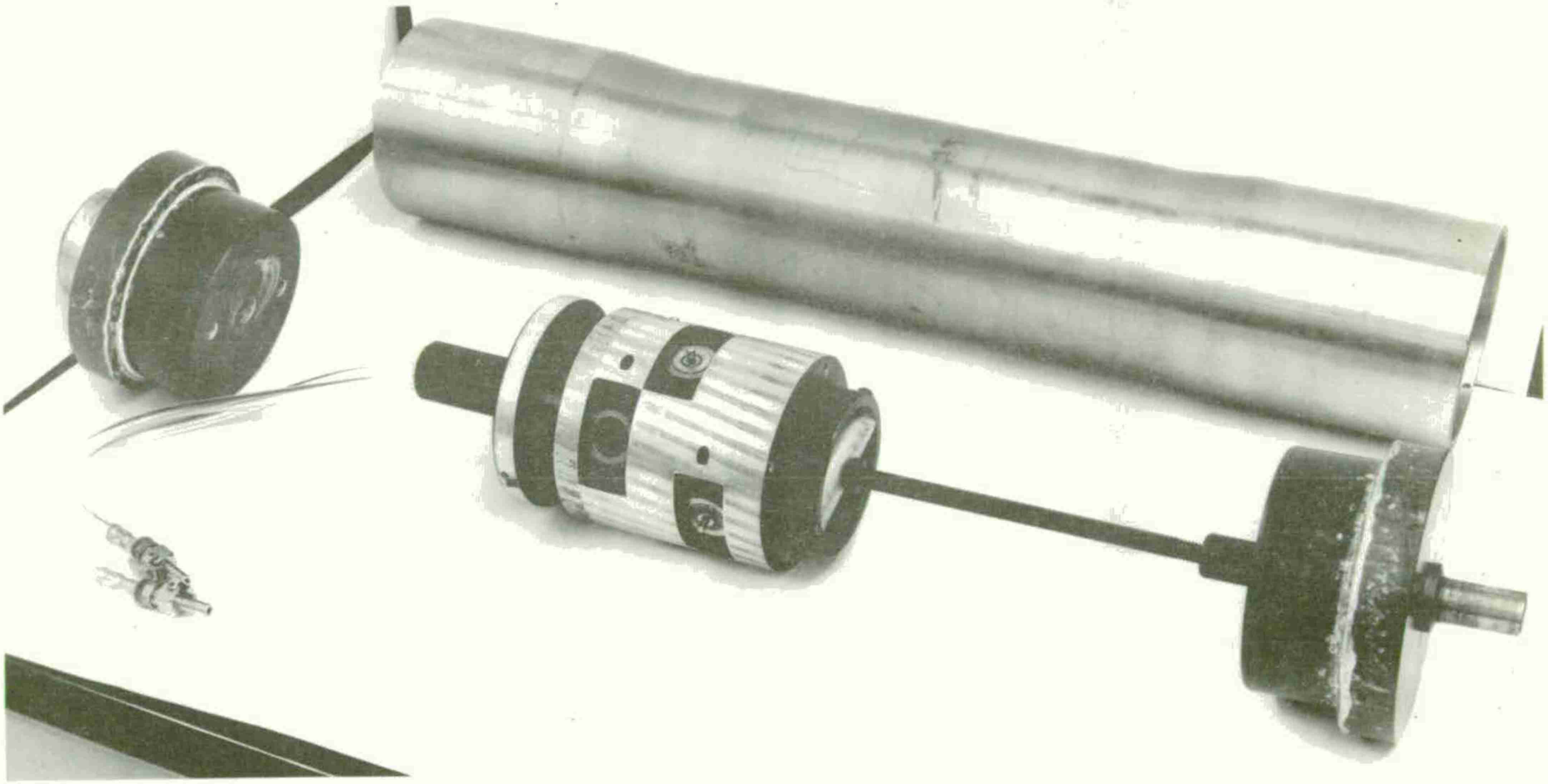

Figure 9. Modified Air Gage Assembly Used for Deflection Measurement During Winding.

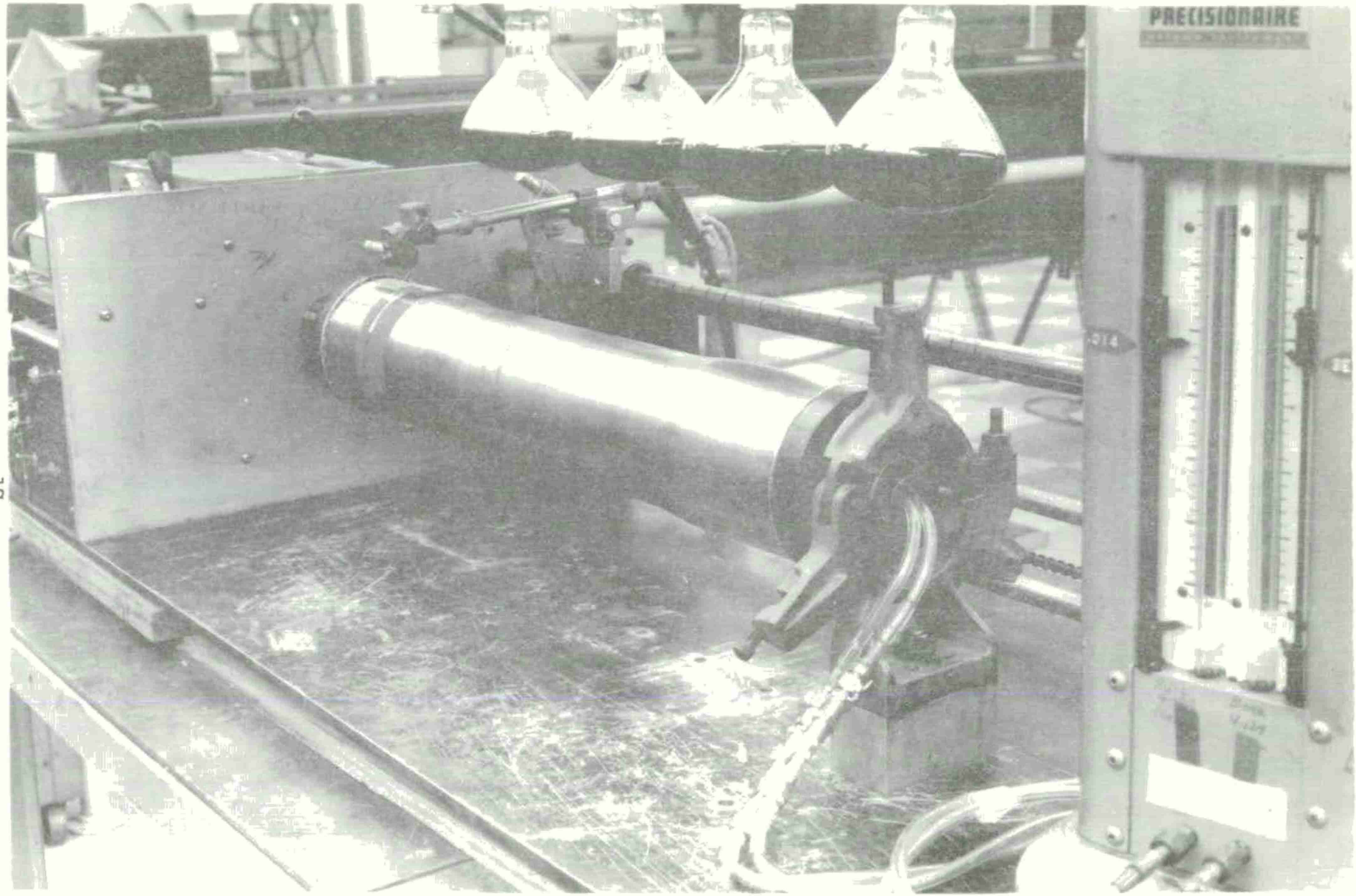

Figure 10. Close-up of Cylinder in Winder Showing Leads from Internal Air Gage to Recording Air Column

The curing cycle for all four cylinders was similar. The wound cylinder was gelled in the winder under four I. R. lamps for 3 hours; was allowed to cool overnight to room temperature and the entire internal diameter profile was measured. After these readings were taken (Fig 11), the cylinder was placed in the oven, brought to a temperature of 350°F. (for approximately an hour) and allowed to cure at this temperature for 2 hours.

OCL-4

This composite cylinder was designed for a pressure of 19.0 ksi. The liner has a minimum wall thickness of 0.047" in the gage area. It was wound with 17 layers of steel wire/epoxy at an average laydown of 161.9 ends/in/layer. The tension of the wire, at the mandrel, was maintained at 3.8#/end. The final diametrical deflection of this tube at the mid-point was -.015" after 17 layers.

OCL-6

This composite cylinder was also designed for 19.0 ksi burst. The liner wall was 0.075" thick. It required 15 layers of the steel wire/epoxy overwrap at an average of 161.7 ends/in. Winding tension was maintained at 3.8#/end. Final mid-point diametrical deflection of this cylinder was -.0115" after the 15 layers.

OCL-10

This composite cylinder was designed for 19.0 ksi burst. The liner wall was 0.100" thick in the gage area. It required 13 layers of overwrap at an average of 157.5 ends/in. Winding tension was again maintained at 3.8#/end throughout the winding. Maximum diametrical deflection after the 13 layers was -0.0085".

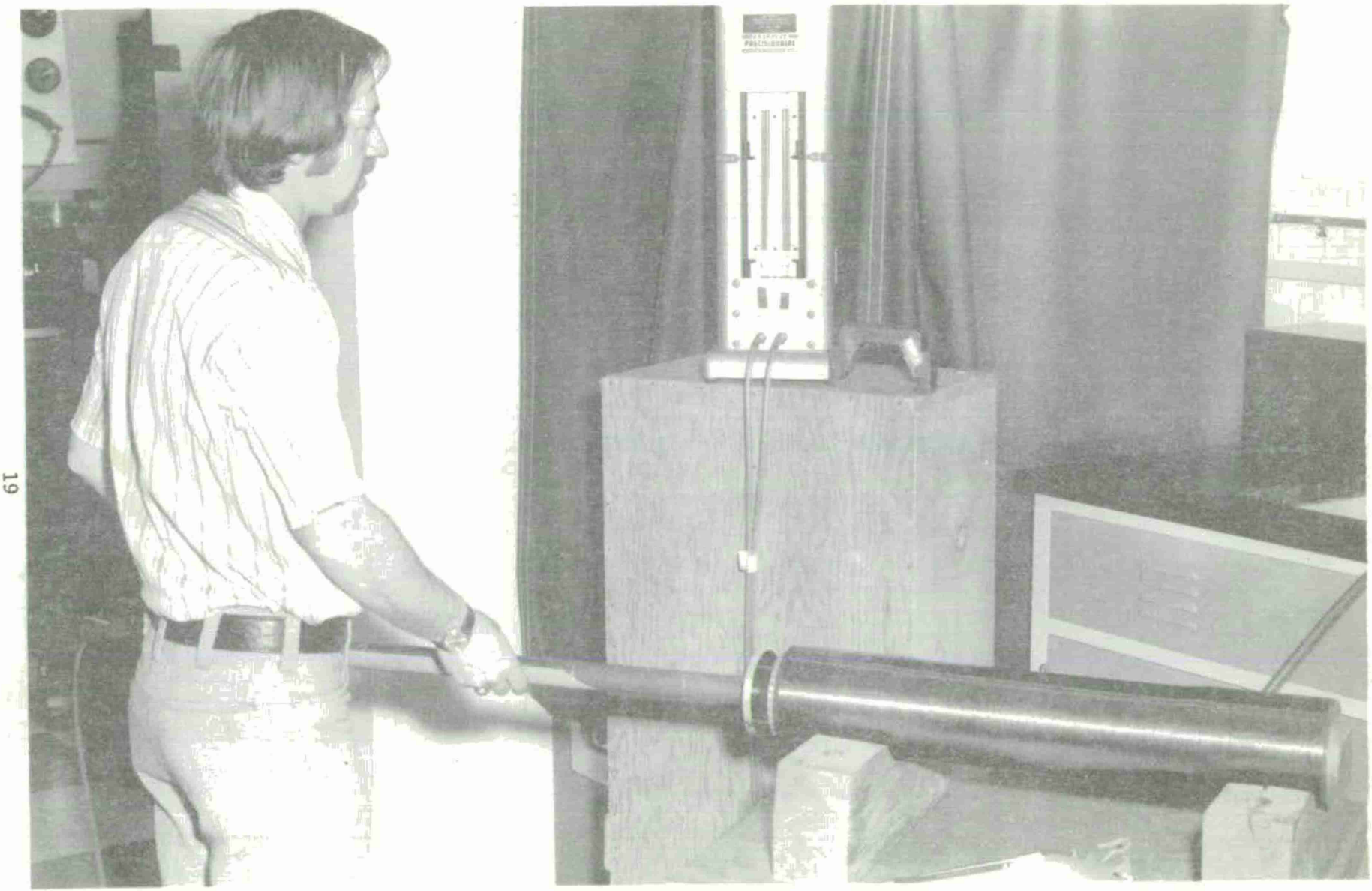

Figure 11. Standard Technique Used to Measure I.D. Profile of Test Cylinders Before Winding, After Gel and After Cure.

OCL-7

This was an additional cylinder with 0.100" liner wall thickness. It was designed for 20 ksi burst and had 14 layers of the composite overwrap.

A winding tension of 3.8#/end was used and final diametrical deflection was -.009" at the mid-point. The average ends/in for this winding was 158.7

Table 4 lists the outside and inside dimensions of the four composite cylinders, and Appendix C lists their I.D. profiles.

THEORY

The primary effects of the tension in the filaments which take place during the uncured state are:

A. The Mandrel Deflection.

B. A resin squeeze-out during winding and after winding up to Gel.

C. A resin shrinkage which takes place from Gel to Full Cure.

D. A differential thermal expansion effect during the curing.

A. Mandrel Deflection Effect

During the winding operation the mandrel will deflect as layers of filaments are wound successively. The deflection of the mandrel is proportional to the number of layers and the stiffness of the material below the layers.

The following analysis considers the pressure applied by each layer as transmitted directly through the mandrel as the layer is wound; this causes the mandrel to deflect and simultaneously relieve tension in all layers except the one being wound. Compatibility and

TABLE 3. PHYSICAL, CHEMICAL, AND MECHANICAL PROPERTIES OF "GUN STEEL"

CHEMICAL		MECHANICAL	
C	.30 - .40	Min Yield Strength (.1% offset)	160,000 psi
Mn	.50 - .90		
P	.015		
S	.015	Min Impact Strength (-40°F "V" - CHARPY)	15 ft-lb
Si	.15 - .35		
Ni	2.75 - 3.25		
Cr	.75 - 1.20	Elastic Modulus	30×10^6 psi
Mo	.45 - .60		
V	.08 - .13		

PHYSICAL

Density (lb/in^3) - .283

Thermal Expansion Coefficient (in/in/°F) - 6.3×10^{-6}

TABLE 4. DIMENSIONS AND DESIGN DATA OF COMPOSITE CYLINDERS

Cylinder	A	B	BO	PA
OCL-4	2.105	2.154	2.256	19000
OCL-6	2.105	2.177	2.267	19000
OCL-7	2.105	2.205	2.289	20000
OCL-10	2.105	2.205	2.283	19000

A = Bore radius (in), B = Liner radius (in)

BO = Jacket radius (in); PA = Max Internal Pressure

equilibrium equations are used to determine this deflection. Considering Figure 12 and the following notation, it can be proved that the final pressures applied by the layers to the mandrel for an arbitrary number of layers can be depicted in a matrix form.

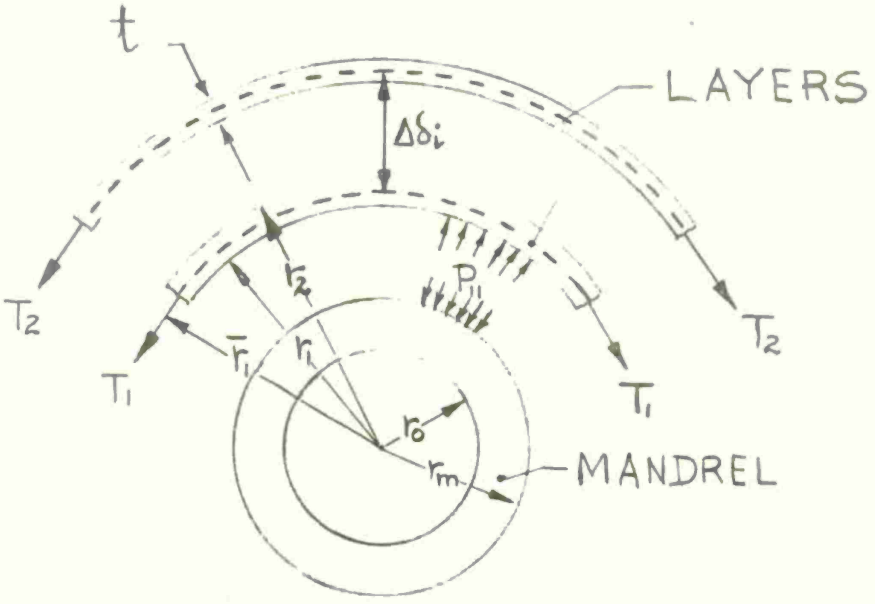

Figure 12. Schematic View Of Pressure Applied By The Layers To The Mandrel

Ti = Layer tension (#) per inch of width for layer (i)

Ri = radius to centerline of layer (i)

Rm, Ro = mandrel outside and inside radii

Pi = pressure applied by any layer (i) at the outer radius of the mandrel during winding of the layer

$\bar{P}i$ = pressure applied by any layer (i) at its own center line during winding

ν = Poisson's ratio

t = material thickness

E = modulus of elasticity

ϵ = unit strain

f = subscript referring to filament

m = subscript referring to mandrel

r = subscript referring to "reduced"

Example:

If one hoop layer of steel filament (one inch wide) under tension Ti is wound on the 106mm liner, it exerts a pressure on the liner of Ti/Rm, and undergoes a strain

$$\epsilon_f = \frac{\sigma_f}{E_f} = \frac{P_1 R_1}{t_f E_f} \tag{1}$$

and the mandrel undergoes strain

$$\epsilon_{m_1} = P_1 K_o \tag{2}$$

where

$$K_o = \frac{1}{E_m}\left[\frac{R_m^2 + R_o^2}{R_m^2 - R_o^2} - \nu_m\right]$$

and

$$\bar{P}_i = P_i \frac{R_m}{R_i} \tag{3}$$

If a second layer is then wound:

$$\epsilon_{m_2} = \left(P_2 + P_{r_1}\right) K_o \tag{4}$$

where

P_2 is the additional pressure applied to the mandrel, and

Pr_1 is the pressure P_1 reduced by P_2

The radial deflection of the mandrel is then

$$(\epsilon_{m_2} - \epsilon_{m_1}) R_m = (\epsilon_1 - \epsilon_{r_1}) R_1 \tag{5}$$

but

$$\epsilon_{r_1} = \frac{P_{r_1} R_1}{t_f E_f} \tag{6}$$

Then using (1), (2), (4), and (6) into (5) we obtain:

$$K_o (P_2 + P_{r_1} - P_1) R_m = \left(\frac{P_1 R_1}{t_f E_f} - \frac{\bar{P}_{r_1} R_1}{t_f E_f} \right) R_1$$

or

$$P_{r_1} = P_1 - P_2 \left(\frac{1}{1 + \frac{a_1}{K_o}} \right) \tag{7}$$

when

$$a_1 = \frac{R_1}{t_f E_f}$$

and the total pressure applied to the liner is

$$P_{m_2} = P_2 + P_{r_1} \tag{8}$$

For an arbitrary number of layers, it can be shown that the final pressure equations can be represented in the following matrix form:

N = 1	N = 2	N = 3	N = 4	N = 5 ---	N = n
P_1	$Pr_{1,1}$	$Pr_{1,2}$	$Pr_{1,3}$	$Pr_{1,4}$ ---	$Pr_{1,(n-1)}$
	P_2	$Pr_{2,1}$	$Pr_{2,2}$	$Pr_{2,3}$ ---	$Pr_{2,(n-2)}$
		P_3	$Pr_{3,1}$	$P_{r3,2}$ ---	$Pr_{3,(n-3)}$
			P_4	$Pr_{4,1}$ ---	$Pr_{4,(n-4)}$
				P_5 ---	$Pr_{5,(n-5)}$
					↓
					Pn

when N = total number of layers

(9)

where

(1) the first subscript of the reduced pressure is the layer number and the second number is the number of times the original pressure as applied has been reduced.

(2) The total pressure applied to the mandrel surface is the sum of all pressures appearing under the appropriate N, for instance for N = 5

$Pm_5 = P_5 + P4_{4,1} + Pr_{3,2} + Pr_{2,3} + Pr_{1,4}$

(3) The reduced pressure for the next to outside layer is

$$P_{r(J-1),1} = P_{(J-1)} - \frac{P_J}{\left[1 - a_{(J-1)}\left(\frac{1}{a_1} + \frac{1}{a_2} + \cdots \frac{1}{a_{(J-2)}} + \frac{1}{K_o}\right)\right]}$$

where:

$$J = 2 \text{ to } n \tag{10}$$

$$a_i = \frac{R_i}{t_i E_i}$$

$$K_o = \frac{1}{E_m}\left[\frac{R_m^2 + R_o^2}{R_m^2 - R_o^2} - \nu_m\right]$$

Note that the only inputs required are the original winding pressures $\left(\frac{T_i}{R_m}\right)$, and the layer and mandrel stiffnesses.

(4) The remaining pressure can be determined from:

$$P_{r_{L,K}} = P_{r_{L,(K-1)}} - \frac{Z_J}{a_L} \tag{11}$$

for

$$3 \leq J \leq n$$

$$2 \leq K \leq J-1$$

$$L = J - K$$

or

$$3 \leq J \leq n$$

$$1 \leq L \leq J-2$$

$$K = J - L$$

and

$$Z_J = \left[a_{(J-1)}\right] \cdot \left[P_{(J-1)} - P_{r(J-1)}\right] \quad \text{for } J = 3 \text{ to } n \tag{12}$$

Once the total pressure is determined then the mandrel strain at Rm can be found, i. e.,

$$P_n = \frac{1}{R_m} \sum T_i \tag{13}$$

$$\delta_m = \frac{P_n R_m}{E_m} \cdot \left[\frac{R_m^2 + R_o^2}{R_m^2 - R_o^2} - \nu_m\right] = P_n R_m K_o$$

or

$$\delta_m = K_o \sum T_i \tag{14}$$

and

$$\epsilon_m = \delta_m / R_m \tag{15}$$

The changes in tension, after winding, is then, directly related to the radial displacement, thus

$$\Delta T_i = T_1 - T_2$$

or

$$\Delta T_i = \frac{\Delta \delta_i}{B_i} \tag{16}$$

where

$$B_i = \frac{R_i}{K_i t_i E_f}$$

This relationship predicts the change in tension for a given radial deflection and layer properties.

This analysis was programmed in TENZIONE, and provision was made to compare graphically test and theory by having as input the actual deflection data monitored during fabrication.

B. Resin Squeeze-Out

A hoop or helical layer, when wound has a resin volume ratio. This ratio is controlled by the manufacturer of the filaments (if a pre-preg spool is used), or by a particular wet-winding set-up. As more layers are wound the resin content will change, this is mostly due to winding under tension. If Ωi represents the resin volume ratio than the change in layer thickness.

$$\Delta t_i = t_i (1-K) \Omega i \tag{17}$$

To obtain the total effect, it can be easily seen that

$$\Delta \delta_i = \left(\frac{\delta i}{2} + \delta_{(i-1)} + \delta_{(i-2)} + \cdots + \delta_1 \right) \tag{18}$$

where

$$\delta_i = \Delta t_i \tag{19}$$

Equation 18 assumes that the filament of the layer considered can move only 1/2 the distance of its own change in thickness, and the equation can be integrated if Ωi is known through the thickness of the laminate. Once $\Delta \delta i$ is found the effect of resin squeeze-out on the tension is found by substituting $\Delta \delta i$ into equation (16).

Example:

Assuming an "n" layer laminate having a triangular resin squeeze-out distribution (Fig 13) or:

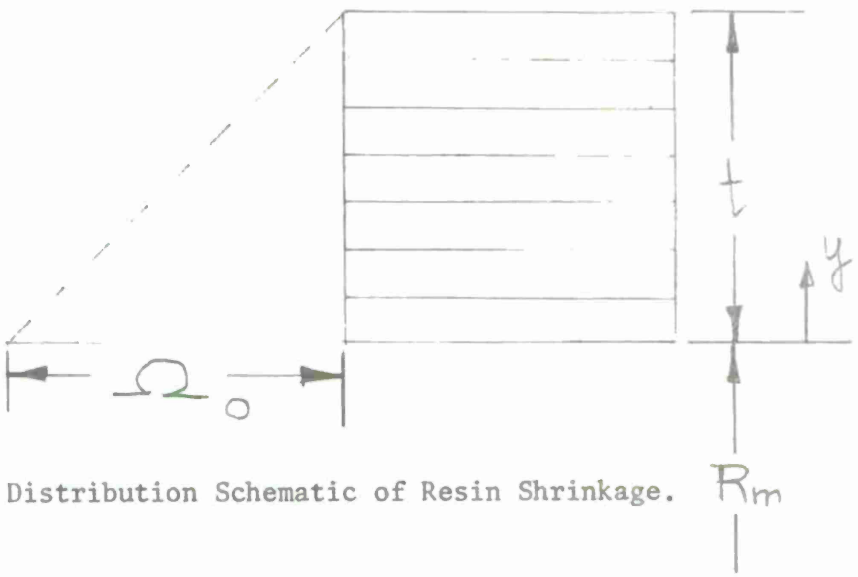

Figure 13. Distribution Schematic of Resin Shrinkage.

$$\Omega = \Omega_o \left(1 - \frac{y}{t}\right)$$

and

$$\delta_i = t_i \left(1 - K\right) \Omega \qquad \text{from 19}$$

then

$$d\delta_y = dy \left(1 - K\right) \Omega_o \left(1 - \frac{y}{t}\right)$$

and

$$\Delta\delta_y = \sum d\delta_y \qquad \text{from 18}$$

then

$$\Delta\delta_y = \Omega_0 (1-K) \int_0^y \left(1 - \frac{y}{t}\right) dy \qquad (20)$$

C. Resin Shrinkage

Resin shrinkage takes place at gel up to the full cure. The percent of shrinkage can be analyzed by placing strain gages on the mandrel or liner.

Consider the whole jacket as a unit layer which will shrink to a radial displacement δ_s (Figure 14); then the following expression would apply, i. e.,

$$\delta_s = t \cdot (\text{resin shrinkage}) \cdot (\text{matrix volume ratio}) \qquad (21)$$

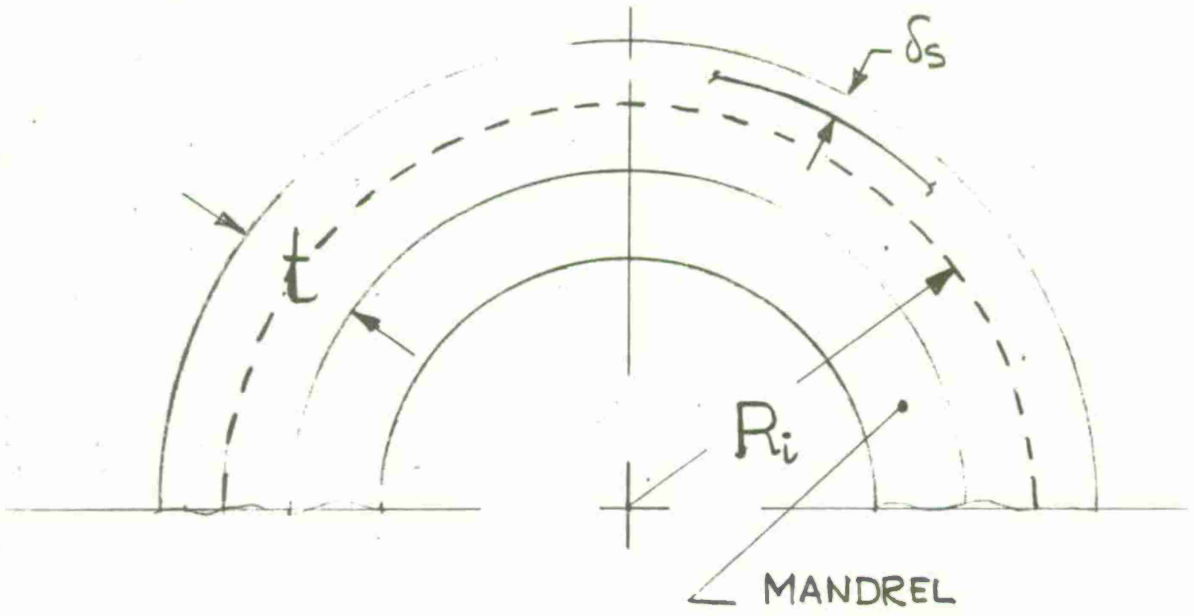

Figure 14. Schematic of Radial Displacement Caused by Resin Shrinkage.

then

$$\text{Resin Shrinkage} = \frac{\Delta\delta}{t(1-K)} \tag{22}$$

where $\Delta\delta$ = Total deflection after winding -

and

t = (filament diameter) (number of layers)

Example:

Cylinder A had a total deflection (after winding) of .005; after gel the δ_s was measured to be .0041, then

$\Delta\delta$ = .0009, t = .048, K = .75

or

$$\text{Resin Shrinkage} = \frac{9 \times 4}{(4.8)} \times 10^{-2}$$

$$= .075$$

The average resin shrinkage in the six 106mm test specimens is $\approx$ 4%. This effect, then, relieves the filament tension as it follows:

Assume Ω_s is constant throughout the thickness then

$$d\delta_y = dy\,(1-K_y)\,\Omega_s \tag{23}$$

In this case the filament content (ky) is considered a variable due to differential resin squeeze out through the thickness. Thus, after the resin squeeze-out

$$K_y = \frac{K}{1-\Omega(1-K)} \tag{24}$$

where Ω is the volumetric change in resin at any point, and K the initial filament volume.

Recall, from the Resin Squeeze-out analysis, that

$$\Omega = \Omega_0 \left(1 - \frac{y}{t}\right) \tag{25}$$

therefore

$$K_y = \frac{K}{1 - \Omega_0 \left(1 - \frac{y}{t}\right)(1-K)} \tag{26}$$

or

$$\Delta\delta_y = \Omega_s \int_0^y (1 - K_y)\, dy \tag{27}$$

$$= \Omega_s \left[y - \int_0^y K_y \, dy \right]$$

the integral when reduced to the form of

$$\int_0^y \frac{dy}{a+by} = -\frac{1}{b} \ln a + \frac{1}{b} \ln (a+by) \tag{28}$$

gives a

$$\Delta\delta_y = \Omega_s \left[y + \frac{K}{b} \ln a - \frac{K}{b} \ln (a+by) \right]$$

where

$$a = 1 - \Omega_0 (1-K) \; ; \; b = \frac{\Omega_0 (1-K)}{t} \tag{29}$$

D. DIFFERENTIAL THERMAL EXPANSION

This effect takes place during the curing process. Assuming that the liner or mandrel is rigid during the temperature rise to cure then

$$\delta_m = R_m \alpha_m \Delta T \tag{30}$$

and at the same time, the composite layers will deflect

$$\delta = R_i \alpha_c \Delta T \tag{31}$$

The difference in the two is then equal to the added radial deflection which the filaments must experience, thus:

$$\Delta \delta_i = \Delta T \left(R_m \alpha_m - R_i \alpha_c \right) \tag{32}$$

Note that α_c is the coefficient of thermal expansion of the composite, i.e. : filament plus matrix.

Tension After Curing

Effects considered in previous analyses assumed a rigid mandrel. Now these effects must be superimposed to find a final mandrel deflection at cure which in turn gives a final tension distribution through the composite.

Let Ti be the tension in a layer "i" due to all effects prior to cure while considering the mandrel rigid, then

$$\bar{P}_i = \frac{T_i}{R_m} \tag{33}$$

is the pressure applied to the mandrel by each layer and

$$P_{im} = \sum_{1}^{N} \bar{P}_i \tag{34}$$

represent pressure on the mandrel under rigid condition.

To set the mandrel in equilibrium with the jacket, the mandrel deflection

$$\delta_m = K_o R_m P_m \tag{35}$$

but

$$P_m = \sum_{1}^{N} \left(\bar{P}_i - \Delta \bar{P}_i \right) \tag{36}$$

where

$\Delta \bar{P}_i$ is the pressure lost due to deflection,

The corresponding tension change in a layer for a $\Delta \bar{P}$ at the liner is:

$$\Delta \bar{P}_i = \frac{\Delta T_i}{R_m} \tag{37}$$

Also, it has been shown that δ_m will cause ΔT equal to δ_m / B_i

Thus $$\Delta \bar{P}_i = \frac{\delta_m}{B_i R_m}$$

or

$$P_m = \sum_{1}^{N} \left(\bar{P}_i - \frac{\delta_m}{B_i R_m} \right) = \frac{\delta_m}{K_o R_m}$$

since $\bar{P}_i = T_i / R_m$

$$\delta_m = K_o \sum_1^N \left(T_i - \frac{\delta_m}{B_i} \right)$$

$$= \frac{K_o \sum_1^N T_i}{1 + K_o \sum_1^N \frac{1}{B_i}}$$

knowing δ_m :

$$\Delta \bar{P}_i = \frac{K_o}{B_i K_m} \cdot \frac{\sum_1^N T_i}{1 + K_o \sum_1^N \frac{1}{B_i}}$$

and

$$\Delta T_i = \frac{K_o}{B_i} \cdot \frac{\sum_1^N T_i}{1 + K_o \sum_1^N \frac{1}{B_i}}$$

whereas

$$\Delta T_n = \frac{\Delta T_i}{n}$$

which represents the change in tension per end.

Parts A through D have been programmed in TENZIONE, and graphical results of particular configurations will be discussed next.

RESULTS AND DISCUSSION OF RESULTS

Computer Program "TENZIONE" provides the design engineer with the necessary tools to proceed with the minimum weight design of composite gun tubes. Recall that Computer Program "GANTU II" described in ref 1 assumes a plastic-elastic interface (ρ) in the liner and an optimum use of the composite jacket (i.e., the maximum contribution of the jacket to the liner strength is achieved when the stress at r=B satisfies the Hill's failure criterion for the jacket); "TENZIONE" allows the engineer, in practice, to realize these assumptions to achieve a minimum weight component.

"TENZIONE" INPUT:

Mandrel's:	Modulus of elasticity	=	EM
	Outside radius	=	RM
	Internal radius	=	RO
	Poisson's ratio	=	XNUM
	Coeff thermal expansion	=	ALPHF
Filament's	Modulus of elasticity	=	EF
	Thickness	=	TI
	Volume ratio	=	XKF
Other Parameters:	Resin squeeze out	=	OMEGA
	Resin shrinkage	=	OMEGS
	Ambient temp	=	TAMB
	Curing temp	=	TCURE
	Coeff of thermal exp of composite jacket	=	ALPHC
	Number of layers	=	N
	Tension of layer #1	=	TI
	Tension of layer N	=	TN

[1]Cullinan, R., et al, "Application of Filament Winding to Cannon and Cannon Components. Part I: Steel Filament Composites," April 1972, Watervliet Arsenal Technical Report WVT-7205.

"TENZIONE" OUTPUT

After Winding:	Diametrical change vs no. of layers Pressure on liner vs no. of layers
After Curing:	Diametrical change vs no. of layers Pressure on liner vs no. of layers Filament residual stress vs no of layers

The experimental results of winding operation are included in Table 5 which presents the uncured diametrical change of cylinders 4, 6, 7 and 10 as a function of the number of layers, and in Table 6 which presents the final deflections of the manufactured cylinders after the GEL and cure state.

These experimental results are then compared with the theoretical results from "TENZIONE". A sample output (OCL-7) is depicted in Figures 15 through 19, the other cases are included in APPENDIX B. Cylinders 4, 6, and 10 were designed to hold the same pressure, thus as we increase the thickness of the liner (i.e. from 0.05" to 0.10") we note a decrease in number of layers which in turn reduce the deflection in the liner as it can be seen in Table 6.

The discrepancy between theory-experiment can be best explained if Fig 17 is considered. In this case the theory assumes a smooth bore cylinder with a liner thickness of 0.0985" and a constant winding tension of 3.83 pounds. These two parameters are actually the controlling factors in obtaining the theoretical diametrical change vs number of layers.

In the real case we have a rifled liner, which contributed to the discrepancy, and a winding tension which is difficult to monitor.

If the winding procedure is reviewed, one finds that the tension

TABLE 5. DIAMETRICAL CHANGE OF COMPOSITE CYLINDERS VS NUMBER OF LAYERS (AFTER WINDING)

No. of Layers	OCL 4	OCL 6	OCL 7	OCL 10
1	12×10^{-4}	10×10^{-4}	5×10^{-4}	5×10^{-4}
2	25	20	15	15
3	35	30	20	25
4	45	35	30	30
5	60	45	40	35
6	70	55	45	45
7	80	60	50	50
8	90	65	55	55
9	95	75	60	60
10	105	80	70	65
11	111	90	75	70
12	115	100	80	75
13	122	105	85	85
14	125	110	90	
15	135	115		
16	140			
17	145			

TABLE 6. FINAL DIAMETRICAL CHANGE OF COMPOSITE CYLINDERS

	DEFLECTIONS	
	AFTER GEL	AFTER CURE
OCL 4	135×10^{-4}	125×10^{-4}
OCL 6	95	100
OCL 7	80	90
OCL 10	70	75

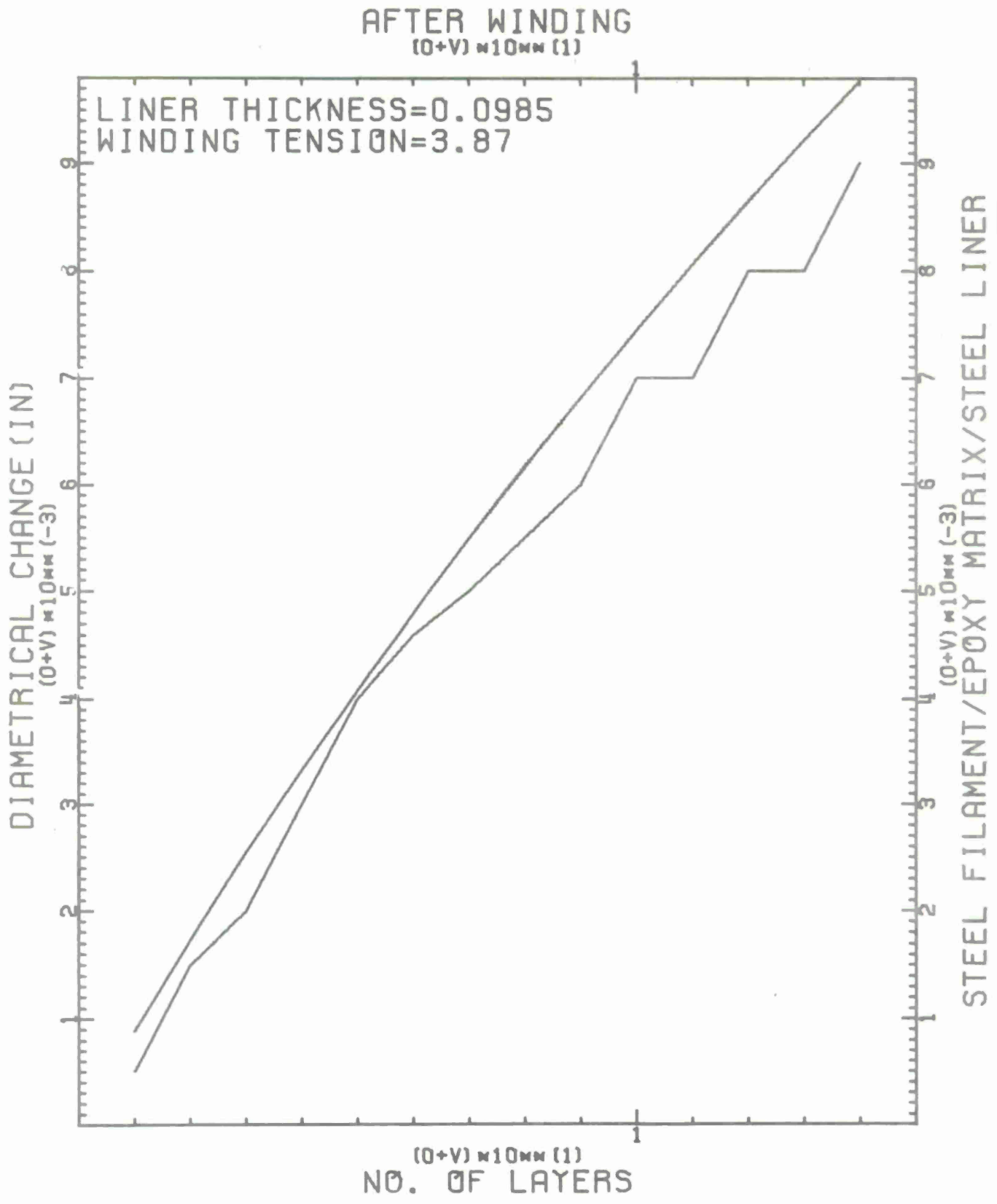

Figure 15. Deflection vs No. of Layers for OCL-7 (After Winding)

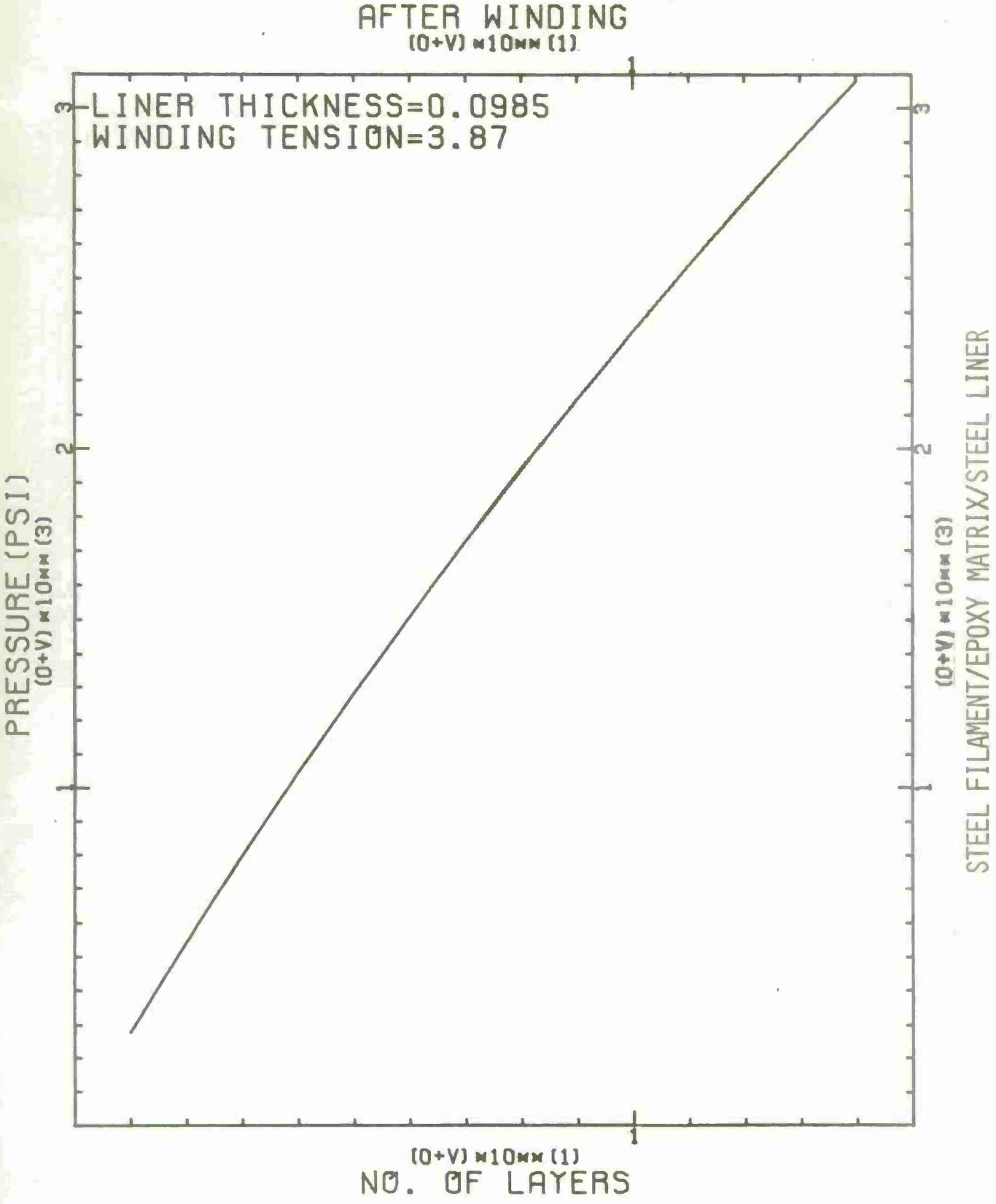

Figure 16. Compressive Liner Pressure for OCL-7 (After Winding)

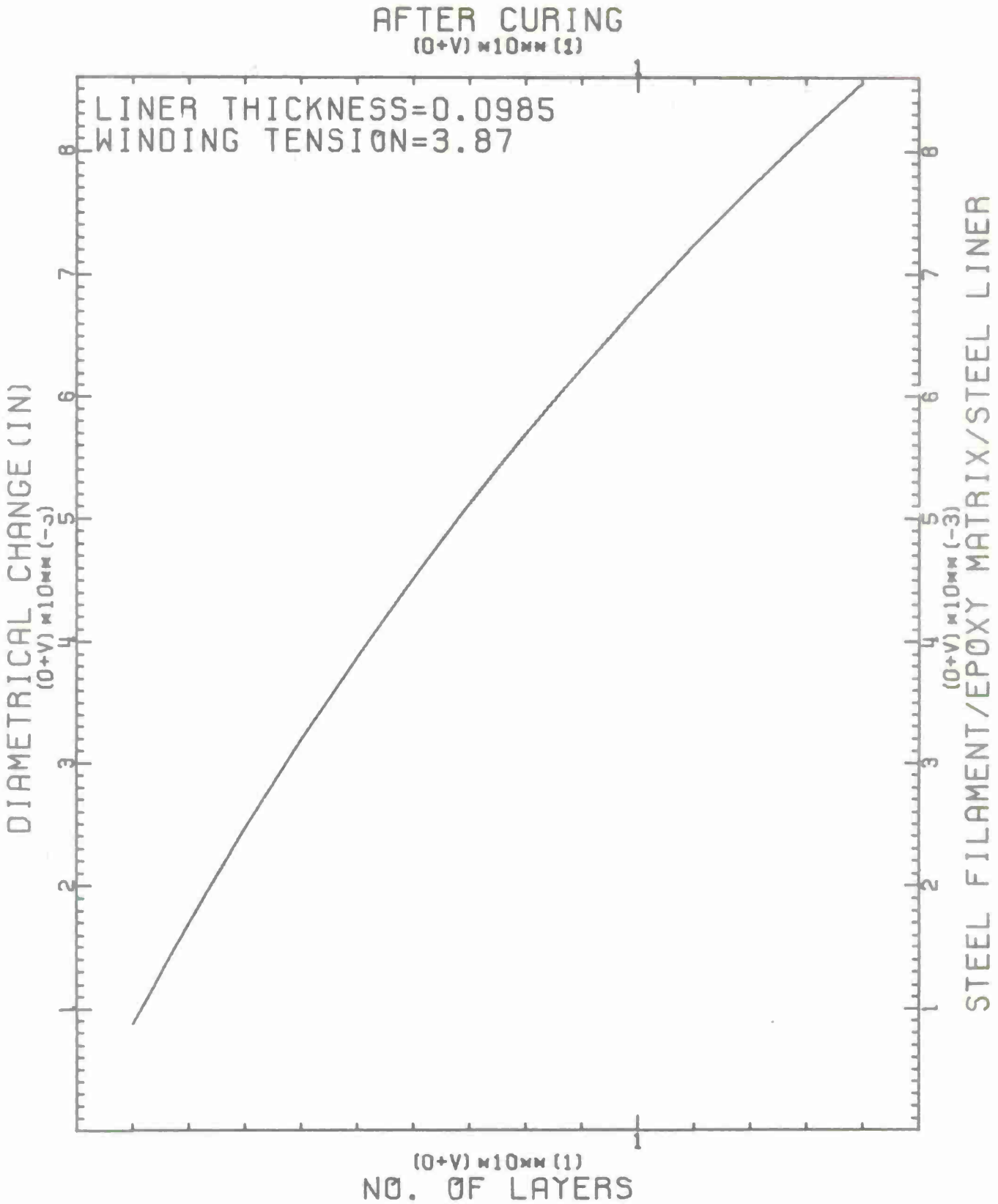

Figure 17. Deflection vs No. of Layers for OCL-7 (After Curing)

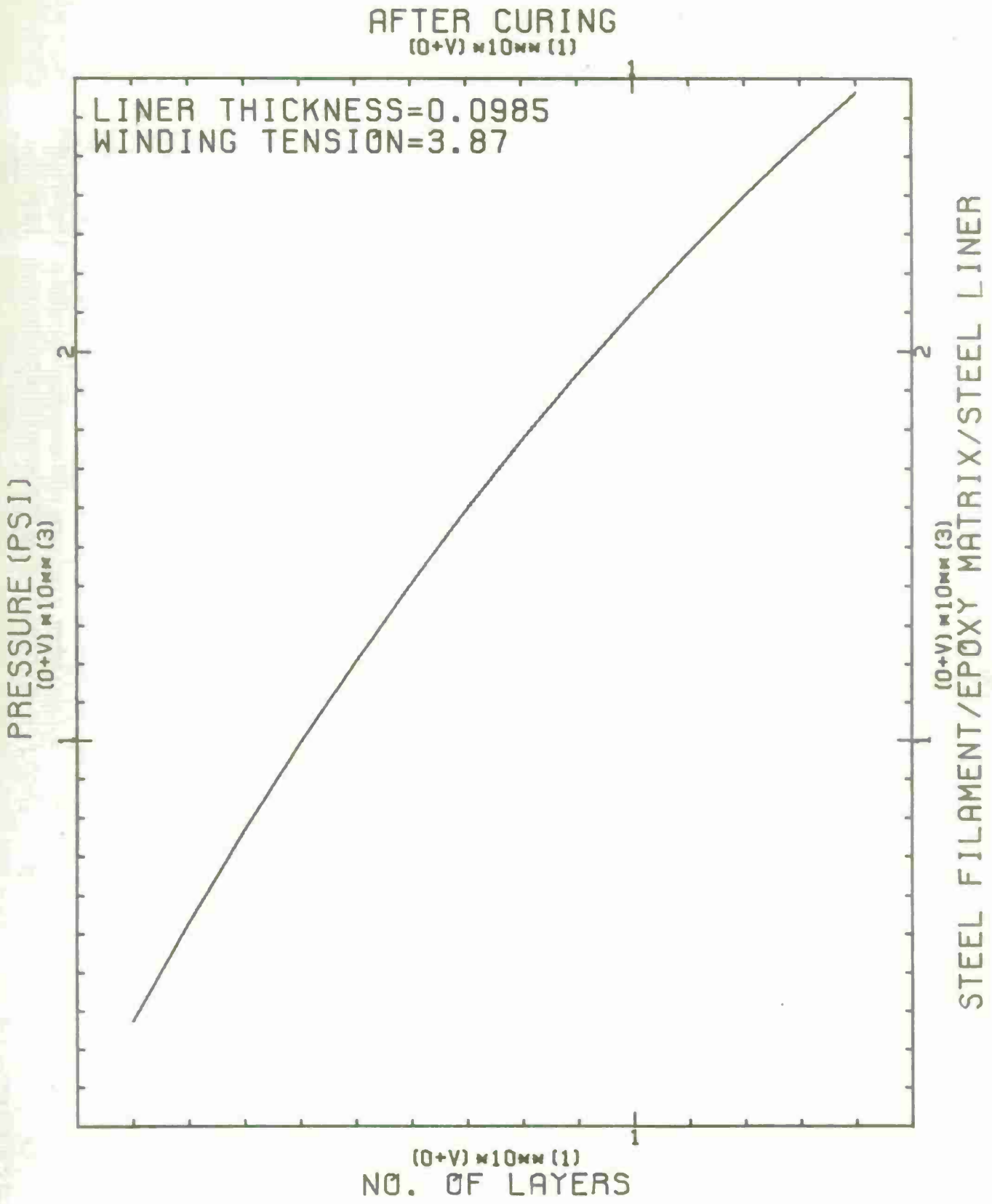

Figure 18. Compressive Liner Pressure for OCL-7 (After Curing)

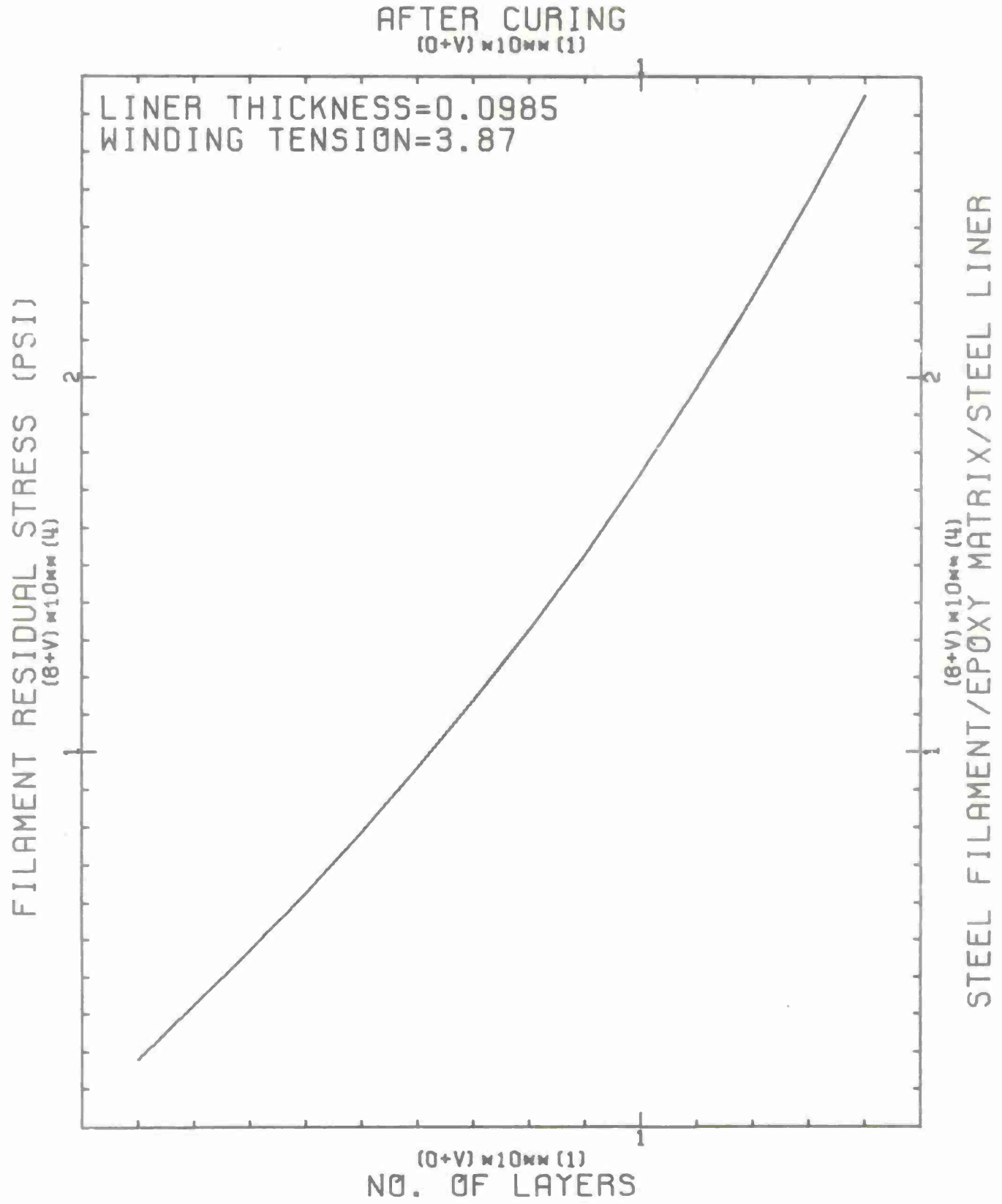

Figure 19. Induced Residual Stresses for OCL-7 (After Curing)

set in the "Constant Tension Device" is not necessarily the tension transferred onto the mandrel. Friction forces must be added because the filament goes through different pulley arrangements before it gets to the mandrel. These friction forces can be constant or varying depending on the set-up and kind of force measuring instrument used. In this project accuracy in measuring force on the mandrel is questionable since a "Fish-scale" type of scale was used. For an accurate reading, a device should be included in the delivery system which monitors tension constantly and also the tensioning devices themselves should provide ease of adjustment for predetermined tension distribution during the winding.

The residual stress analysis from "TENZIONE" has been successfully used in the wrapping of several axi-symmetric components. Perhaps the question which would arise from this work is: "how is this information used?"

The complete picture can be obtained if references 5, 6, and 7 are reviewed. The following example is presented to illustrate the usefulness of the program "TENZIONE". The cylinder which will be analyzed is

---

[5]D'Andrea, G., "Composite Cylindrical Pressure Vessels Related to Gun Tubes. Part I: Theoretical Investigation," September 1968, Watervliet Arsenal Technical Report WVT-6821.

[6]D'Andrea, G., "Composite Cylindrical Pressure Vessels Related to Gun Tubes. Part II: Minimum Weight Design," September 1971, Watervliet Arsenal Technical Report WVT-7125.

[7]D'Andrea, G. and Cullinan, R., "Development of: Design Analyses, Manufacturing and Testing of the 81mm XM73 Fiberglass-Epoxy Recoilless Rifle," June 1974, Watervliet Arsenal Technical Report WVT-TR-74014.

OCL-7, which was pressure cyled 10 times at 15,000 psi, 12 times at 20,000 psi, and then brought to rupture at a pressure of 21,900 psi. After the first 10 cycles at 15,000 ksi, the I.D. profile of the cylinder was again measured (as shown in Table 7) and there was no noticeable dimensional change.

Figure 20, obtained from GANTU II (Ref 5) shows the ideal hoop stress distribution of the OCL-7 composite cylinder when subjected to a pressure of 20,000 psi. At this pressure, the OCL-7 exhibits a tangential or hoop service stress A-A when the residual stresses of the form B-B are introduced in the structure. With these residual stresses, the cylinder will rupture simultaneously at the bore, liner-jacket interface and jacket outside diameter. Curve C-C represents the elastic stresses that would prevail if the cylinder were elastic under the action of the 20,000 psi pressure. (Curve C-C can also be obtained by adding curves A-A and B-B).

Figure 21 depicts the theoretical residual stresses as obtained from "TENZIONE" which is very close to the actual stresses induced during the manufacturing of the OCL-7 (see Figure 15). It is now obvious that with these (Fig 21) residual stresses, OCL-7 will not respond as originally designed (Fig 20).

To check the behavior of the manufactured cylinder under the action of an internal pressure, the following procedure is undertaken:

---

[5]D'Andrea, G., "Composite Cylindrical Pressure Vessels Related to Gun Tubes. Part I: Theoretical Investigation," September 1968, Watervliet Arsenal Technical Report WVT-6821.

Assuming the same yielding criteria used in obtaining Figure 20 and the residual stresses obtained from "TENZIONE", the limit pressure or the pressure that produces the first yielding can be found by investigating, separately, yielding at the bore, liner-jacket interface, and the jacket outside diameter. Appendix D shows procedure for obtaining the following

TABLE 7. INTERNAL DIMENSIONS OF OCL-7 BEFORE AND AFTER CURING

TRAVEL (IN)	AFTER CURE		AFTER CYCLING*	
	BORE	RIFLING	BORE	RIFLING
2.5	4.1320	4.2095	4.1330	4.2095
3.5	4.1325	4.2100	4.1330	4.2100
4.5	4.1325	4.2085	4.1330	4.2090
5.5	4.1310	4.2050	4.1320	4.2060
6.5	4.1275	4.2030	4.1290	4.2040
7.5	4.1260	4.2030	4.1270	4.2045
8.5	4.1265	4.2025	4.1280	4.2040
9.5	4.1270	4.2020	4.1275	4.2040
10.5	4.1265	4.2015	4.1275	4.2030
11.5	4.1265	4.2020	4.1270	4.2035
12.5	4.1270	4.2020	4.1275	4.2035
13.5	4.1270	4.2020	4.1270	4.2030
14.5	4.1270	4.2020	4.1270	4.2030
15.5	4.1270	4.2020	4.1270	4.2030
16.5	4.1270	4.2020	4.1270	4.2030
17.5	4.1265	4.2020	4.1270	4.2030
18.5	4.1260	4.2050	4.1265	4.2050
19.5	4.1295	4.2090	4.1290	4.2085
20.5	4.1325	4.2095	4.1320	4.2090
21.5	4.1330	4.2095	4.1330	4.2090
22.5	4.1330	4.2100	4.1330	4.2095

*10 Cycles @ 15 KSI/CYC.

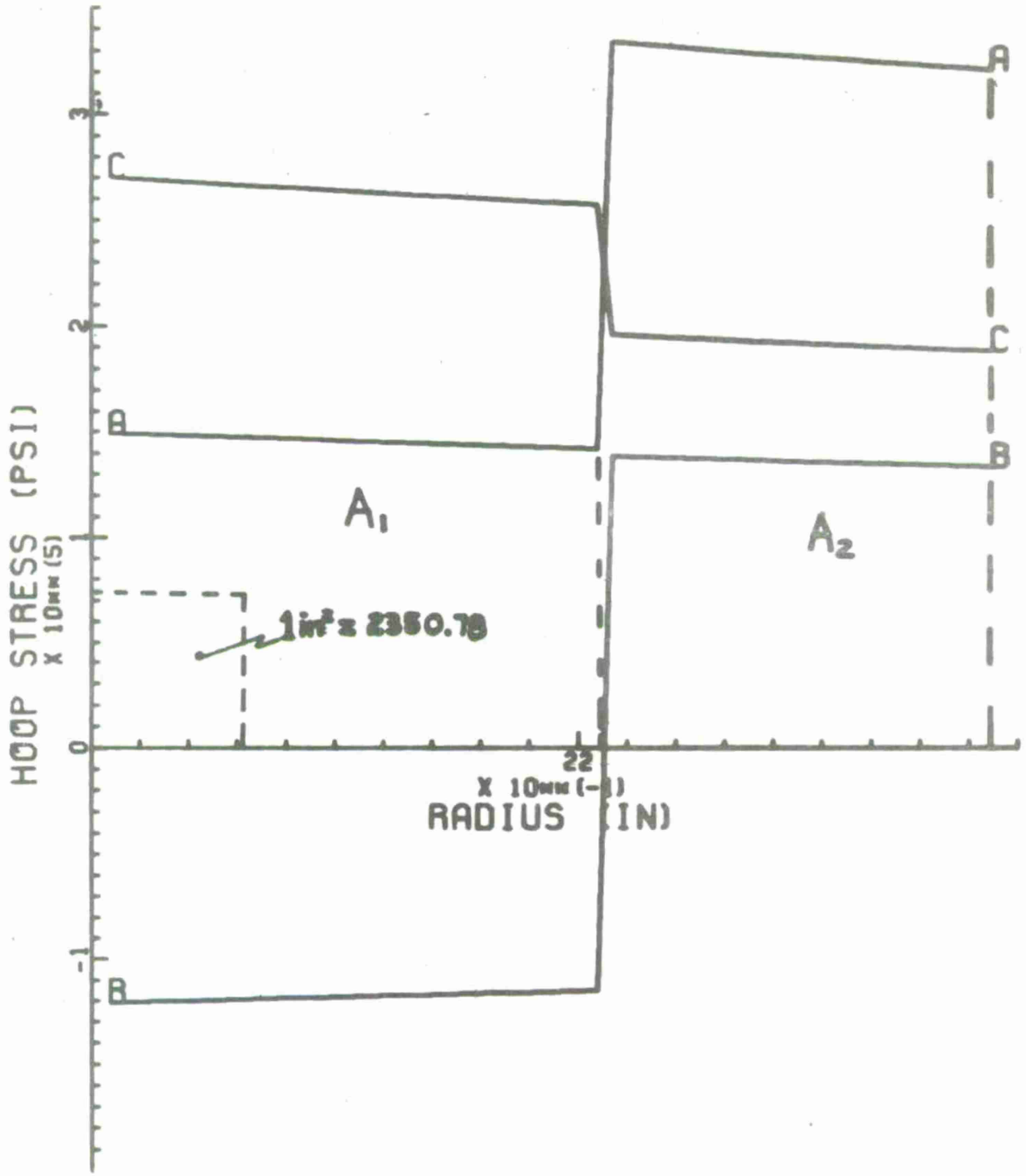

106 MM TEST CYLINDER
(PRESSURE= 20000 PSI)
SERVICE = A-A, RESIDUAL = B-B, ELASTIC = C-C

Figure 20. "GUNTUC" Liner and Jacket Stress Distribution for OCL-7

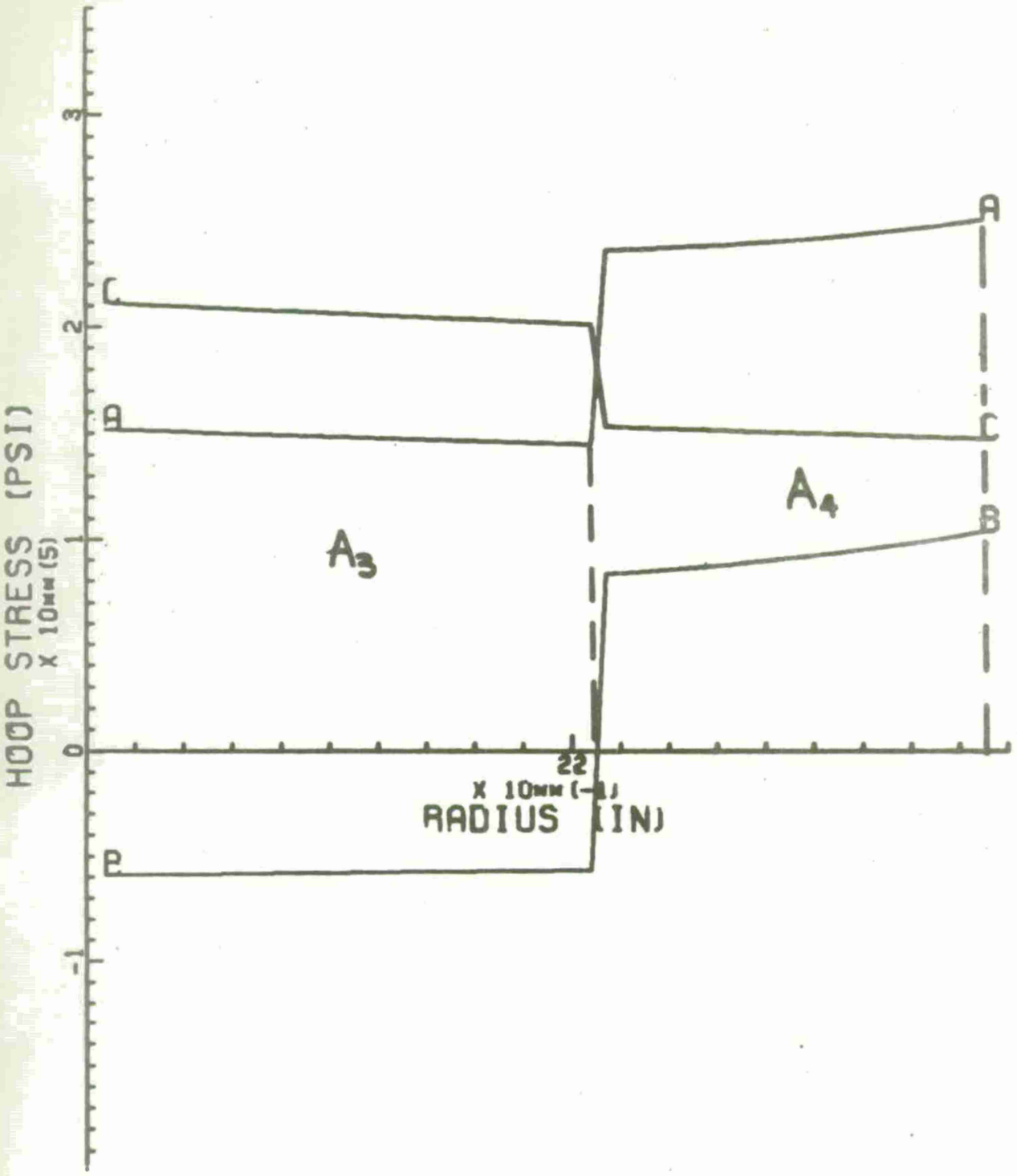

Figure 21. "TENZIONE" Liner and Jacket Stress Distribution for OCL-7.

cases:

(1) Yielding of the bore will commence at a pressure of 15,614 psi

(2) Yielding of the interface will commence at a pressure of 25,734

(3) Yielding of the jacket's outside diameter will commence at a pressure of 25,153 psi.

The area of concern is then the initial failure at the bore, or case (1). Figure 21 depicts case (1) and the following comments are presented:

1. At a pressure of 15,614 psi:
   a. the liner has reached its maximum capability and
   b. it is obvious that the jacket has not been properly used since its yielding stress is at a higher level as shown in Figure 20.

2. After the 15,614 psi pressure, the liner cannot share any longer the increase in pressure with the jacket; it keeps its stress level and its plastically deforms as the pressure is increased. Meanwhile the jacket has to take all of the additional stress developed, until it also reaches the yielding point or limit as shown in Figure 20 (curve A-A).

This behavior can be simply explained if the area under the hoop stress versus cylinder's radius is considered. Appendix D shows how this area is related to the applied pressure. In Figure 20, if the curve A-A is divided into two areas as shown, we can calculate A_1 and relate it to a pressure of 7129 psi and A_2 to 12,469 psi. Similarly in Figure 21, A_3 corresponds to 7129 psi and A_4 to 8922 psi. This means that after the liner has yielded A_4 it has to take all the

additional area or pressure until it reaches the yielding or limit as shown in Figure 20. In other words, A_4 has to increase to produce (P_2-P_4), (12,469-8,900), or 3569 psi pressure. In turn when this pressure is added to P_3 and P_4, the total pressure capacity of 19,620 psi is obtained.

3. From comments 1 and 2 it can be concluded that if the cylinder is subjected to 20,000 psi (let us assume for the moment that the cylinder will not rupture at this pressure) then upon release of this pressure the hoop stress distribution will be the curve C-C of Fig 20, and a new residual stress state will be induced in the structure. This stress state should be very close to the ideal case (B-B) depicted in Figure 20. This step introduces a change in the cylinder's internal diameter. After this process, known as autofrettage, the composite cylinder's stress-strain curve, upon further pressurization, will behave linearly.

4. Figures 22 through 25 depicting the pressure cycling of the OCL-7, verify the aforementioned comments.

a. Figures 22 and 23 depict the first and tenth cycles at a pressure of 15,600 psi. This checks with the results of Figure 21. Note linearity or elastic behavior.

b. Figure 24 depicts the first time OCL-7 was brought to a 20,000 psi pressure. Note: (1) Non-linearity after the 15,600 psi. (2) OCL-7 did not rupture here as theoretically predicted. This can be due to the variation of the many input parameters in obtaining Figure 20.

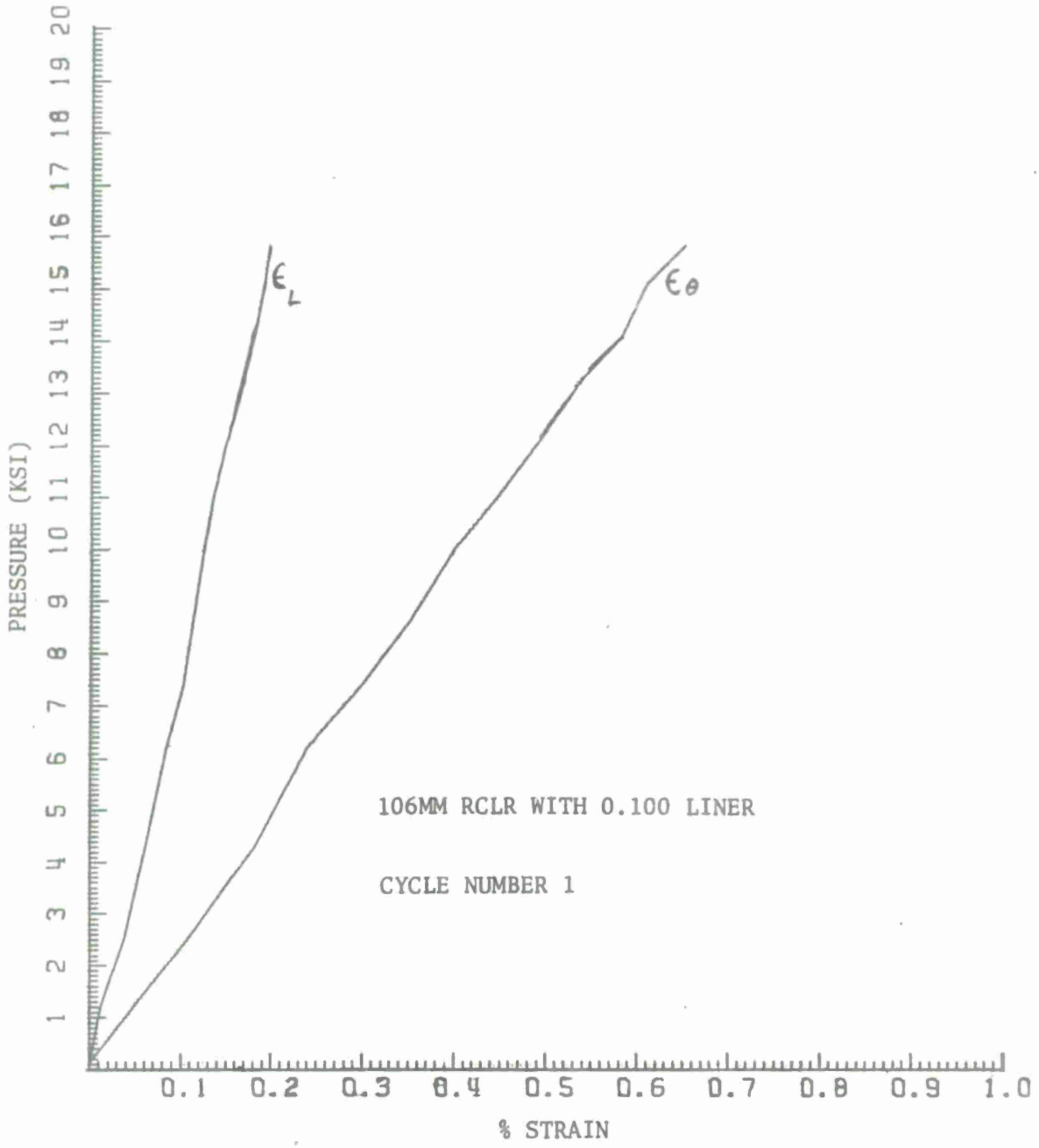

Figure 22. P vs ϵ Curve for 1st Cycle (15.6 KSI) on OCL-7.

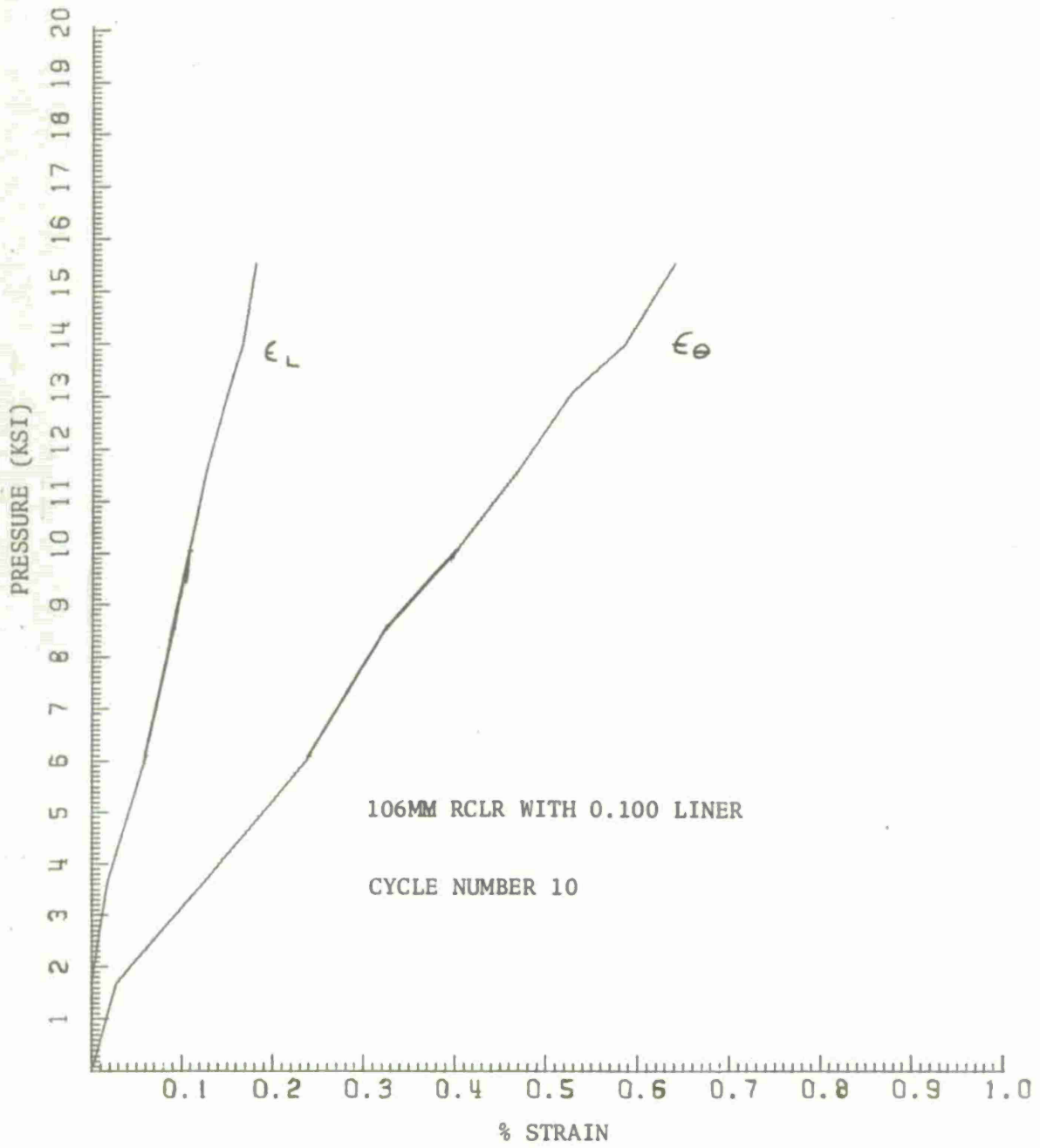

Figure 23. P vs ϵ Curve for 10th Cycle (15.6 KSI) on OCL-7.

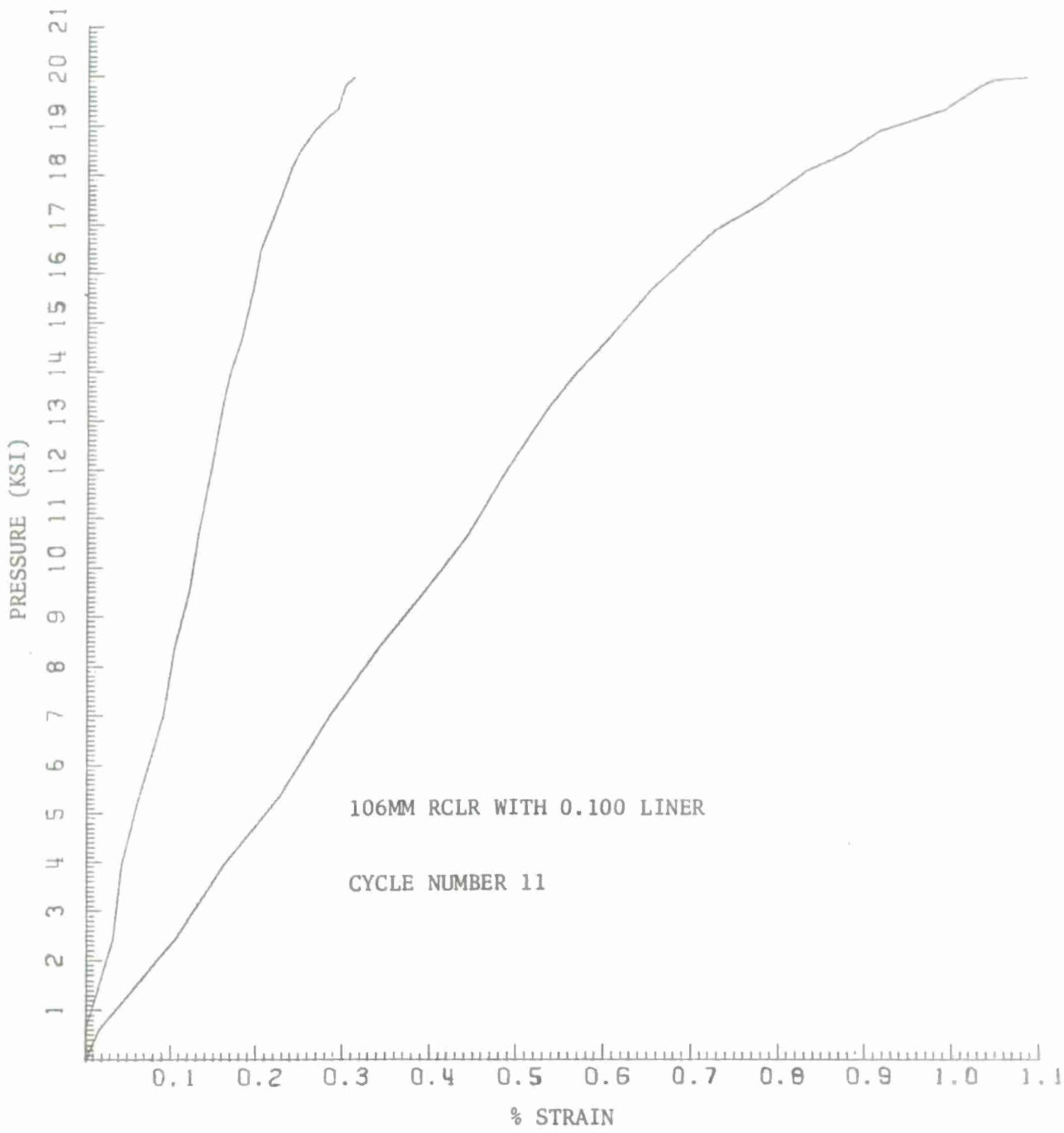

Figure 24. P vs ϵ Curve for 11th Cycle (20 KSI) on OCL-7.

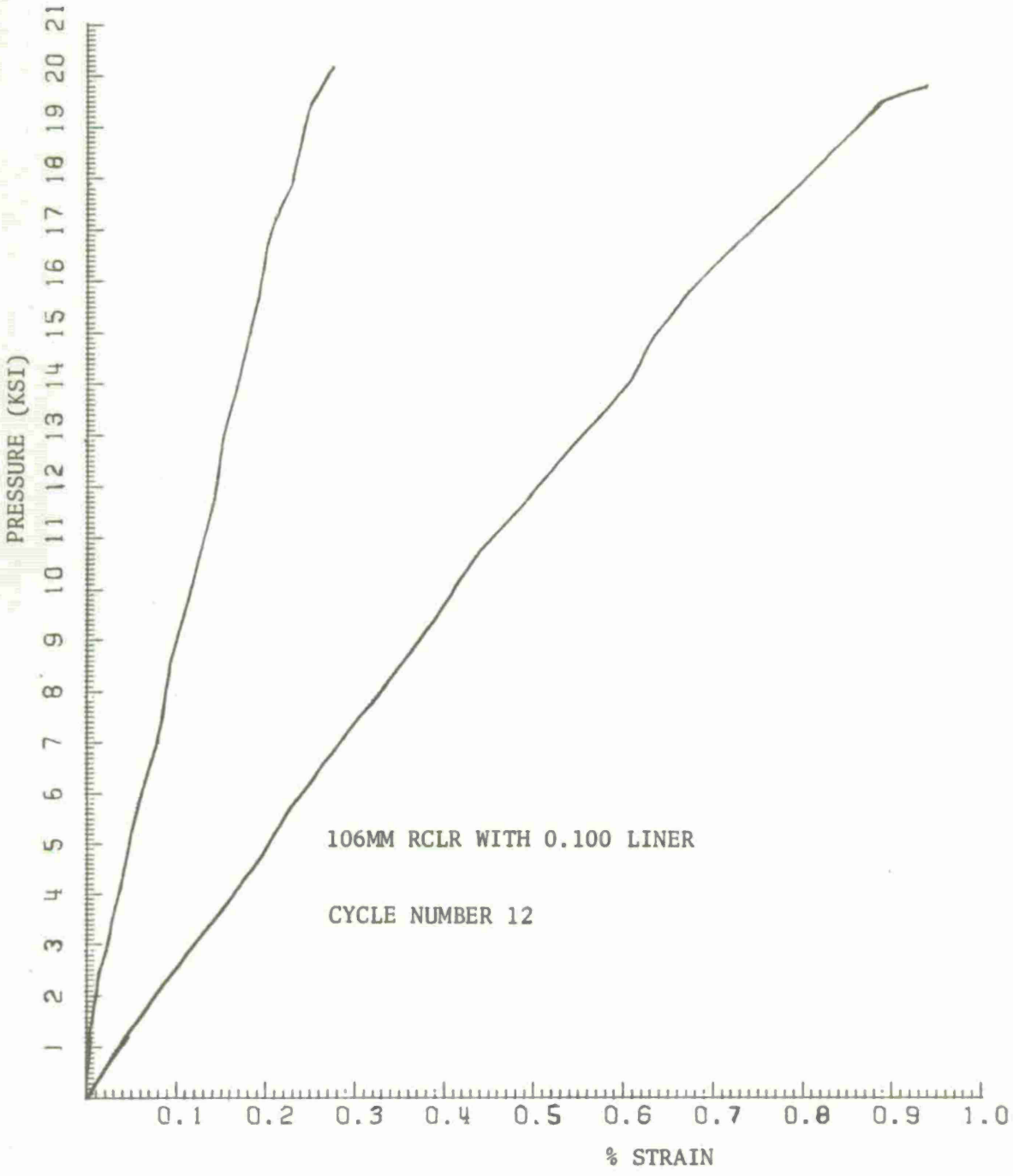

Figure 25. P vs ϵ Curve for 12th Cycle (20 KSI) on OCL-7.

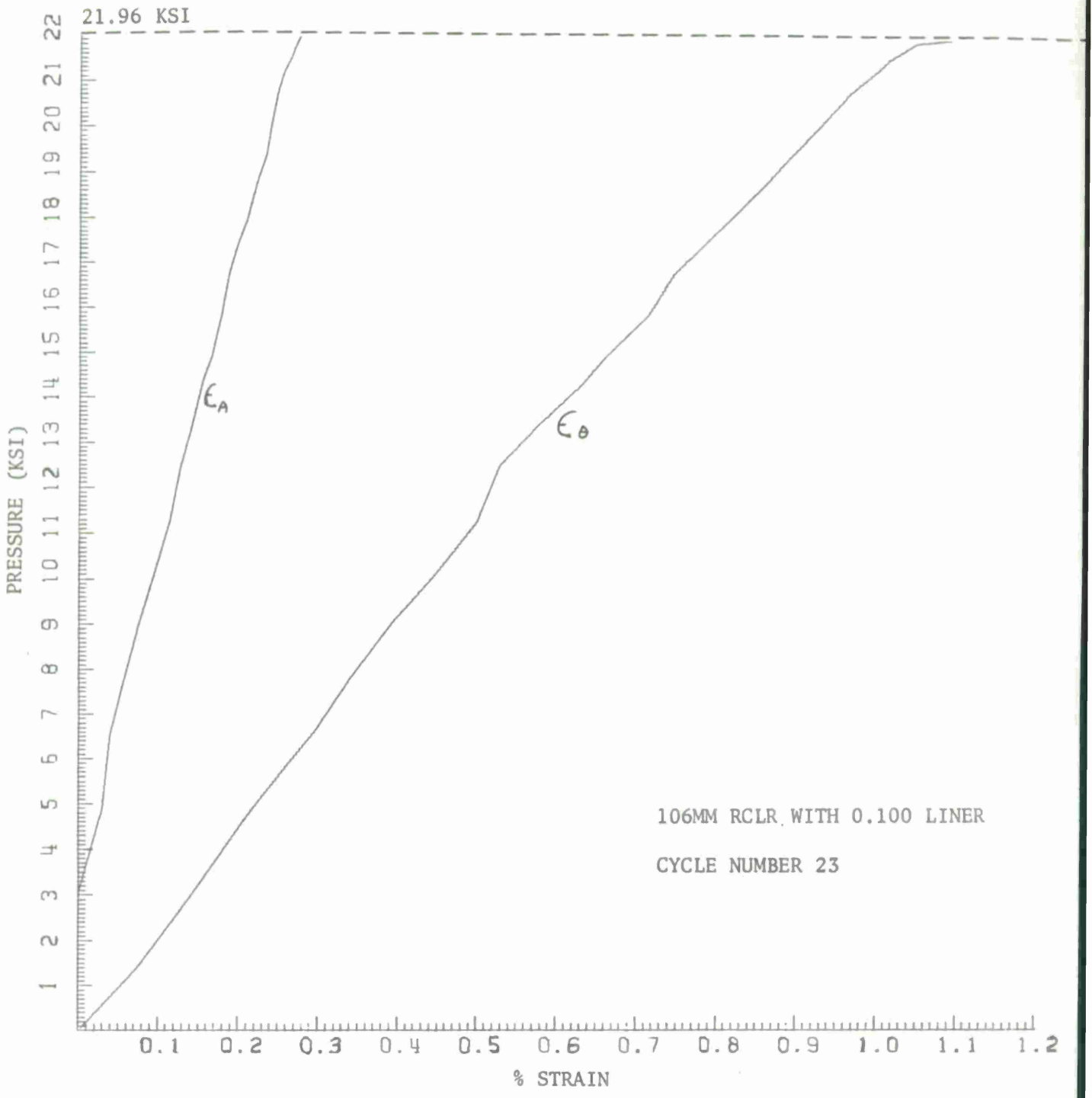

Figure 26. P vs ϵ Curve for Burst Cycle (21.9 KSI) on OCL-7.

c. Figure 25 depicts the second time OCL-7 was brought up to 20,000 psi. Note the linearity as explained in comment 3. A close look between Figures 22 and 25 will reveal a shift in slope between the hoop strain curve as it is expected.

d. Figure 26 depicts the burst cycle. The burst pressure is 21,900 psi or 9.5% above the theoretical value.

e. A check in the measured hoop strain reveals the following:

From reference 5

$$\epsilon_\theta \Big|_{THEOR.} = \beta_{12}\sigma_r + \beta_{11}\sigma_\theta$$

$$\sigma_r \Big|_{at\ r=b_o} = 0$$

or $$\epsilon_\theta = \beta_{11}\sigma_\theta = (.043\times10^{-6})\sigma_\theta \ in/in$$

$$\beta_{11} = .043\times10^{-6}\ in^2/\#$$

(1) From Figure 20 (curve C-C)

$$\sigma_\theta \Big|_{20Ksi} = 188{,}000\ psi$$

$$\epsilon_\theta = (.188)(.043) = .8\%$$

From Figures 24 and 25 $\epsilon_\theta \Big|_{EXPERIMENT} \simeq .92\%$

---

[5] D'Andrea, G., "Composite Cylindrical Pressure Vessels Related to Gun Tubes. Part I: Theoretical Investigation," September 1968, Watervliet Arsenal Technical Report WVT-6821.

(2) From Figure 21 (curve C-C)

$$\sigma_\theta \Big|_{15.6\ Ksi} \simeq 147{,}000 psi$$

$$\epsilon_\theta \Big|_{THEOR.} = (.147)(.043) = .63\%$$

From Figures 22 and 23

$$\epsilon_\theta \Big|_{EXPERIMENT} \simeq .64\%$$

CONCLUSIONS

1. Theoretical and experimental analyses of the 106mm RCLR composite test specimens indicate that programmed tensions are feasible, and predetermined residual stresses in the liner and jacket can be introduced to obtain a structurally sound and lightweight composite vessel.

2. Computer Program "TENZIONE" is suitable for evaluating composite cylinders made of filament wrapped materials. Its clear response, in the form of graphical output, can quickly and easily be used by the engineer who is interested in lightweight, high strength structures. Figures 20, 21, and Appendix B depict its usefulness.

3. The filament winding fabrication technique, shown in Figures 1 through 6 and explained in detail in reference 1, indicates that high strength, high-modulus composite cylinders can be fabricated of high strength (450 KSI), small diameter (.006 in) steel filaments with conventional epoxy matrices.

---

[1]Cullinan, R., et al, "Application of Filament Winding to Cannon and Cannon Components. Part I: Steel Filament Composites," April 1972, Watervliet Arsenal Technical Report WVT-7205.

4. The measurement of internal diametrical deflection before, after and during the winding operation has been successful. The techniques and air gage equipment utilized are explained and shown in Figures 7 through 11.

5. In-house pressurization of fabricated 106mm test cylinders to corrolate theory and experiment has been accomplished. Typical results of a 23 cycle test are shown in Figures 22 to 26.

6. In the computer analysis "TENZIONE" of the resultant residual stresses introduced from the winding operation, the theoretical diametrical change and stress was utilized rather than the experimental values. The slight difference in theory vs experimental is a result of the rifling in the cylinders and possibly a lack of extreme accuracy in measuring the winding tension at the delivery eye.

7. Graphical output depicted in Figure 21 suggests that (if during the filament winding operation, the predetermined residual stresses cannot or were not obtained) any pressure greater than the one which induced yielding at the liner, will introduce (upon depressurization) the desired residual stresses in the structure. This process, known as autofrettage, was experimentally verified in Figures 24 and 25.

8. The next and final technical report will provide a comprehensive summary of the work performed under the MM&T project of "Application of Filament Winding to Cannon and Cannon Components." Details on Design, Fabrication and Firing Tests of a full size 106mm Composite Recoilless Rifle will be presented and fully analyzed.

REFERENCES

1. Cullinan, R., et al, "Application of Filament Winding to Cannon and Cannon Components. Part I: "Steel Filament Composites," April 1972, Watervliet Arsenal Technical Report WVT-7205.

2. Stone, F. E., "Study of Residual Stresses in Thick Glass-Filament-Reinforced Laminates," October 1965, AD623051.

3. Stone, F. E., "Study of Residual Stresses in Thick Glass-Filament-Reinforced Laminates," September 1964, AD606406.

4. Rosato, D. V. and Grove, C. S., "Filament Winding," John Wiley & Son, New York, N. Y. 1964, p 180.

5. D'Andrea, G., "Composite Cylindrical Pressure Vessels Related to Gun Tubes. Part I: Theoretical Investigation," September 1968, Watervliet Arsenal Technical Report WVT-6821.

6. D'Andrea, G., "Composite Cylindrical Pressure Vessels Related to Gun Tubes. Part II: Minimum Weight Design," September 1971, Watervliet Arsenal Technical Report WVT-7125.

7. D'Andrea, G. and Cullinan, R., "Development of: Design Analyses, Manufacturing and Testing of the 81mm XM73 Fiberglass-Epoxy Recoilless Rifle, June 1974, Watervliet Arsenal Technical Report WVT-TR-74014.

APPENDIX A

FABRICATION SHEETS OF CYLINDERS OCL-4,6,7, and 10

NO:

OCL-4

TENSION: 11.5 lb

NO. OF SPOOLS: 3

	LAYERS	ENDS IN	BORE DIAM	RIFLING DIAM	REMARKS
1	F ⟶ F	123	19.0	19.0	20 = 0 Deflection
2	F ⟵ F	216	17.0	17.5	
3	" ⟶ 19 1/2	147	16.0	16.5	
4	4 7/8 ⟵ "	173	14.5	15.5	
5	" ⟶ F	156	13.5	14.5	
6	F ⟵ "	173	12.5	13.0	
7	" ⟶ 19 3/8	158	11.5	12.0	
8	5 ⟵ "	173	10.5	11.0	
9	" ⟶ F	153	9.5	10.5	
10	F ⟵ "	146	9.0	9.5	
11	" ⟶ 19 1/4	136	8.0	9.0	
12	10 1/8 ⟵ "	188	7.0	8.5	
13	" ⟶ F	172	6.5	8.0	
14	F ⟵ "	158	6.0	7.5	I.R. Lamps Turned On For Layers 14 and 15 For Better Resin Flow
15	" ⟶ "	143	4.5	6.5	
16	" ⟵ "	163	3.5	6.0	
17	" ⟶ "	175	3.0	5.5	
	AVG =	161.9			

NO:

OCL-6

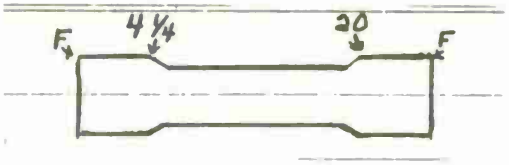

TENSION: 11.5 lb

NO. OF SPOOLS: 3

	LAYERS	ENDS IN	BORE DIAM	RIFLING DIAM	REMARKS
1	F → F	144	19.0	19.0	20 = 0 DEFLECTION
2	" ← "	157	18.0	18.0	
3	" → 20	160	17.0	17.5	
4	4 1/4 ← "	147	16.5	17.0	
5	" → 19 7/8	217	15.5	16.0	
6	4 3/8 ← "	148	14.5	15.5	
7	" → F	139	14.0	15.0	
8	4 1/2 ← "	164	13.5	14.5	
9	" → 19 3/4	171	12.5	14.0	
10	F ← "	177	11.5	13.5	Turn I-R Lamps On For Layers 10 and 11 To Allow Better Resin Flow
11	" → F	123	11.0	13.0	
12	4 5/8 ← "	172	10.0	12.5	
13	" → 19 5/8	160	9.5	11.0	
14	F ← "	182	9.0	8.5	
15	" → F	165	8.5	7.5	
		AVG = 161.7			

NO:

OCL-7

TENSION: 11.5 lb

NO. OF SPOOLS: 3

	LAYERS	ENDS IN	BORE DIAM	RIFLING DIAM	REMARKS
1	F → F	160	15.0	15.5	16 = 0 Deflection
2	" ← "	198	14.0	14.5	
3	" → 19 7/8	103	13.5	14.0	
4	4 3/4 ← "	160	13.0	13.0	
5	" → 19 3/4	153	12.5	12.0	
6	4 7/8 ← "	167	12.0	11.5	
7	" → F	186	11.0	11.0	
8	F ← "	178	10.5	10.5	
9	" → 19 5/8	181	10.0	10.0	
10	5 ← "	133	9.0	9.0	
11	" → 19 1/2	147	8.5	8.5	
12	5 1/8 ← "	136	8.0	8.0	
13	" → F	157	7.5	7.5	
14	F ← "	161	7.0	7.0	
		AVG = 158.7			

NO:

OCL-10

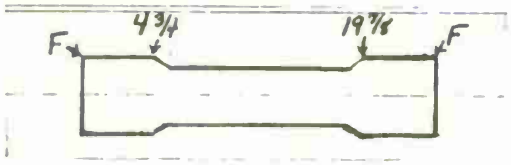

TENSION: 11.5 lb

NO. OF SPOOLS: 3

	LAYERS	ENDS IN	BORE DIAM	RIFLING DIAM	REMARKS
1	F ⟶ 19 7/8	139	19.5	DID	20.0 = 0 Deflection
2	4 3/4 ⟵ "	199	18.5		
3	" ⟶ F	152	17.5		
4	4 7/8 ⟵ "	168	17.0		
5	" ⟶ 19 3/4	157	16.5		
6	F ⟵ "	181	15.5		
7	" ⟶ 19 5/8	137	15.0	NOT	
8	5 ⟵ "	151	14.5		
9	" ⟶ F	145	14.0		
10	5 1/8 ⟵ "	154	13.5		
11	" ⟶ 19 1/2	141	13.0		
12	F ⟵ "	163	12.5		Last 2 Layers Wound With I-R Lamps On In Order To Get Better Resin Flow
13	" ⟶ "	160	11.5	RECORD	
	AVG =	157.5			

APPENDIX B

INPUT AND OUTPUT OF COMPUTER PROGRAM TENZIONE

FOR CYLINDERS OCL-4,6,7, and 10

"TENZIONE" - INPUT AND EXPERIMENTAL DIAMETRICAL CHANGES (DC) FOR THE OCL-4 SPECIMEN

			L	DC (in)
Modulus of Mandrel	= EM	30×10^6	1	.0012
Outside radius of Mandrel	= RM	2.1540	2	.0025
Internal radius of Mandrel	= RO	2.1055	3	.0035
Poisson's ratio of Mandrel	= XNUM	.28	4	.0045
Modulus of Filament	= EG	30×10^6	5	.006
Thickness of Filament	= TI	.006	6	.007
Area of Filament	= AN	$.283 \times 10^{-4}$	7	.008
Resin squeeze out	= OMEGA	.20	8	.009
Filament volume ratio	= XKF	.75	9	.0095
Resin shrinkage	= OMEGS	.04	10	.0105
Coeff Thermal exp of mandrel	= ALPHM	6.0×10^{-6}	11	.011
Coeff Thermal exp of composite	= ALPHG	6.15×10^{-6}	12	.0115
Ambient Temperature	= TAMB	75	13	.0122
Curing Temperature	= TCURE	350	14	.0125
			15	.0135
Number of layers	= N	17	16	.014
Tension of Layer #1	= T1	3.83	17	.0145
Tension of Layer N	= Tn	3.83		
D.C. After Gel	= 0.0135"			
D.C. After Cure	= 0.0125"			

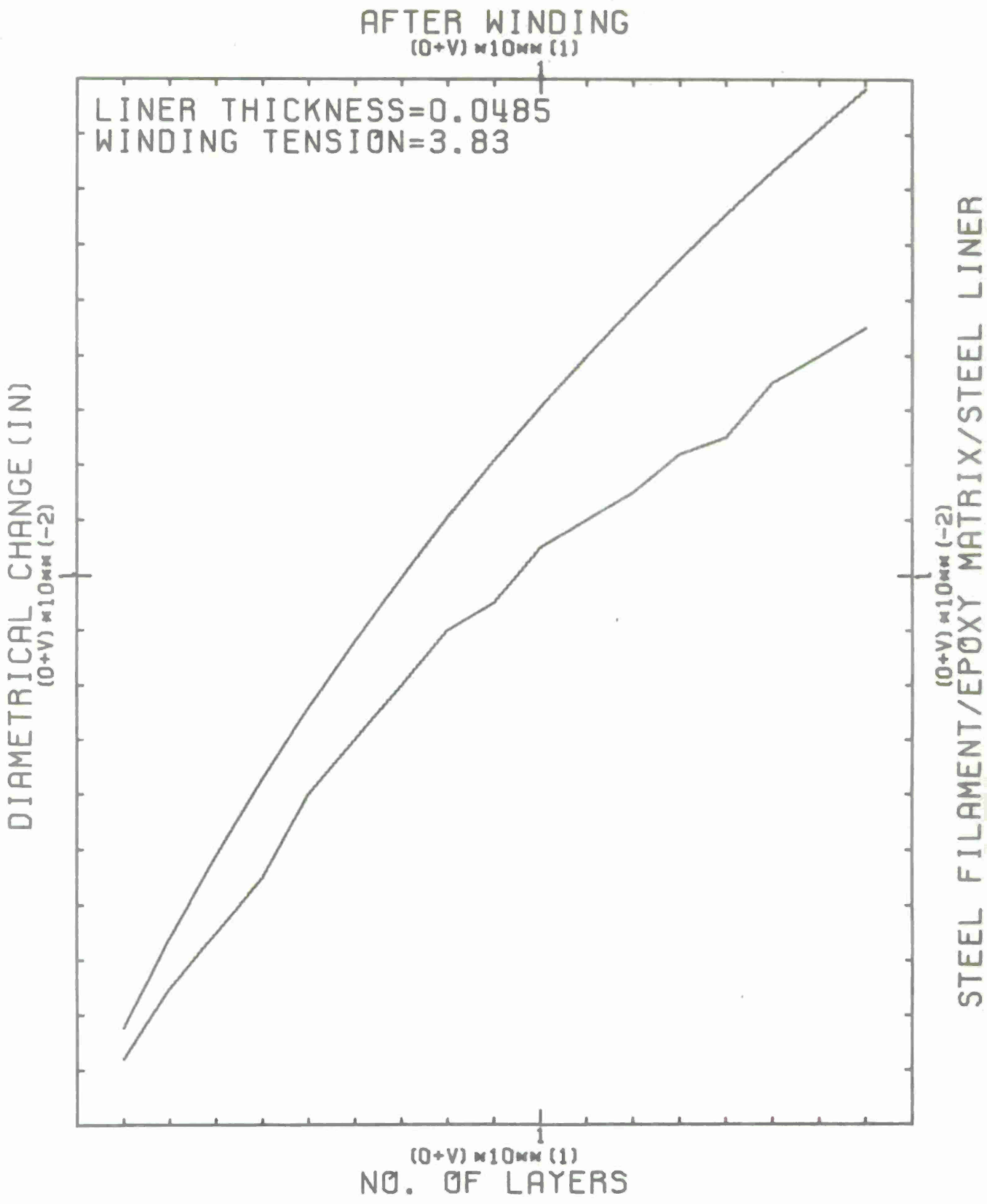

Figure B-1. Deflection vs No. of Layers for OCL-4 (After Winding)

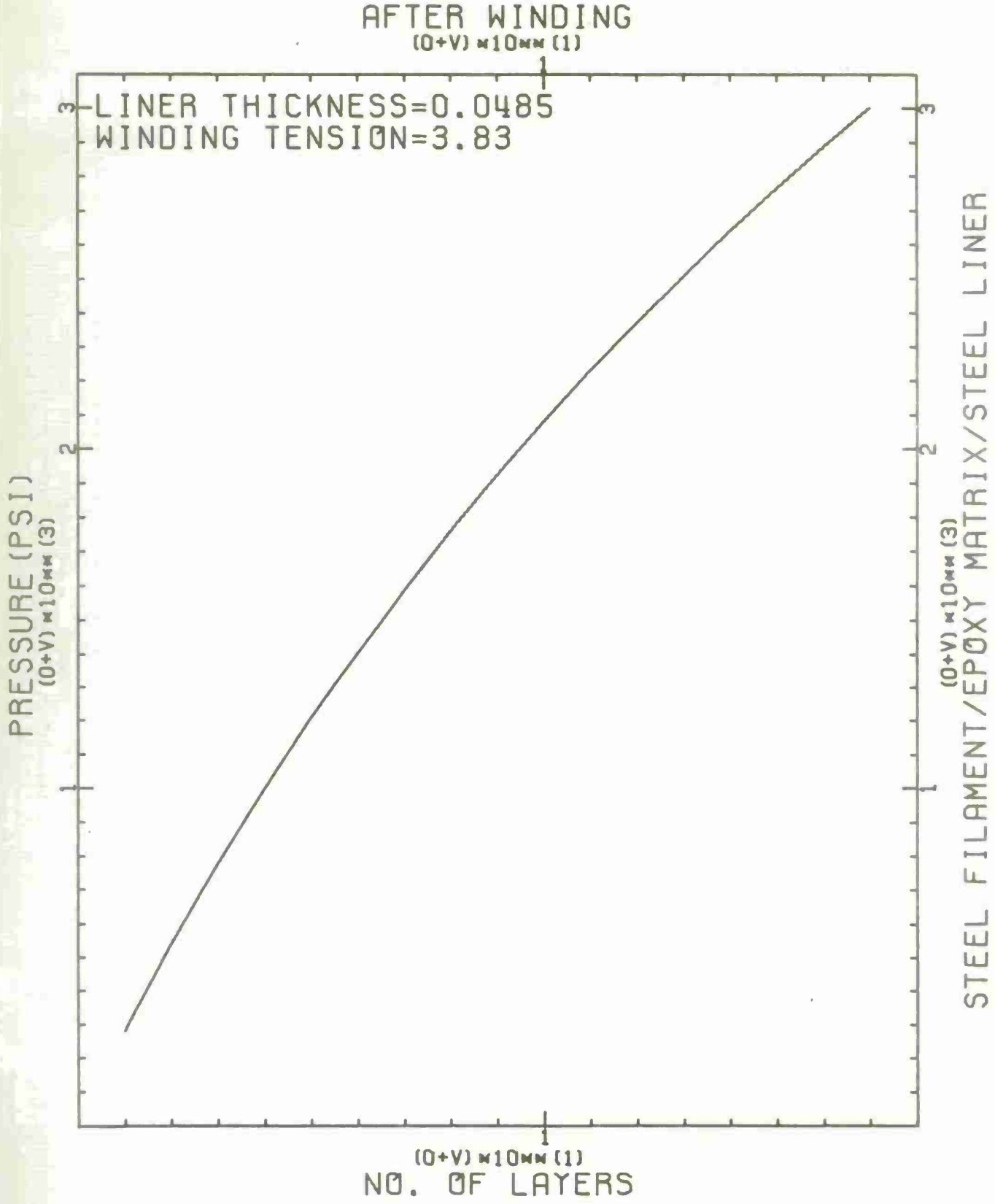

Figure B-2. Compressive Liner Pressure for OCL-4 (After Winding)

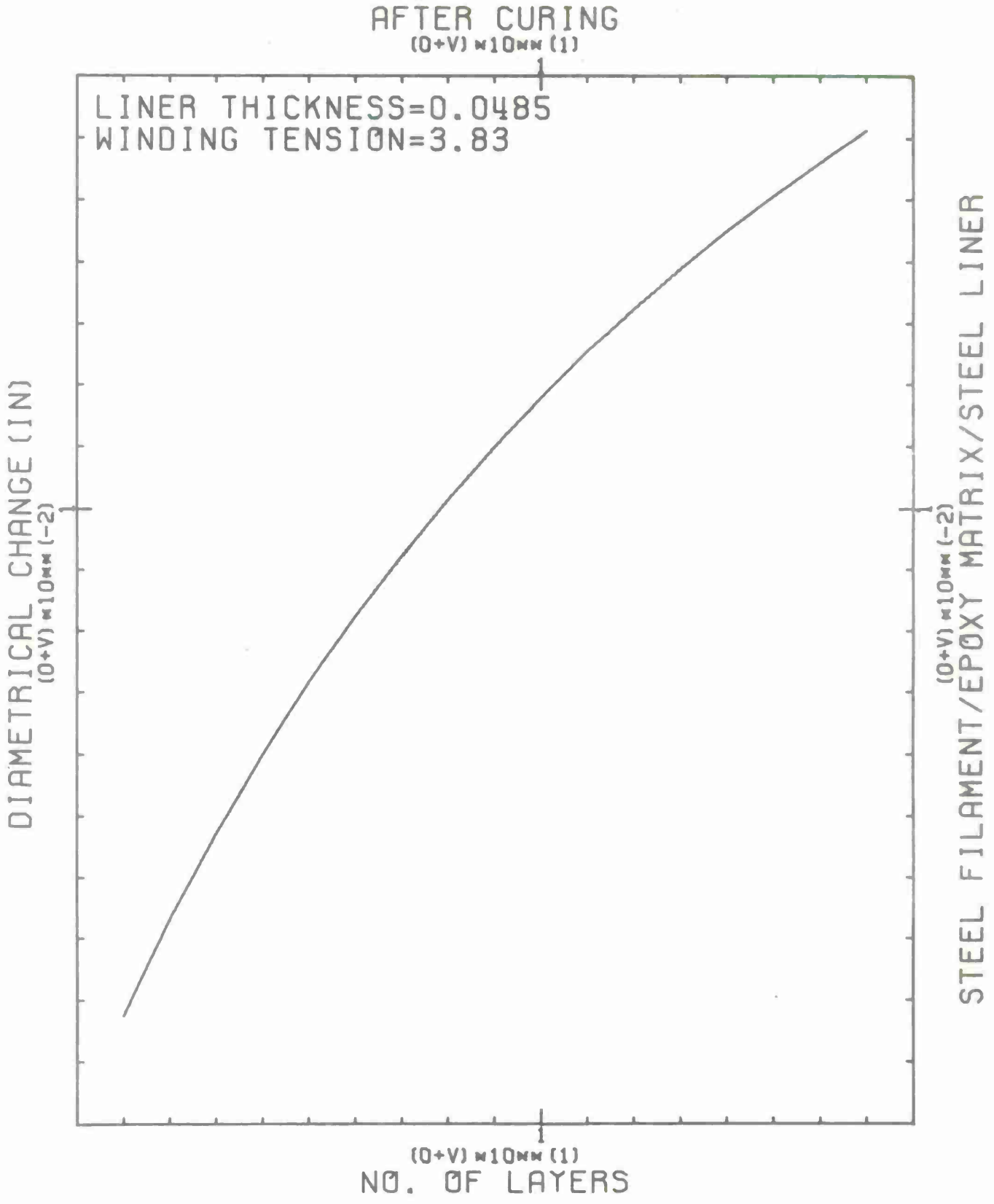

Figure B-3. Deflection vs No. of Layers for OCL-4 (After Curing)

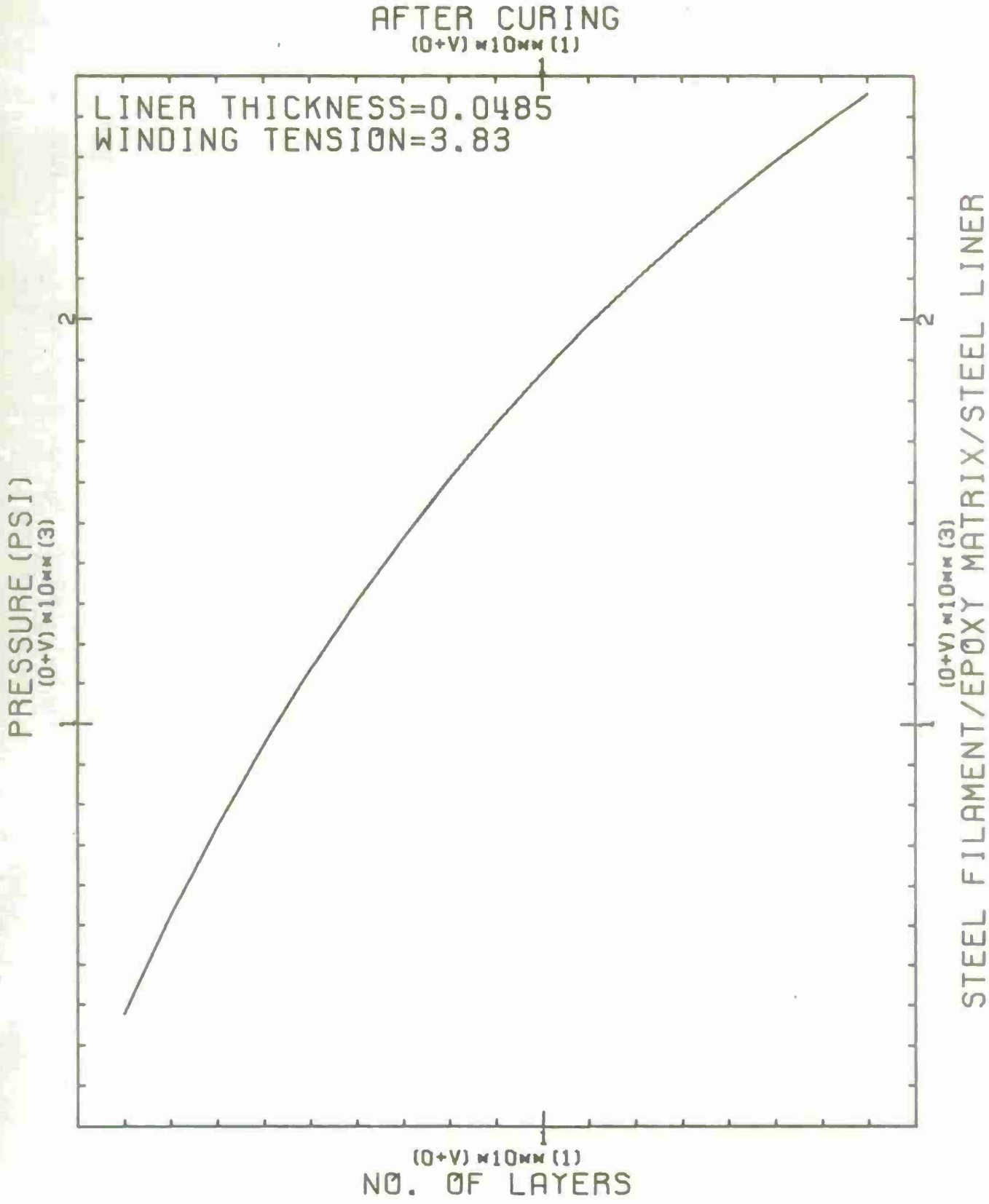

Figure B-4. Compressive Liner Pressure for OCL-4 (After Curing)

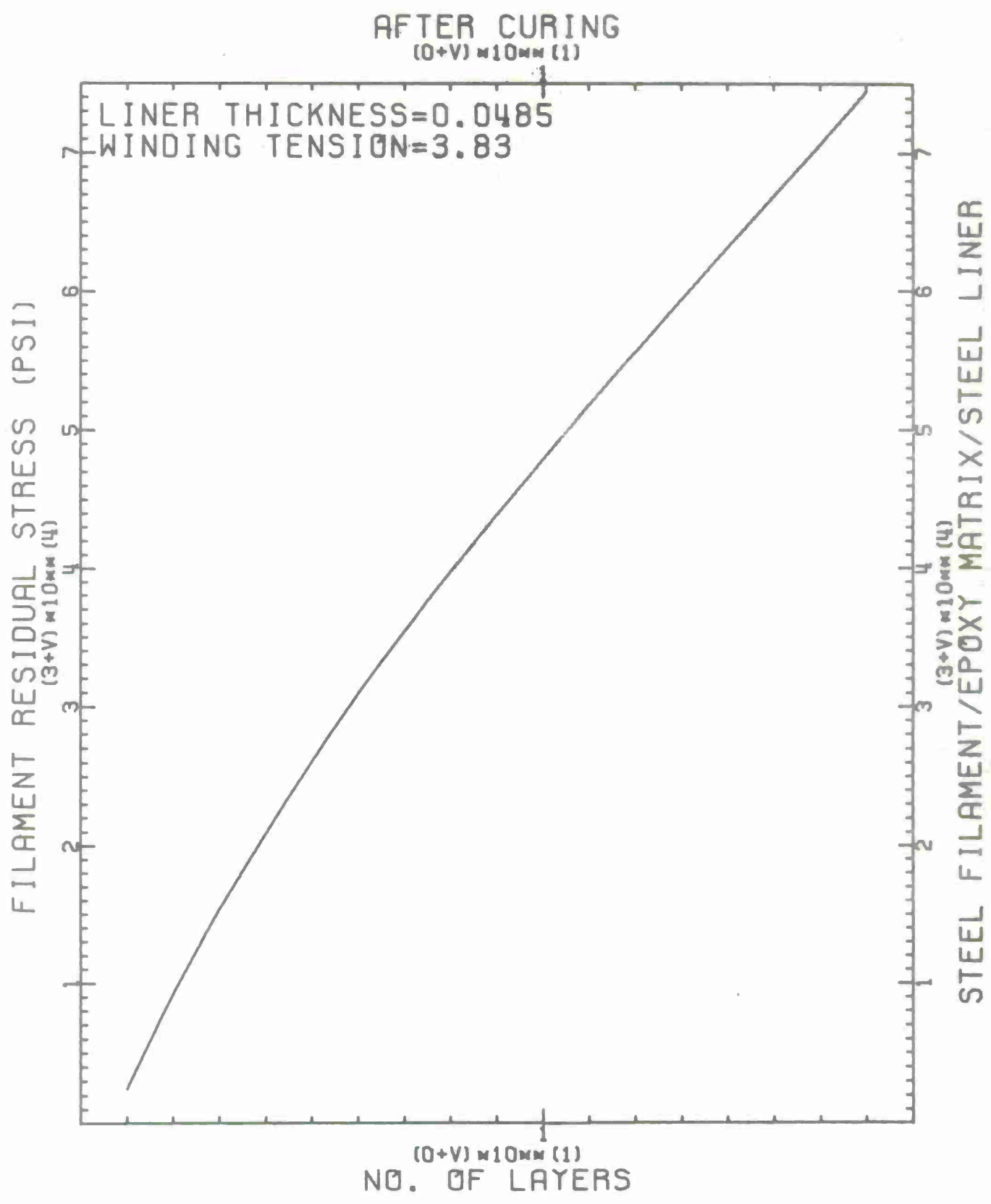

Figure B-5. Induced Residual Stresses for OCL-4 (After Curing)

"TENZIONE" - INPUT AND EXPERIMENTAL DIAMETRICAL CHANGES (DC) OF THE OCL - 6 SPECIMEN

			L	DC (in)
Modulus of Mandrel	= EM	30×10^6	1	.001
Outside radius of Mandrel	= RM	2.177	2	.002
Internal radius of Mandrel	= RO	2.105	3	.003
Poisson's ratio of Mandrel	= XNUM	.28	4	.0035
Modulus of Filament	= EG	30×10^6	5	.0045
Thickness of Filament	= TI	.006	6	.0055
Area of Filament	= AN	$.283 \times 10^{-4}$	7	.006
Resin squeeze out	= OMEGA	.20	8	.0065
Filament volume ratio	= XKF	.75	9	.0075
Resin shrinkage	= OMEGS	.04	10	.008
Coeff Thermal exp of Mandrel	= ALPHM	6.0×10^{-6}	11	.009
Coeff Thermal exp of Composite	= ALPHG	6.15×10^{-6}	12	.010
Ambient Temperature	= TAMB	75	13	.0105
Curing Temperature	= TCURE	350	14	.011
			15	.0115
Number of layers	= N	15		
Tension of Layer #1	= T1	3.8		
Tension of Layer N	= TN	3.7		
D.C. After Gel	= 0.0095			
D.C. After Cure	= 0.010			

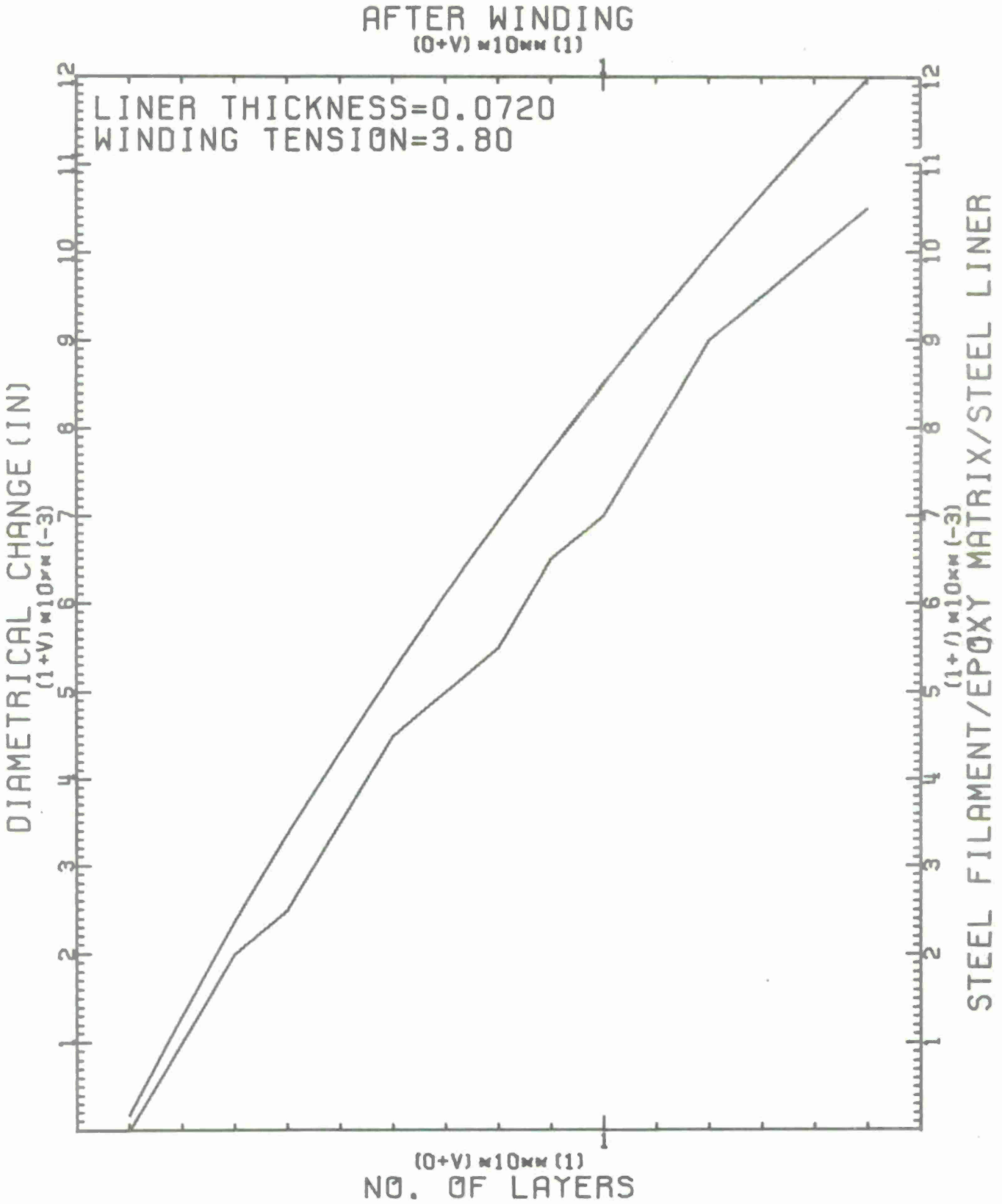

Figure B-6. Deflection vs No. of Layers for OCL-6 (After Winding)

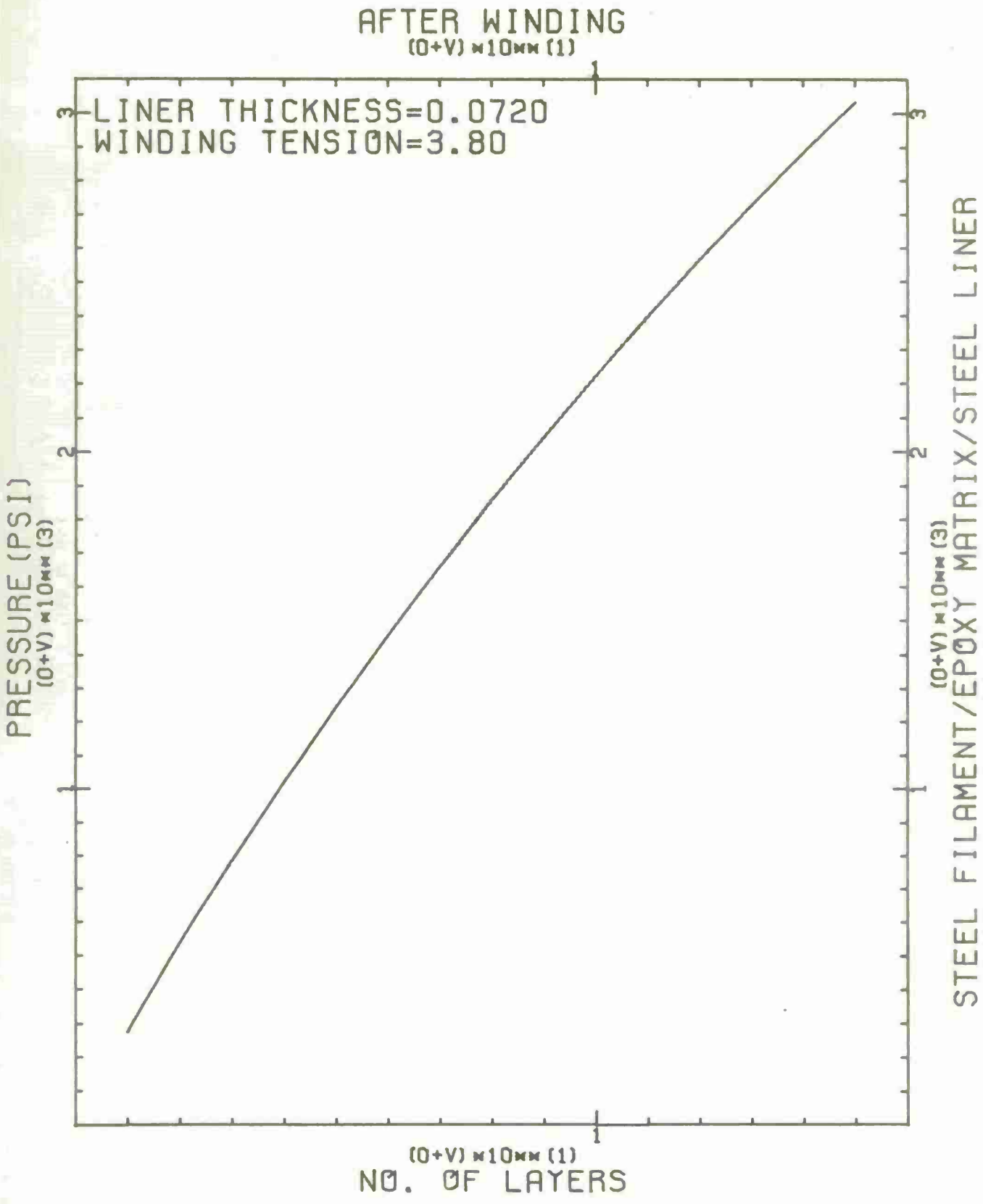

Figure B-7. Compressive Liner Pressure for OCL-6 (After Winding)

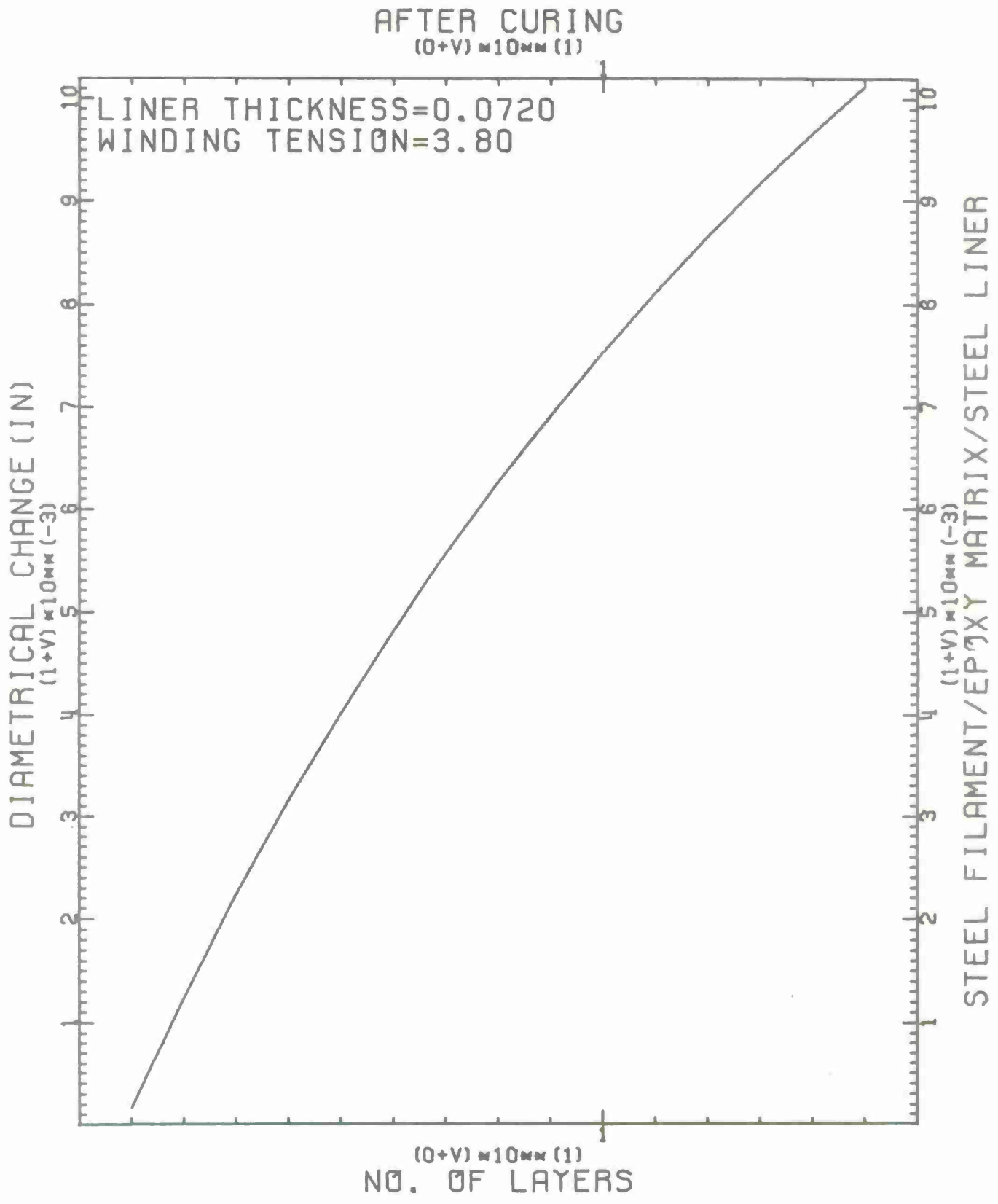

Figure B-8. Deflection vs No. of Layers for OCL-6 (After Curing)

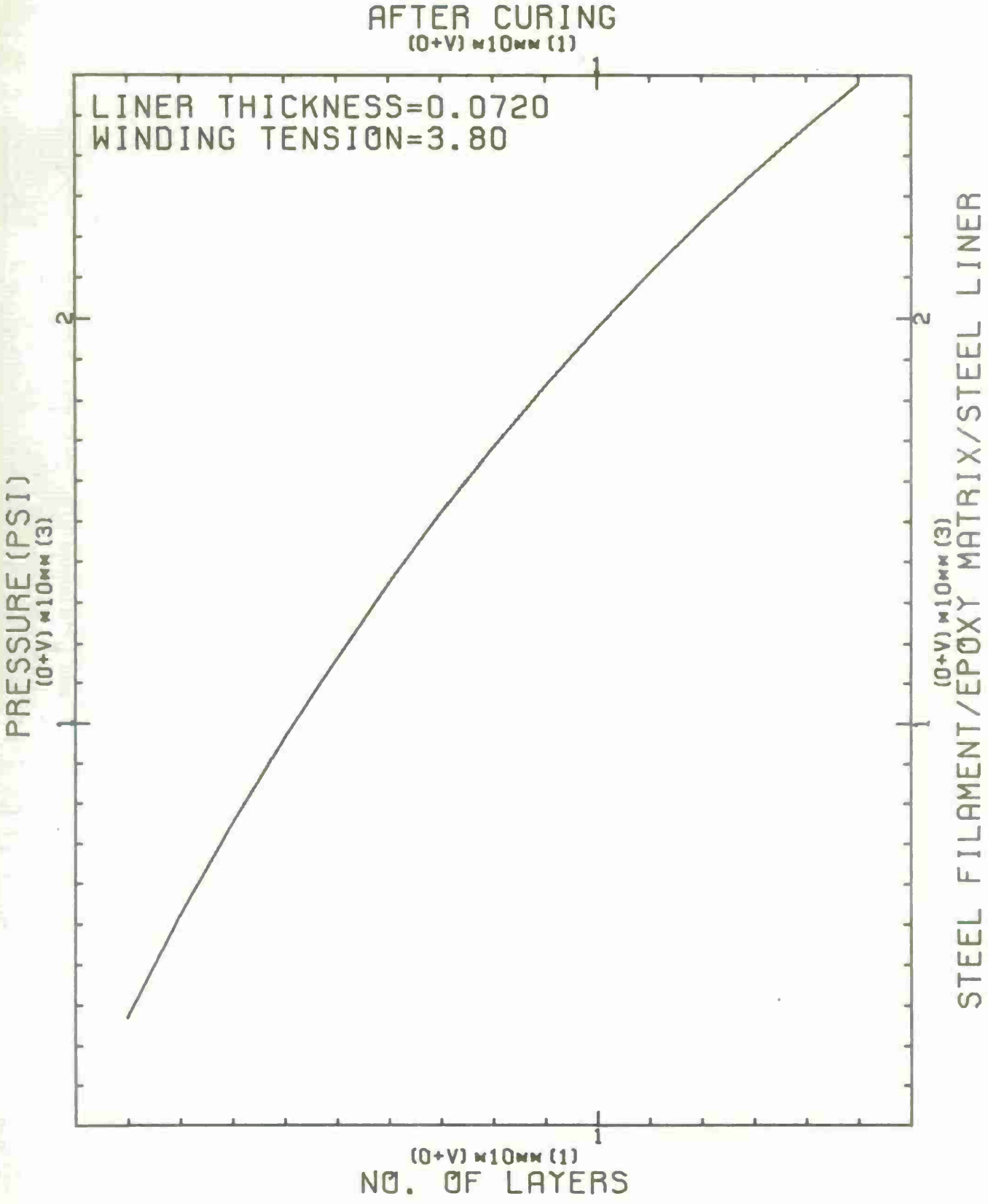

Figure B-9. Compressive Liner Pressure for OCL-6 (After Curing)

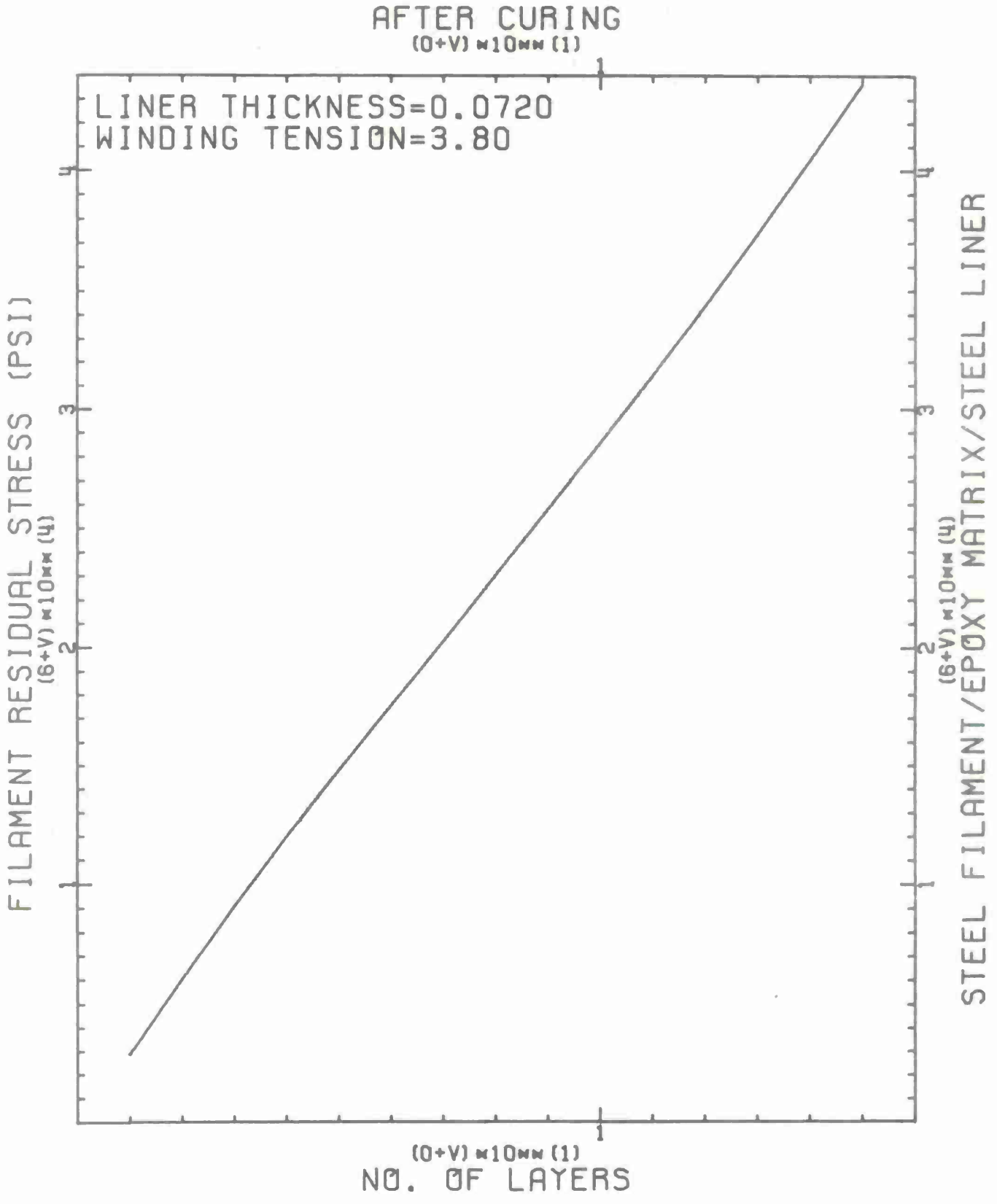

Figure B-10. Induced Residual Stresses for OCL-6 (After Curing)

"TENZIONE" - INPUT AND EXPERIMENTAL DIAMETRICAL CHANGES (DC) FOR THE OCL- 7 SPECIMEN

			L	DC (in)
Modulus of Mandrel	= EM	30×10^6	1	.0005
Outside radius of Mandrel	= RM	2.204	2	.0015
Internal radius of Mandrel	= RO	2.1055	3	.002
Poisson's ratio of Mandrel	= XNUM	.28	4	.003
Modulus of Filament	= EG	30×10^6	5	.004
Thickness of Filament	= TI	.006	6	.0045
Area of Filament	= AN	$.283 \times 10^{-4}$	7	.005
Resin squeeze out	= OMEGA	.20	8	.0055
Filament volume ratio	= XKF	.75	9	.006
Resin shrinkage	= OMEGS	.02	10	.007
Coeff Thermal exp of Mandrel	= ALPHM	6.0×10^{-6}	11	.0075
Coeff Thermal exp of Composite	= ALPHG	6.15×10^{-6}	12	.008
Ambient Temperature	= TAMB	75	13	.0085
Curing Temperature	= TCURE	350	14	.009
Number of layers	= N	14		
Tension of Layer #1	= T1	3.87		
Tension of Layer N	= TN	3.8		
D.C. After Gel	= 0.008"			
D.C. After Cure	= 0.009"			

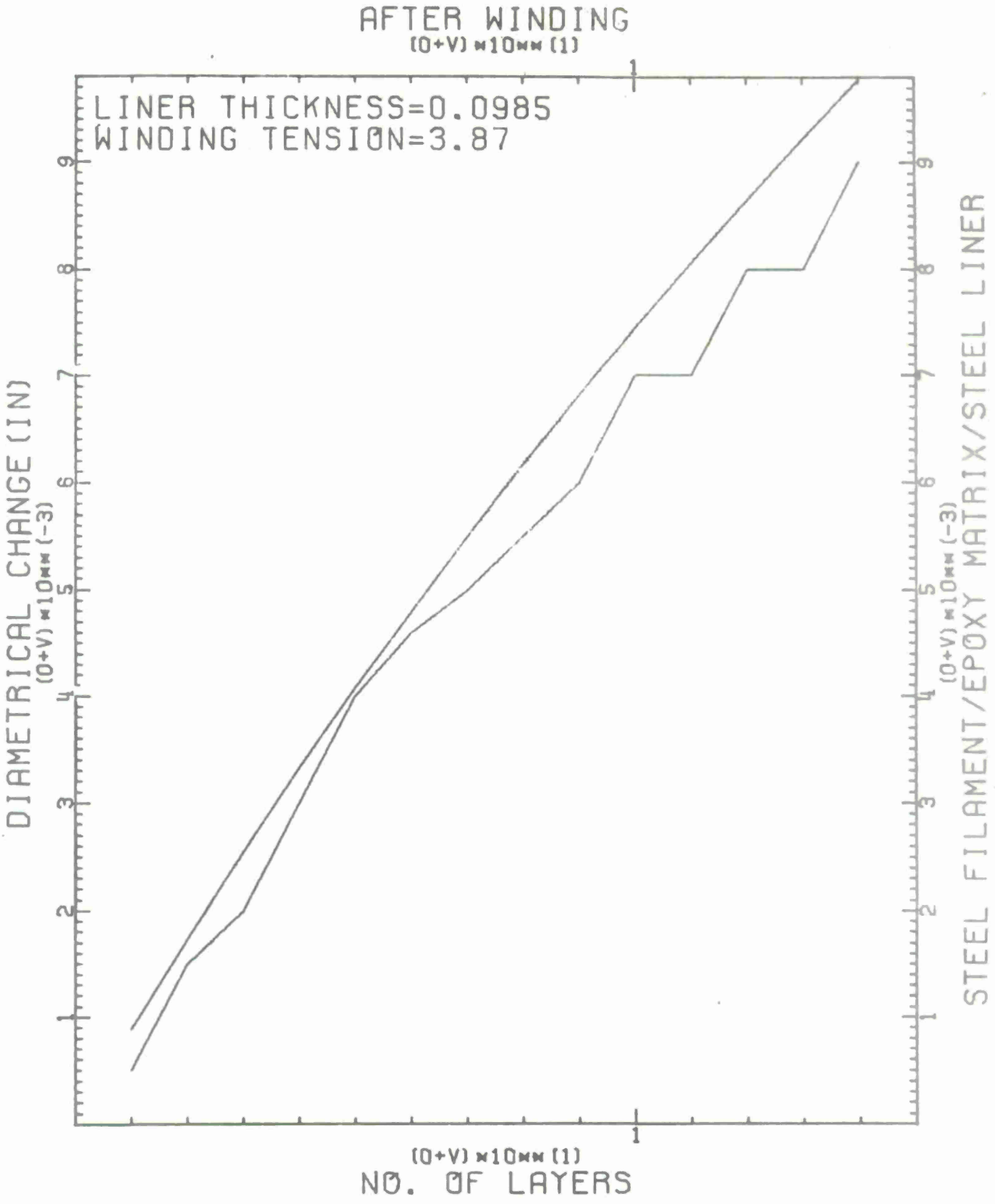

Figure B-11. Deflection vs No. of Layers for OCL-7 (After Winding)

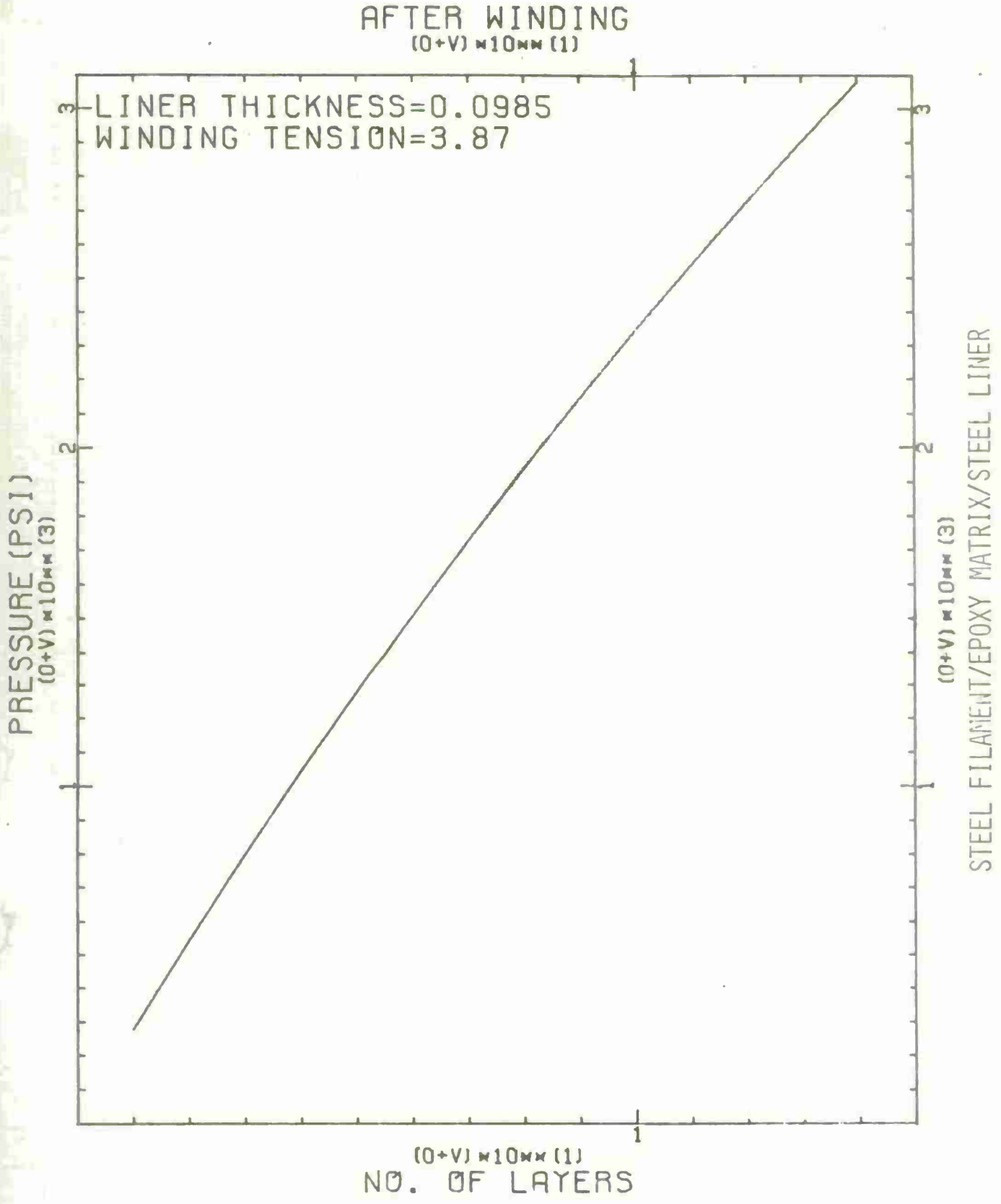

Figure B-12. Compressive Liner Pressure for OCL-7 (After Winding)

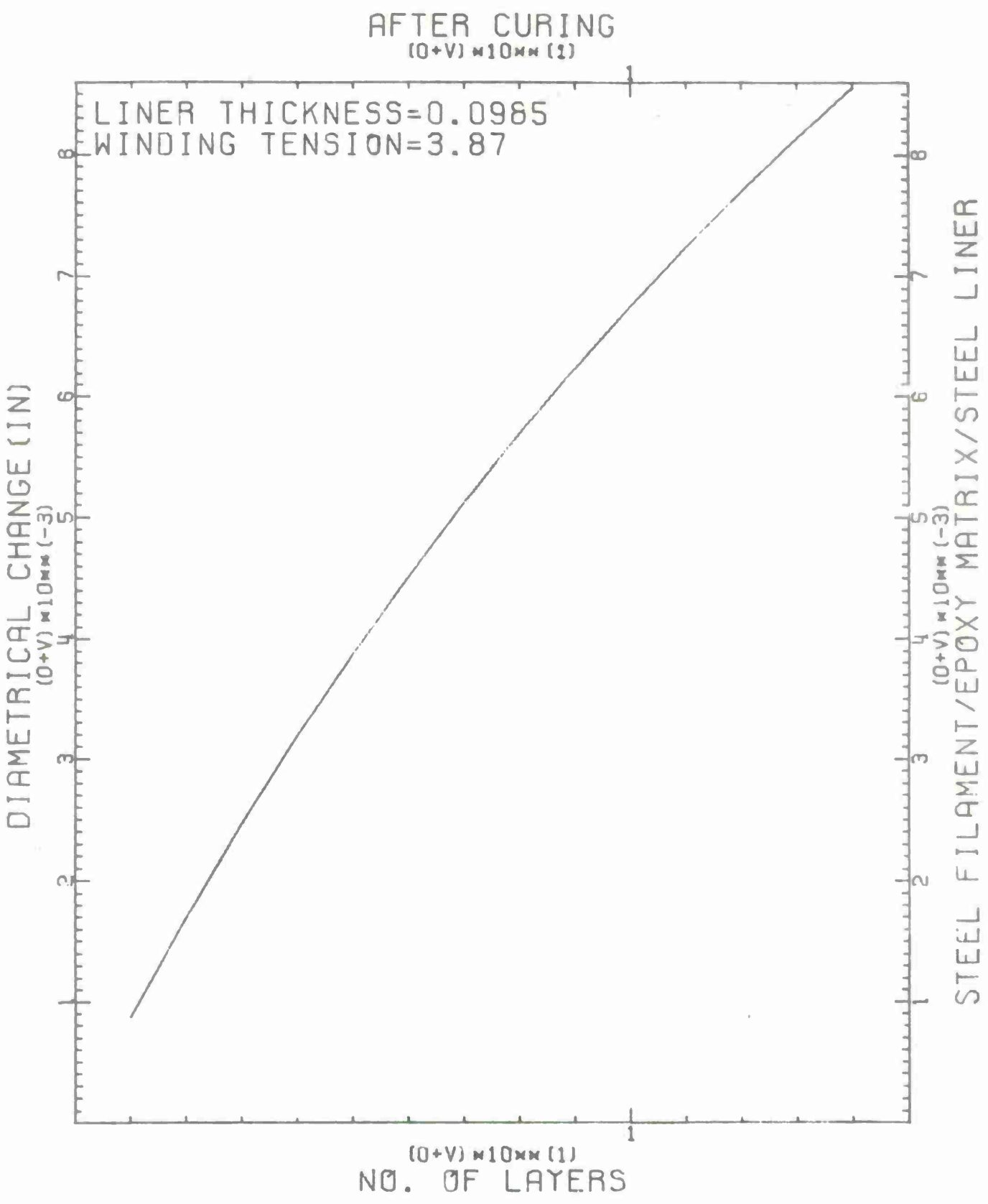

Figure B-13. Deflection vs No. of Layers for OCL-7 (After Curing)

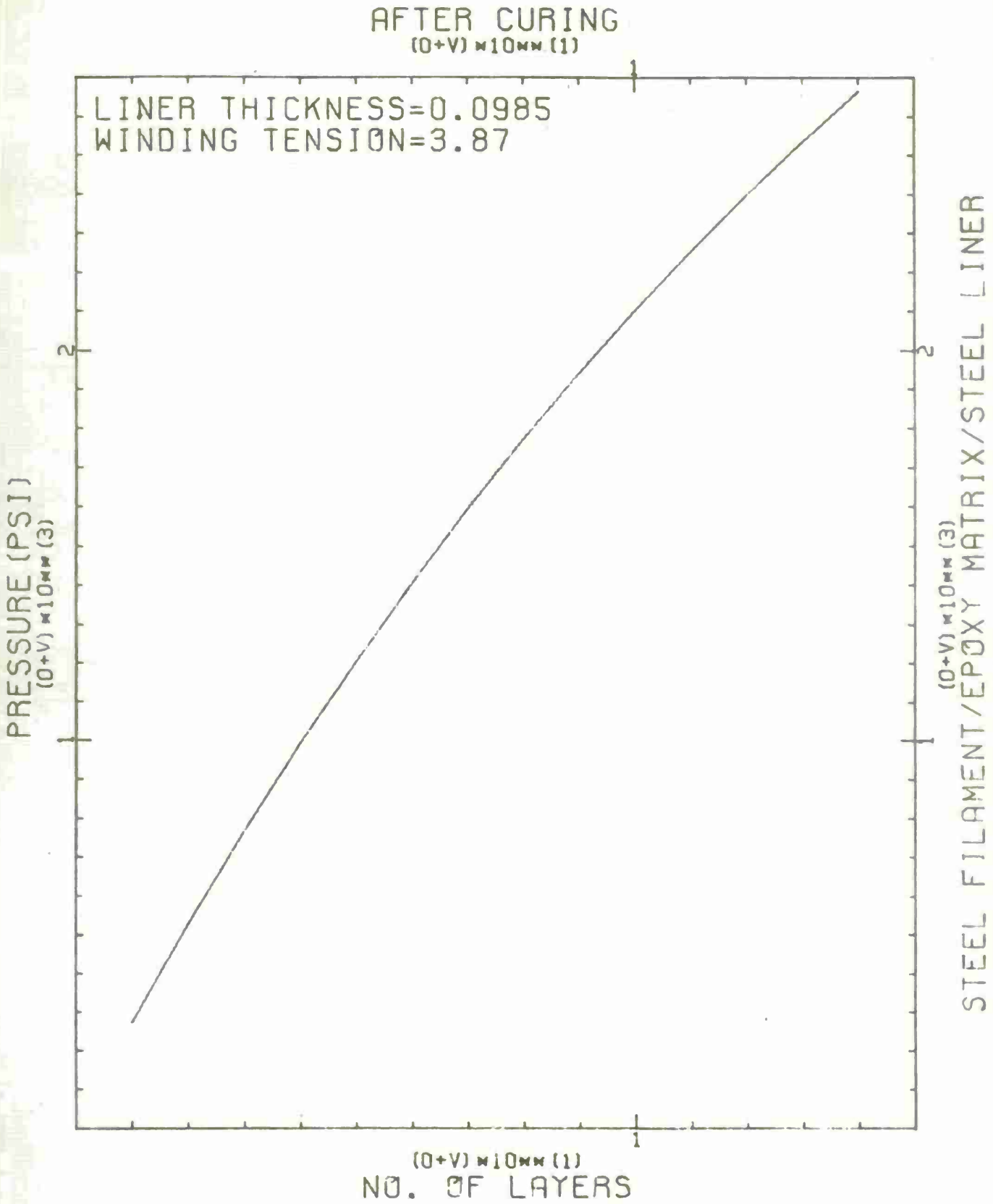

Figure B-14. Compressive Liner Pressure for OCL-7 (After Curing)

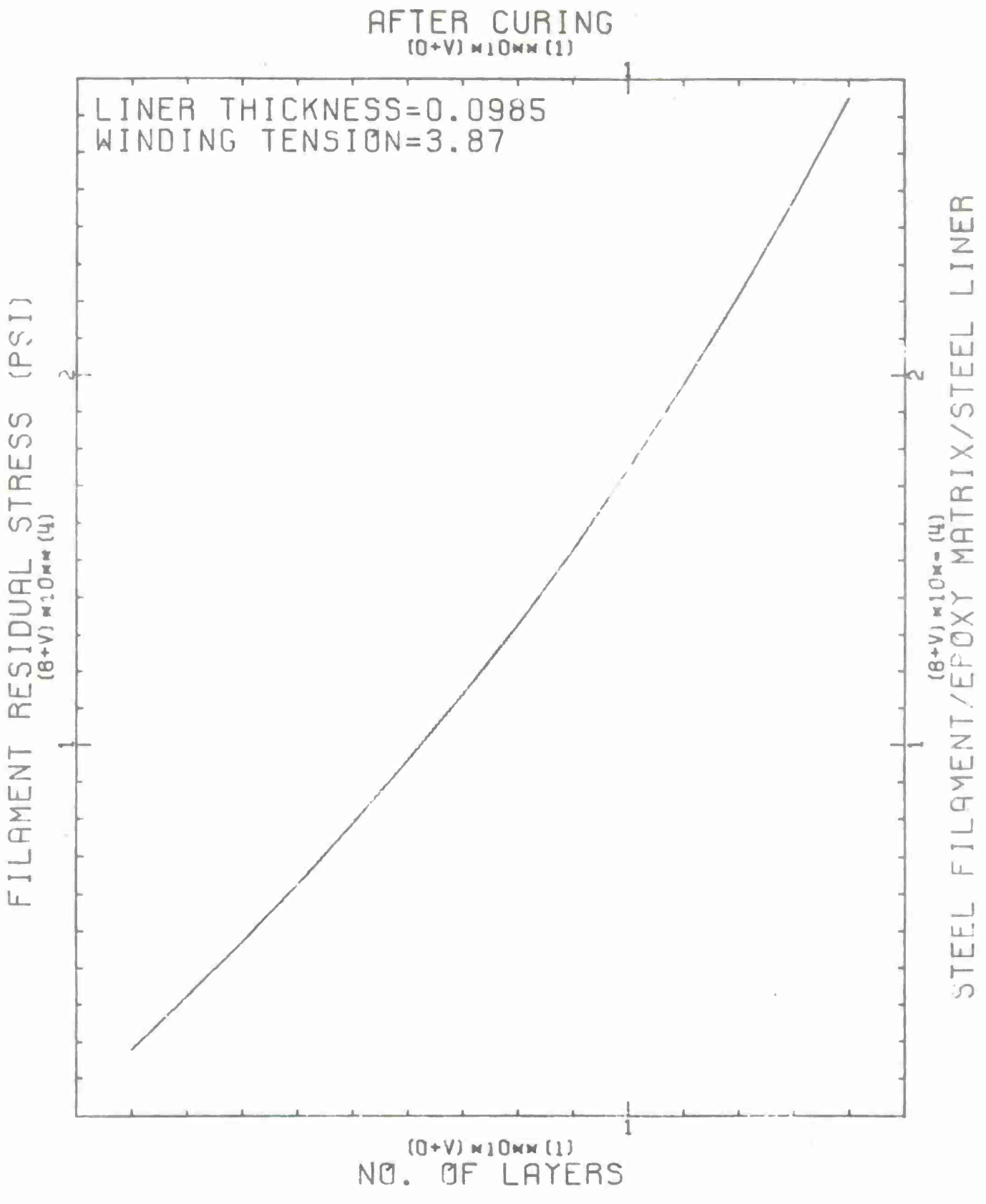

Figure B-15. Induced Residual Stresses for OCL-7 (After Curing)

"TENZIONE" - INPUT AND EXPERIMENTAL DIAMETRICAL CHANGES (DC) FOR THE OCL-10 SPECIMEN

			L	DC (in)
Modulus of Mandrel	= EM	30×10^6	1	.0005
Outside radius of Mandrel	= RM	2.205	2	.0015
Internal radius of Mandrel	= RO	2.105	3	.0025
Poisson's ratio of Mandrel	- XNUM	.28	4	.003
Modulus of Filament	= EG	30×10^6	5	.0035
Thickness of Filament	= TI	.006	6	.0045
Area of Filament	= AN	$.283 \times 10^{-4}$	7	.005
Resin squeeze out	= OMEGA	.20	8	.0055
Filament volume ratio	= XKF	.75	9	.006
Resin shrinkage	= OMEGS	.04	10	.0065
Coeff Thermal exp of Mandrel	= ALPHM	6.0×10^{-6}	11	.007
Coeff Thermal exp of Composite	= ALPHG	6.15×10^{-6}	12	.0075
Ambient Temperature	= TAMB	75	13	.0085
Curing Temperature	= TCURE	350		
Number of layers	= N	13		
Tension of Layer #1	= T1	3.83		
Tension of Layer N	= TN	3.83		
D.C. After Gel		.75		
D.C. After Cure		.75		

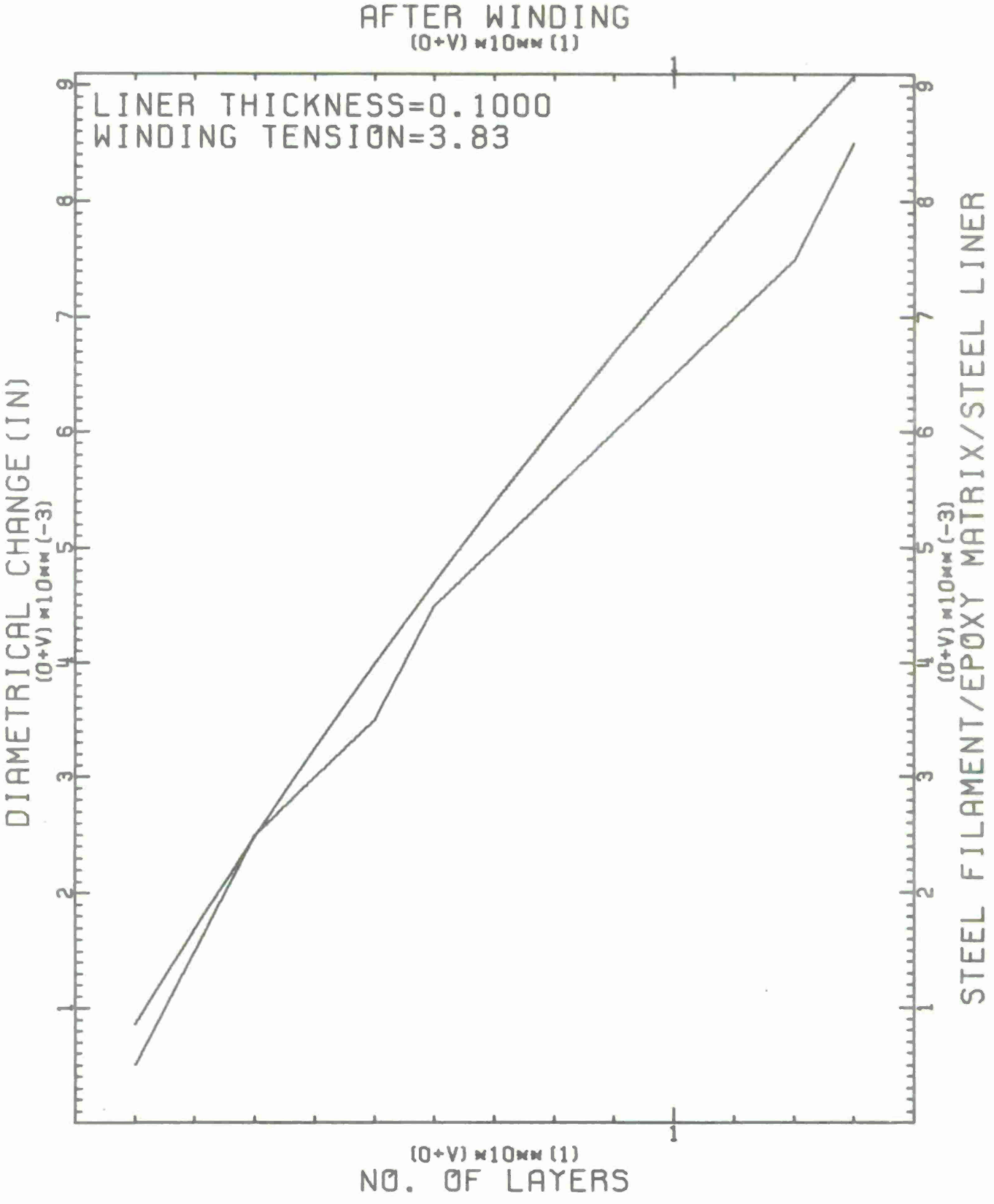

Figure B-16. Deflection vs No. of Layers for OCL-10 (After Winding)

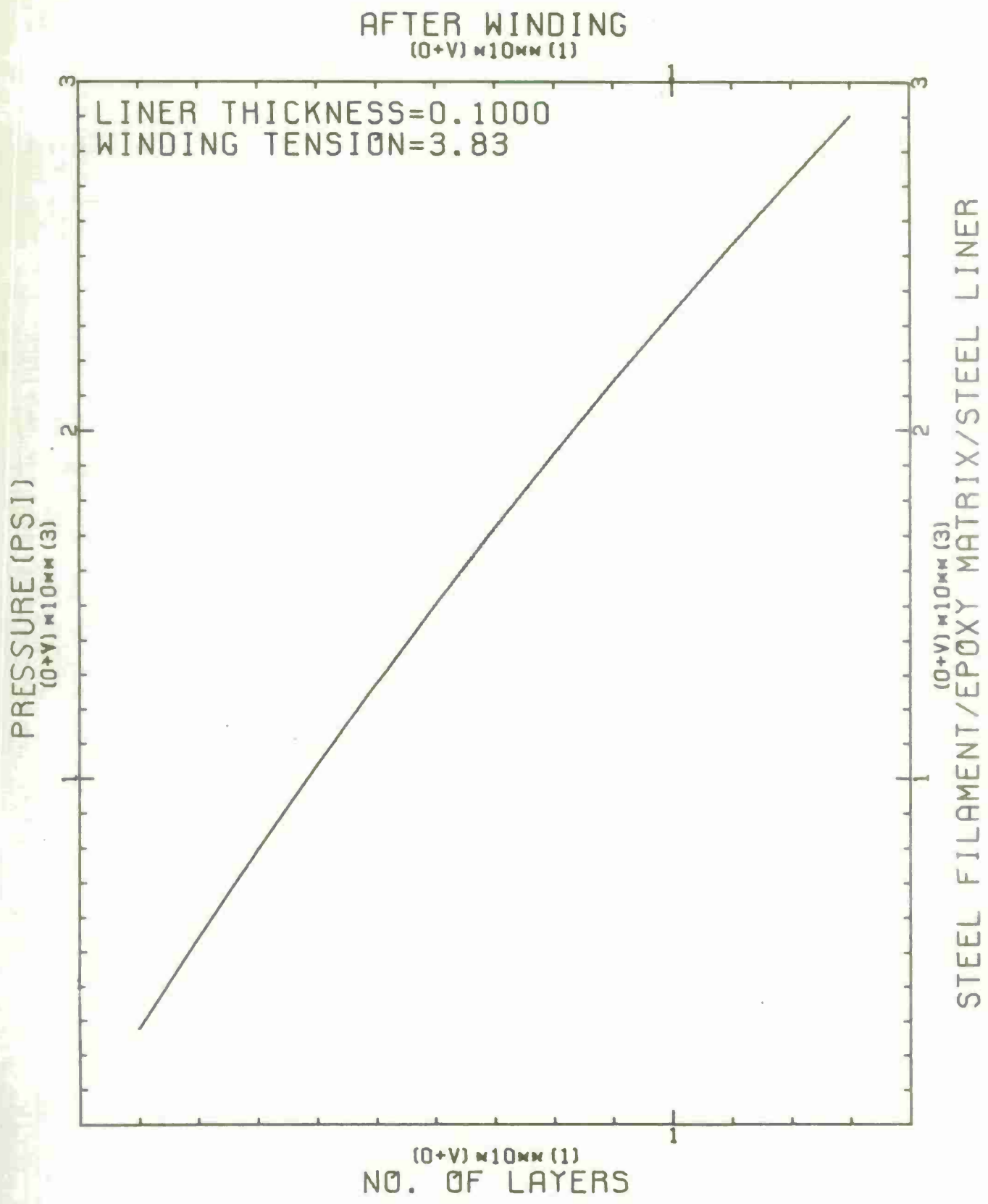

Figure B-17. Compressive Liner Pressure for OCL-10 (After Winding)

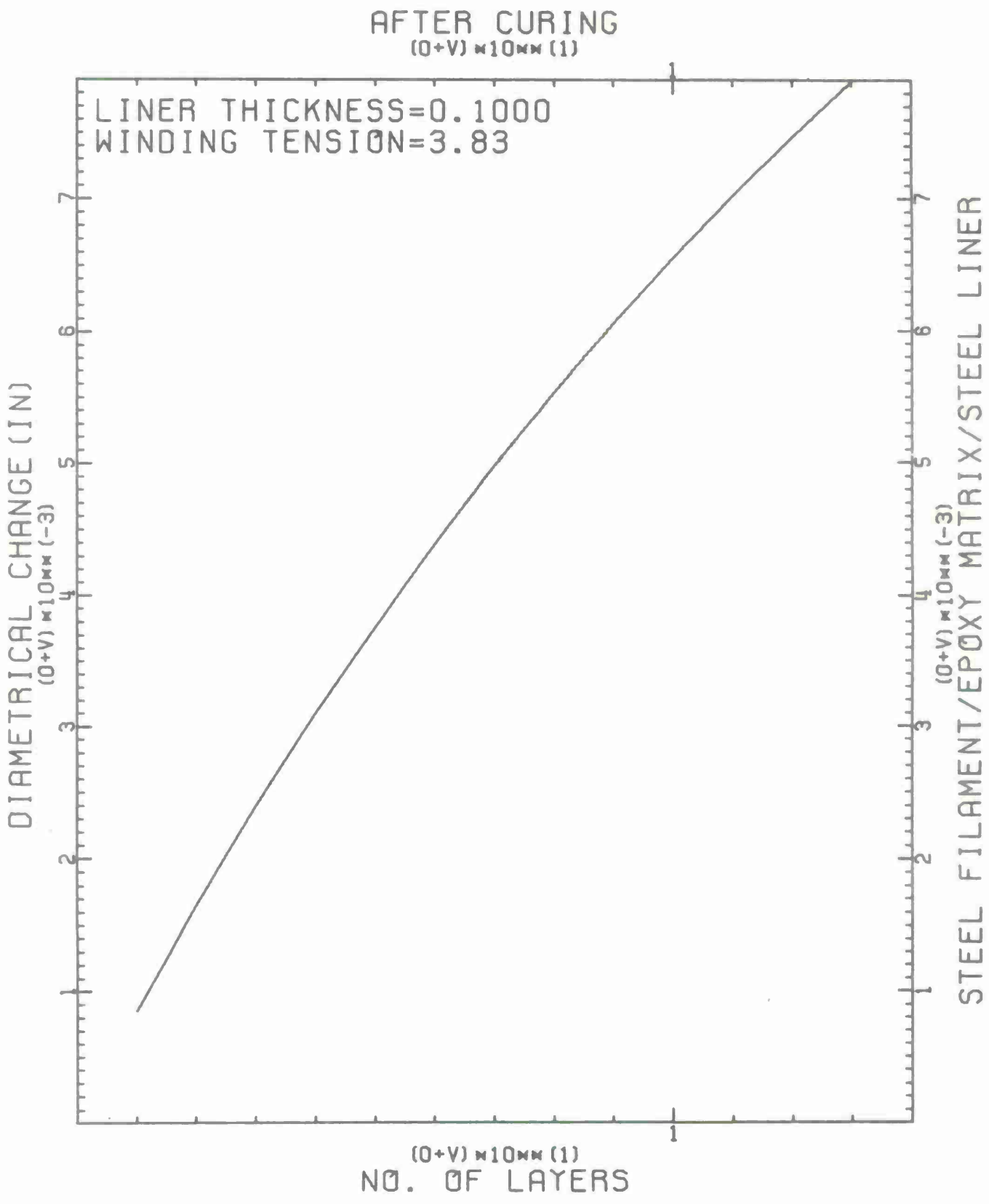

Figure B-18. Deflection vs No. of Layers for OCL-10 (After Curing)

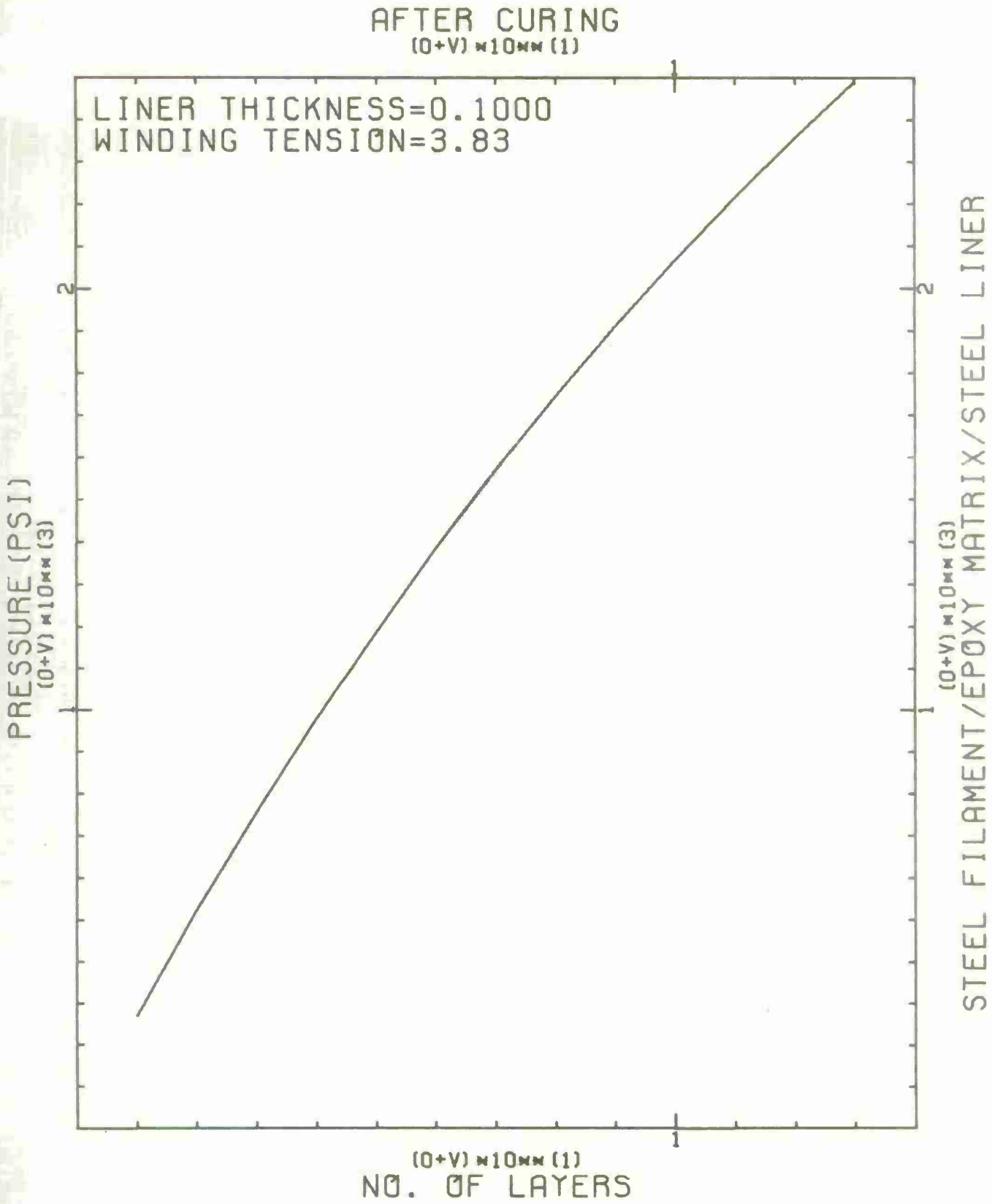

Figure B-19. Compressive Liner Pressure for OCL-10 (After Curing)

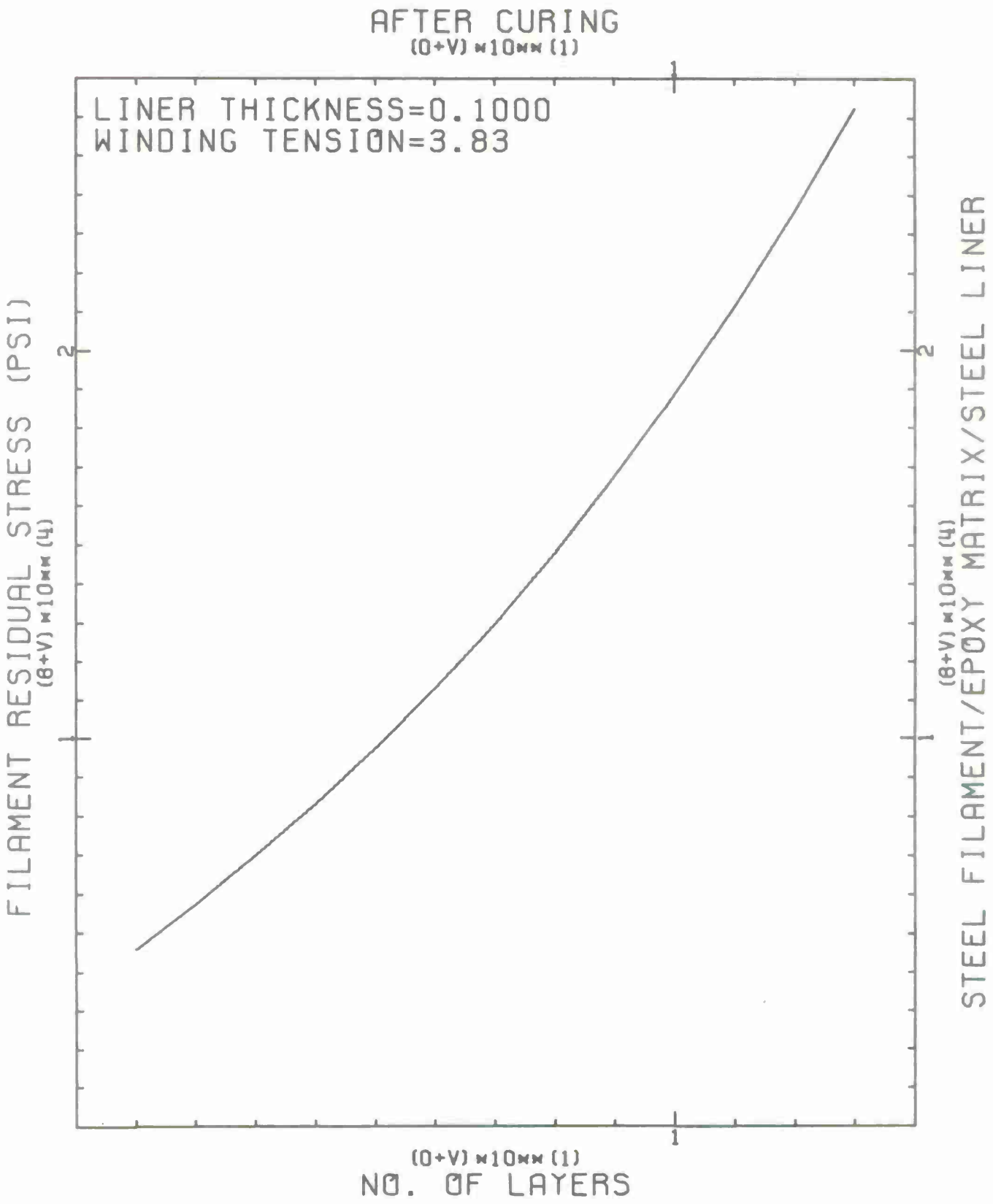

Figure B-20. Induced Residual Stresses for OCL-10 (After Curing)

APPENDIX C

THE DIMENSIONAL (INTERNAL) PROFILES OF CYLINDERS OCL 4,6,7, and 10 BEFORE WINDING, AFTER GEL, AND AFTER CURE

OCL-4 (0.050" LINER)

Travel (INS)	BEFORE WINDING		AFTER GEL		AFTER CURE	
	Bore	Rifling	Bore	Rifling	Bore	Rifling
2	-	4.2110	-	4.2075	-	4.2075
4	4.1355	4.2110	4.1315	4.2070	4.1315	4.2080
6	4.1350	4.2120	4.1290	4.1990	4.1290	4.2000
8	4.1355	4.2120	4.1215	4.1970	4.1210	4.1980
10	4.1355	4.2115	4.1230	4.1975	4.1225	4.1980
12	4.1350	4.2110	4.1225	4.1960	4.1220	4.1970
14	4.1355	4.2110	4.1220	4.1960	4.1210	4.1965
16	4.1360	4.2110	4.1195	4.1940	4.1185	4.1960
18	4.1360	4.2100	4.1170	4.1965	4.1175	4.1975
20	4.1360	4.2090	4.1280	4.2070	4.1275	4.2080
22	4.1355	4.2110	4.1310	4.2070	4.1305	4.2070
24	-	-	-	-	-	-

OCL-6 (0.075" LINER)

2	-	4.2120	-	4.2100	-	4.2100
4	4.1345	4.2115	4.1330	4.2095	4.1325	4.2100
6	4.1345	4.2110	4.1300	4.2015	4.1305	4.2030
8	4.1365	4.2110	4.1240	4.1995	4.1240	4.2005
10	4.1365	4.2100	4.1240	4.2000	4.1245	4.2010
12	4.1355	4.2105	4.1245	4.2015	4.1240	4.2015
14	4.1360	4.2105	4.1260	4.2020	4.1255	4.2025
16	4.1355	4.2110	4.1260	4.2010	4.1250	4.2020
18	4.1360	4.2100	4.1255	4.2005	4.1250	4.2010
20	4.1360	4.2100	4.1295	4.2065	4.1290	4.2065
22	4.1355	4.2110	4.1335	4.2095	4.1335	4.2095
24	-	-	-	-	-	-

OCL-7 (0.100" LINER)

Travel (INS)	BEFORE WINDING Bore	BEFORE WINDING Rifling	AFTER GEL Bore	AFTER GEL Rifling	AFTER CURE Bore	AFTER CURE Rifling
2	-	4.2115			-	4.2090
4	4.1350	4.2115			4.1325	4.2100
6	4.1350	4.2115	NOT		4.1310	4.2050
8	4.1350	4.2100			4.1260	4.2030
10	4.1355	4.2100			4.1270	4.2020
12	4.1355	4.2100	AVAILABLE		4.1265	4.2020
14	4.1355	4.2100			4.1270	4.2020
16	4.1350	4.2100			4.1270	4.2020
18	4.1355	4.2100			4.1265	4.2020
20	4.1355	4.2100			4.1295	4.2090
22	4.1360	4.2100			4.1330	4.2095
24	-	-			-	-

OCL-10 (0.100" LINER)

2	-	4.2105	-	4.2095	-	4.2085
4	4.1345	4.2100	4.1330	4.2085	4.1335	4.2080
6	4.1345	4.2100	4.1310	4.2025	4.1315	4.2025
8	4.1350	4.2100	4.1280	4.2025	4.1285	4.2025
10	4.1355	4.2100	4.1290	4.2030	4.1295	4.2025
12	4.1355	4.2095	4.1290	4.2025	4.1290	4.2020
14	4.1355	4.2100	4.1285	4.2025	4.1285	4.2025
16	4.1350	4.2100	4.1275	4.2020	4.1275	4.2020
18	4.1355	4.2090	4.1270	4.2025	4.1275	4.2025
20	4.1350	4.2105	4.1300	4.2085	4.1300	4.2085
22	4.1350	4.2105	4.1330	4.2090	4.1335	4.2090
24	-	-	-	-	-	-

APPENDIX D

CALCULATIONS FOR THE VESSEL LIMITING PRESSURE

1. Calculations for the Limit Pressure.

CASE 1. Yielding commencing at the bore.

$$\sigma_\theta\Big|_a^{\text{RESIDUAL}} + \sigma_\theta\Big|_a^{\text{ELASTIC}} = \sigma_\theta\Big|_a^{\text{YIELDING}}$$

$$-60{,}200 + \left(A^* + \frac{B^*}{2}\right) = \frac{1}{2}\left[\sigma_r + \sqrt{3}\sqrt{\frac{4}{3}\sigma_o^2 - \sigma_r^2}\right]$$

OR

$$-60{,}200 + \left[6.185 + \frac{31.81}{(2.104)^2}\right]P = \frac{P}{2} + \frac{\sqrt{3}}{2}\sqrt{\frac{4}{3}(160{,}000)^2 - (-P)^2}$$

$$\Rightarrow \quad P = 15{,}838 \text{ psi}$$

CASE 2. Yielding commencing at the Liner-Jacket interface

$$\sigma_\theta\Big|_b^{R} + \sigma_\theta\Big|_b^{E} = \sigma_\theta\Big|_b^{Y}$$

$$82{,}000 + \left(n_1 c_1^* b^{n_1-1} + n_2 c_2^* b^{n_2-1}\right) = \frac{1}{2}\left[\sigma_r + \sqrt{3}\sqrt{\frac{4}{3}\theta_o^2 - \sigma_r^2}\right]$$

where

$$\sigma_r = A^* - \frac{B^*}{b^2}$$

$$\Rightarrow P = 24{,}610 \text{ psi}$$

CASE 3. Yielding commencing at the jacket OD

$$\sigma_\theta\Big|_{b_o}^{R} + \sigma_\theta\Big|_{b_o}^{E} = \sigma_\theta\Big|_{b_o}^{Y}$$

$$108{,}000 + \left(n_1 C_1^* b_o^{n_1-1} + n_2 C_2^* b_o^{n_2-1}\right) = \frac{1}{2}\left[\sigma_r + \sqrt{3}\sqrt{\frac{4}{3}\theta_o^2 - \sigma_r^2}\right]$$

$$\Rightarrow P = 22{,}568 \text{ psi}$$

where

$$\sigma_r\Big|_{b_o} = 0$$

NOTE:

From Reference 5

$A^* = 6.185\ P$	$b = 2.209"$
$B^* = 31.81\ P$	$b_o = 2.288"$
$C_1^* = .735\ P$	$n_1 = 2.45$
$C_2^* = 30.57\ P$	$n_2 = 2.45$
$J_o = 160$ KSI	$\theta_o = 340$ KSI

[5] D'Andrea, G., "Composite Cylindrical Pressure Vessels Related to Gun Tubes. Part I: Theoretical Investigation," September 1968, Watervliet Arsenal Technical Report WVT-6821.

2. Derivation of the pressure parameter as it is related to the area under the A-A curves of Figures 20 and 21.

A cylinder under pressure can be illustrated per the following sketch:

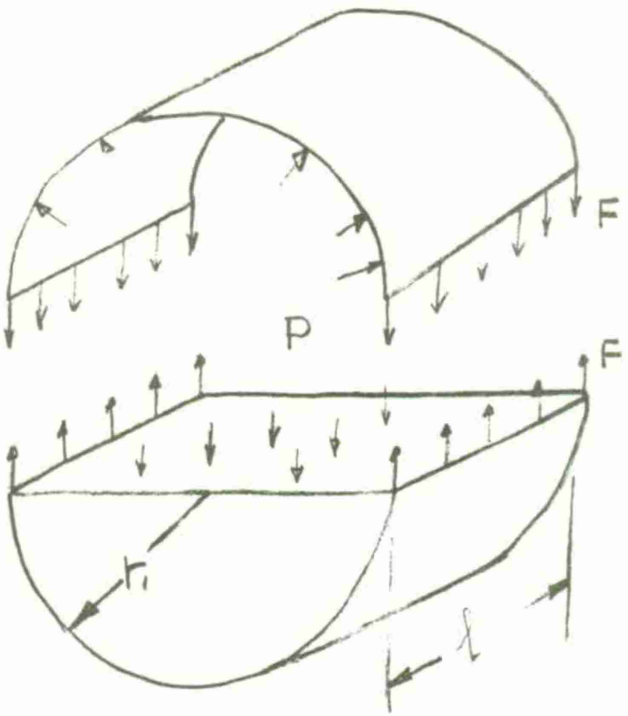

This sketch represents the distribution of gas pressure exerted by the gas in the upper half upon the semi-cylindrical wall and upon the gas occupying the lower half of the cylinder. From this diagram the force F is readily calculated from the condition for static equilibrium of the lower part, i.e.,

$2F = p \times \text{projected area}$

$= p \times 2 r_1 \ell$

OR

$F = p r_1 \ell$

Next, the unit tensile stress (or hoop stress) in the wall of thickness t is readily obtained from:

$$\sigma_\theta = \frac{F}{A} = \frac{P r_1 \ell}{t \ell} = \frac{P r_1}{t}$$

In the integral form the pressure P is

$$P = \frac{1}{r_1} \int_{r_1}^{r_2} \sigma_H \, dr$$

This integral $\left(\int_{r_1}^{r_2} \sigma_H \, dr \right)$ represents the area under the curve of the hoop stress versus the radius, and it is also called the stress resultant in the units of #/in.

From Figures 20 and 21 we can obtain the scale factor K which is equal to 2350.78 #/in. Knowing this factor (1 in^2 = 2350.78 #/in) and the actual area under the A-A curve we can obtain the value of the pressure P.

Then

$$P_1 = \frac{A_1}{2.104} = \frac{(3.16)(2.02)(2350.78)}{2.104}$$

$$= 7129 \text{ psi}$$

Similarly,

	P_2 =	12,469 psi	A_1	15,000	A_3
	P_3 =	7,129 psi	A_2	26,235	#/in
and	P_4 =	8,922 psi	A_4	18,772	#/in